12-2016

Models for Decanting Gaseous Fuel Tanks: Simulations with GFSSP Thermal Model

Kailash Kumar Jain Munoth
University of Nebraska-Lincoln, kailashjain.m@gmail.com

Models for Decanting Gaseous Fuel Tanks: Simulations with GFSSP Thermal Model

By

Kailash Kumar Jain Munoth

A THESIS

Presented to the Faculty of

The Graduate College at the University of Nebraska

In Partial Fulfillment of Requirements

For the Degree of Master of Science

Major: Mechanical Engineering and Applied Mechanics

Under the Supervision of Professor Kevin D. Cole

Lincoln, Nebraska

December, 2016

Models for Decanting Gaseous Fuel Tanks: Simulations with GFSSP Thermal Model

Kailash Kumar Jain Munoth, M.S.

University of Nebraska, 2016

Advisor: Kevin D. Cole

Transport of fuel from distillation/storage plant to different parts of the world has always been challenging task for Engineers. Different methods have been proposed over the time for transporting fuel efficiently and at low cost which include Marine vessels, Pipelines, Rail Cars and Trucks. In order to transport useful amount of fuel in a reasonably sized tank, we have to liquefy it. While few fuels are easy to liquefy there are great number of fuels which liquefy only under extreme pressure/temperature conditions. Methane has a boiling point of -161.7°C at atmospheric pressure which means it has to be cooled to a much lower temperature in order to turn it into to liquid that can be stored in a tank. In short, Methane is not stored in household tanks because it is hard to liquefy. So large carbon epoxy fiber tanks were developed to transport Methane around the world in gaseous state at high pressures. But when the tank decanting was done in places where ambient temperatures were well below 0°C, it was found that ideal conditions for Methane liquefaction were formed.

Gaseous Methane has to lose a lot of energy to liquefy which means that liquid Methane would be much colder than its gaseous counterpart. Now the liquid Methane would cool the tank walls more rapidly than its gaseous counterpart present in the tank and thus this difference in temperature would impart additional thermal stresses on the tank walls. These thermal stresses are result of uneven contraction/expansion of the tank walls and may lead to crack formation in the wall surface which we intend to avoid in all circumstances. The present study is concentrated in identifying different tank decanting conditions where there may arise favorable conditions for liquid Methane formation.

Tank decanting simulations were performed for different system temperatures ranging from -50°C to 20°C and flow rates of 0.064kg/s, 0.11975 kg/s and 0.3kg/s respectively were selected for each system temperature. A similar study on Biogas tank decanting was performed and different system conditions were identified where possibility of liquefaction arouse within the tank.

Through the tank decanting study carried out on Methane and biogas fuels, few decanting conditions were identified where there was a possibility of liquefaction within the tank. If the decanting was continued from these points of liquefaction, the tank walls would experience immense thermal stresses and there may arise a point where cracking in the tank wall takes place. The tank decanting, either has to be stopped or the decanting flow rate should be reduced further at these points. As the decanting flow rate is reduced the tank wall would have enough time to pump heat into the system and thus avoiding liquefaction within the tank. This process can continue only until the tank wall temperature and the fuel temperature within the tank reaches equilibrium or the fuel temperature reaches its critical point, whichever comes earlier. After this, decanting has to be stopped because any further temperature drop would result in liquefaction which has to be avoided under any circumstances as this would in turn result in tank liner failure.

ACKNOWLEDGEMENT

I would like to thank all the people who contributed in some way or the other to the work described in this thesis. First and foremost, I thank my academic advisor, Professor Kevin D. Cole, for accepting me into his group. During my tenure, he contributed to a rewarding graduate school experience by giving me intellectual freedom in my work, engaging me in new ideas, and demanding a high quality of work in all my endeavors. Additionally, I would like to thank my committee members Dr. George Gogos and Dr. Zhaoyan Zhang for their interest in my work. Special thanks to Brittney Bridger-Burton for her valuable insights on ASPEN Plus.

I would like to acknowledge the Department of Mechanical Engineering and Applied Mechanics at University of Nebraska-Lincoln. My graduate experience benefitted greatly from the courses I took, the opportunities I had and the high-quality seminars that the department organized.

I would also like to acknowledge the Department of Mechanical Engineering at Padmasri Dr. B. V. Raju Institute of Technology. I was first introduced to Thermal Sciences by my college professor Dr. V. Murali Krishna whose lectures on Heat Transfer intrigued my interest towards the subject. Whether it may be the mind boggling theories of heat transfer phenomenon or heated debates on perpetual motion machines, all in all add to my perseverance to get more insight in the theories of thermal sciences.

Finally, I would like to acknowledge friends and family for providing me with unfailing support and continuous encouragement throughout my years of study and through the process of researching and writing this thesis. This accomplishment would not have been possible without them. First and foremost, I would like to thank Mom (Nirmala), Dad (Rajendra), Santosh, Vijaya, Archana and Nagendar for their constant love and support. I would also like to thank Bhushit, Srinidhi, Sirish, Rakshitha to name a few and all my friends in Lincoln who made my time here at UNL a lot more fun. I would also like to thank Manish, Akshi for believing in me and encouraging me through all my endeavors.

Author

Kailash Kumar Jain Munoth

Table of Contents

List of Tables

List of Figures

List of Symbols

Symbol	Description
A	Area (m^2)
a	Length (m)
C	Heat Capacity ($J°C^{-1}$ or $J°K^{-1}$)
C_L	Flow Coefficient
$C_{I,k}$	Mass Concentration of k^{th} Specie at i^{th} Node
C_p	Specific Heat (J/g°C or J/kg-K)
C_v	Flow Coefficient for a Valve
D	Diameter (m)
f	Darcy Friction Factor
g	Gravitational Acceleration (m/s^2)
g_c	Conversion Constant (=32.174 lb-ft/lb_f-sec^2)
h	Enthalpy (J)
h_{ij}	Heat Transfer Coefficient ($W/(m^2K)$)
J	Mechanical Equivalent of Heat (4.22 J/(g°C))
K_f	Flow Resistance Coefficient
K	Thermal Conductivity (W/m-K)
L	Length (m)
M	Molecular Weight
m	Resident Mass (kg)
$\dot{m}$	Mass Flow Rate (kg/sec)

P	Pressure (Pascal's)
P_o	Poiseuille Number
Pr	Prandtl Number
Re	Reynolds Number
R	Gas Constant (J/(mol-K))
r	Radius (m)
s	Entropy (J/K)
T	Fluid Temperature (°C)
T_s	Solid Temperature (°C)
u	Velocity (m/s)
V	Volume (m^3)
v	Specific Volume (m^3/kg)
z	Compressibility Factor

Greek Symbols

ρ	Density (kg/m^3)
η	Efficiency
μ	Viscosity (kg/m-s)
υ	Kinematic Viscosity (m^2/s)
$\bar{\rho}$	Molar Density (kg-mol/m^3)
ϒ	Specific Heat Ratio
δ_{ij}	Distance between two solid nodes (m)
$\Delta\tau$	Time step (sec)
τ	Time (sec)

σ	Stephan Boltzman Constant (=5.67*10^{-8}W/(m^2K^4))

Subscript

a	Ambient
c	Cold
Dis	Discharge
F	Fluid
h	Hot
S	Solid
i	Node
ij	Branch
trans	Transverse
gen	Generation
eff	Effective
or	Orifice
f	Liquid
g	vapor

Chapter 1 : Introduction

1.1 Motivation

Methane is the simplest alkane and the main component of natural gas. Methane, which comes out of the ground as a gas, is produced when microorganisms known as methanogens feed on organic matter in environments with little or no oxygen. Methane can be captured where it naturally occurs or produced in a controlled environment like an anaerobic digester. After it is captured or produced, it is cleaned (by removing carbon dioxide and other liquids); compressed to a higher pressure; odorized (it's odorless and lethal in high doses in its natural state); and piped into our homes, power plants, and factories for heat and power.

Methane, like all fossil fuels, can be combusted (reacted with oxygen) to form energy and water. In fact, a relatively large and growing part of world's electricity comes from Methane. It is the simplest fossil fuel – a single carbon atom with four hydrogen atoms, or CH_4.

The basic Methane combustion reaction is:

CH_4 (Methane) + $2O_2$ (Oxygen) = CO_2 (Carbon dioxide) + $2H_2O$ (Water) + Energy (~810KJ/mole of Methane)

Because of its simplicity and lack of additional compounds, Methane is the cleanest of the fossil fuel to combust. When we say cleanest, though we often mean different things. In terms of the production of carbon dioxide (i.e., the major greenhouse gas), Methane has the lowest density, meaning we get more energy per unit of carbon dioxide than we do with other fuels. (Laurell, 2014) It releases 29% less carbon than oil, 43% less than coal, and 20-30% less lifecycle carbon than oil when used as transportation fuel.

In addition, unlike other fuels, Methane combustion results in basically no NOx (nitrous oxide), Sox (sulfur dioxide), or particulate matter being released into the atmosphere. These all gases are all dangerous to our health and regulated under the Clean Air Act.

One of the potential ways for transporting natural gas would be by using tanks. Natural gas would be filled in tanks at refueling stations or at extraction sites and the fuel would be transported over lands to different accessible parts of the country. Natural gas refueling stations can either be CNG, LNG, or LCNG stations. LCNG stations can offer compressed, liquefied or both types of natural gas. LCNG stations are supplied with LNG, and CNG is produced with a vaporizer. Apart from this, CNG stations can either be fed from the natural gas grid directly, or fed from LNG which is then vaporized and put under pressure in order to get it settled to 200 bar or corresponding equilibrium pressure at ambient temperature conditions.

Even though the end product of the use of CNG and LNG for vehicular applications is essentially the same, the general properties affecting safety are quite different. On one hand, LNG is a more refined and consistent product with none of the problems associated with corrosive effects on tank storage associated with water vapor and other contaminants. On the other, the cryogenic temperature makes it extremely difficult or impossible to add an odorant. Therefore, with no natural odor of its own, there is no way for personnel to detect leaks unless the leak is sufficiently large to create a visible condensation cloud or localized frost formation. The cryogenic temperature associated with LNG systems creates a number of generalized safety considerations for bulk transfer and storage. Most importantly, LNG is a fuel that requires intensive monitoring and control because of the constant heating of the fuel which takes place due to the extreme temperature differential between ambient and LNG fuel temperatures.

Even with highly insulated tanks, there will always be a continuous build-up of internal pressure and a need to eventually use the fuel vapor or safely vent it to the atmosphere. When transferring LNG, considerable care has to be taken to cool down the transfer lines in order to avoid excessive amounts of vapor from being formed.

Given identical compositions, those characteristics that differ between LNG and CNG and that affect their use in some way are shown below (Consultants, 1991):

	CNG	LNG
Physical State	Gas	Liquid
Temperature in vehicle tank	Ambient	-162°C
Typical Pressure in Tank	17.3-24.9 MPa	170-446kPa
Typical Specific Gravity	0.13 – 0.19	0.42
Typical Energy Density (LHV)	6,500-9,500 MJ/L	21,000 MJ/L

In order to maintain it in a liquid state, LNG must be kept cold by storing and transporting it in double-walled, vacuum-insulated containers. All containers let some heat leak in, causing LNG to boil-off and pressure to build up in vapor space. Unless either vapor or liquid is withdrawn at a rate sufficient to counteract the boil-off rate, tank pressure will increase until the pressure setting of the relief valve is exceeded and some gas is vented to the atmosphere. This process will continue until eventually the entire liquid contents of the tank have been vaporized. By contrast, natural gas can be stored as CNG indefinitely without loss.

Use of LNG or CNG also depends on the energy consumed during fuel production and transportation process. To achieve reasonable values of tank weight and volume, CNG has to be compressed to 17-25Mpa and as no pipelines work in this pressure range mobile tanks are used for CNG transportation. The energy required for compression not only depends on initial, final pressure but also on the process of compression. (Consultants, 1991) J.E. Sinor identified two processes for compression which are slow fill process and fast fill process. In slow fill, a compressor is connected to all vehicle tanks at once, and, over a period of several hours, the pressure is increased to final fill pressure. This system requires the least energy for compression. In the fast fill technique, the compressor first fills an intermediate storage vessel or vessels, at least one of which is at an appreciably higher pressure than the desired vehicle fill pressure. A single tank can then be filled in just a few minutes by connecting it to the storage vessel. Because the gas has to be compressed to a higher pressure in the intermediate storage vessel than the final vehicle fill pressure, a fast fill system uses more energy than the slow fill system. The excess energy required is usually reduced by using a series of vessels at successively high pressure, called cascade and filling the vehicles from each in turn. (Consultants, 1991)It was found that the typical energy requirement for compression was in the order of 400Btu/lb, or about 2% of energy value of natural gas being compressed. Also refueling time in fast fill process has great economic importance as time spent refueling 'unproductive time', creating no value for the enterprise. Thus driver time spent in refueling carries a 'lost opportunity' cost, which may not be accounted in usual energy and economic analyses. (Consultants, 1991)If a driver's labor plus overhead rate in a company is $30/h, an extra 10 minutes consumed in refueling carries the lost opportunity cost of $5. If the average fill is 20gal of diesel fuel equivalent, the lost opportunity cost because of extra refueling time is $0.25/gal, a significant fraction of fuel cost. The above analysis is applicable to tank decanting and has a similar lost opportunity cost depending on the time required for tank decanting.

Fast-fill CNG systems also have a problem caused by heating effect when the gas in the tank is compressed and thereby heated. This temperature rise makes it impossible to put as much mass in the tank as can be done in slow-fill process. The penalty may be as much as 5%-10% of tank capacity. Although LNG system has inherent advantages for fast fueling, the cryogenic nature of fuel creates other problems that probably evens out the comparison.

The pressure at which CNG can be stored in a tank also depends on the system temperature. For a given mass and fixed volume of gas, if the system temperature is high, then the system initial pressure would also be high as they are directly proportional according to Gay-Lussac's Law. Similarly, if the system initial temperature is low then the system initial pressure will also be low for a given volume of gas. But during decanting as the amount of fuel in the tank decreases, the left over fuel in the tank has larger space to occupy and as a result the fuel cools rapidly. This cooling will have a greater effect as the system temperature is decreasing because the range of cooling required to reach the critical point decreases as the system temperature decreases i.e. Methane at -20°C has to be cooled relatively lower than Methane at 20°C to reach the critical point of -82.59°C. So the chances of Methane liquefaction increases as the system initial temperature is lowered. And as the fuel temperature approaches the critical point the chances of tank liner failure increases as the tank wall would experience immense sudden cooling effect due to liquid fuel formation which may lead to cracking. And if this occurs relatively early during the decanting process when the pressure in the system is high then explosion of tank is a possibility which may lead to loss of property and even life if any personnel are in vicinity of the tank. This has to be avoided under any circumstances and identifying the point where there is possibility of fuel liquefaction is of utmost importance.

Throughout the report all the mentioned problems are discussed elaborately and addressed technically using two very well-known tank decanting simulation software packages GFSSP and ASPEN Plus. A detailed literature review was carried in **Chapter 2** where inference on natural gas behavior during fast filling and rapid decanting conditions was drawn from the studies made by (Javad Khadem, 2015), (Khamforoush, et al., 2015), (Cole, June 12, 2015), (Brittney Bridger Burton, 2016), (Melideo D., n.d.), (Shipley, 2002) and (Mazyan, et al., 2016). In **Chapter 3** Mathematical basis for GFSSP was discussed in detail. This was followed by **Chapter 4**, where Methane tank decanting simulations were performed in GFSSP and different decanting conditions were identified where Methane liquefaction was observed. In the following **Chapter 5**, similar analysis was performed on Biogas and detailed discussions on the observations made were presented. **Chapter 6** was dedicated to study Methane, but this time with a different approach i.e. by utilizing ASPEN Plus for carrying out the decanting simulations. Summary of all the observations made and also possible solution to avoiding damage to the tank was presented in **Chapter 7**.

Chapter 2 : Literature Review

Natural Gas has become one of the most desired energy sources after oil discovery for its efficient combustion and low carbon dioxide emissions. (Mazyan, et al., 2016) have reviewed all the various processes associated with natural gas including extraction, transportation, storage and treatment as well as the natural gas costs and its market in different parts of the world. The mentioned paper also includes liquefaction and re-gasification processes available in the market in addition to emerging technologies proposed in these areas. Different practices, several emerging technologies including the use of the solar power and thermos-acoustic cycles in the refrigeration cycles, and natural gas solidification for natural gas storage are brought to light.

Fuel tank emptying characteristic has been a topic of study for many researchers around the world and different methods have been developed to simulate tank emptying process. CFD numerical modelling is the most widely used method to simulate thermal models during tank decanting.

2.1 CFD Investigation for Emptying Fuel Tank

A CFD study on hydrogen tanks during fast fill and decanting was performed by (Melideo D., n.d.). It was found that during the filling of hydrogen tanks high temperatures can be generated inside the vessel because of the gas compression while during the emptying low temperatures can be reached because of the gas expansion. Excessively high or excessively low temperatures could affect the mechanical properties of the tank materials. In the work mentioned both filling and emptying are considered for a type 3 tank and a comparison between experiments and simulations was carried out for the gas temperatures, the temperatures at the interface between the liner and the composite layer, and for the temperature on the external surface of the tank, providing a more complete picture of the capabilities of the CFD model.

(Melideo D., n.d.) conducted experiments on compressed hydrogen gas tanks which consisted of fast filling, simulating the refueling of the tank at the service station, followed by an emptying phase, representing the gas consumption during driving. Several parameters were monitored to evaluate the tank performance, such as tank wall temperature, temperature inside the material, internal gas temperature at different positions and deformation of the tank walls as well as the possible leakage or permeation of hydrogen.

The tank tested was a 40liter type 3 with two metallic bosses, a metallic liner and an external wrapping of carbon fiber re-enforced composite. **Figure 2-1** is a sketch of tank with the location of thermocouples where TT's, TC's and EWT's represent different thermocouples.

The CFD simulation was carried out in ANSYS CFX V14.0 with numerical time scheme based on Second Order Backward Euler scheme. A residual convergence criterion for RMS (root mean square) mass-momentum equation of 10^{-4} has been applied, ensuring the attainment of convergence of results. It was found that the pressure at the beginning of defueling reached 750bar and at such high pressures ideal gas laws were unable to describe hydrogen properties so real gas equation of state was used to describe hydrogen properties. The computational model adopted for tank decanting simulations consisted of five subdomains: one fluid part (i.e. Interior of tank filled with hydrogen), the internal metallic liner, the external composite carbon fiber wrap (CFRC) and the two bosses at the tank ends.

The comparison between the CFD results and the experimental data for hydrogen tank decanting is shown in **Figure 2-2**. The yellow and green color of the lines in the figure represent the results from the two decanting simulations and their respective experimental results where the continuous lines represent the CFD simulations and the crosses represent the experiments.

It can be seen from **Figure 2-3** that a faster depressurization generates a larger drop in the gas temperature for the first 500s in the EM-EXP03 case. As the tank decanting progresses the pressure decrease inside the vessel causes a decrease in gas temperature because the gas left over inside the tank expands into the available volume and thus its temperature decreases. While the heat transfer from the environment to the tank walls tends to produce the opposite effect of heating the gas inside the tank. The two effects are competing against each other for the entire decanting process and during most of the tank decanting, depressurization is dominant but towards the end the rate of pressure drop inside the tank decreases and effect of heat transfer from the walls prevails. The end result being increase in gas temperature during the last phase of tank decanting.

2.2 Non-Linear Regression Routine for Modelling Fuel Tank Decanting

Thermal modelling of fuel tank decanting is growing area of research around the world. A similar research for modelling of tank decanting was done at University of Nebraska-Lincoln by (Cole, June 12, 2015). In this research a thermal model for tank decanting was developed which was validated by corresponding experimental data.

In this research different parameters that greatly affected the decanting simulations and also the parameters with very negligible affect were identified. It was found that parameters such as effective outlet valve diameter, heat transfer coefficients of the wall and time constant for thermal sensor were the most predominant parameters while wall thermal conductivity and wall volumetric heat capacity were of low sensitivity for thermal modelling simulations.

A nonlinear regression routine was used to fit the model and the decanting data. The pressure and temperature data were simultaneously fit by minimizing the sum of square error between model temperature, model pressure and experimental temperature and experimental pressure. As the model is nonlinear in parameters, a starting value was required for each parameter.

The starting values were improved by fitting one parameter at a time, then as the values improved multiple parameters were fit at the same time. But for the final multiple-parameter fitting, only the most important parameters (mentioned above) were simultaneously fit.

It was found that there was an error of ±2Kelvin for temperature, also there were some negative errors during the start of decanting, some positive errors towards the end of decanting process which suggested that the model might not contain all the physical effects present in the experiment.

2.3 Fast Filling at CNG refueling stations

Considerable amount of research has been done on studying refueling of Natural Gas Vehicles(NGVs) at refueling stations. NGVs are alternate fuel vehicles that use CNG or LNG as a cleaner alternative to other fossil fuels. Natural gas vehicles connect to the high pressure reservoir tanks at refueling stations during filling process. The major problems with NGVs were found to be the large filling time, high operation costs. An urging need to develop a simulation to optimize the refueling process was identified and thus many research papers were published by different researchers addressing different problems faced and their suggested solutions. Some of those will be briefly discussed in the following paragraphs:

A research study carried out by (Khamforoush, et al., 2015) on the behavior of compressed natural gas in NGVs during fast fill process (FFP) found that the main reason for low driving range of NGVs lies behind the under-filling phenomenon which occurs during FFP in CNG stations. Analysis was carried on two kinds of fuel supply tanks, namely single gas supply tank(SSS) and cascade gas supply tank(CSS). FFP was modeled based on mass conservation law together with the first law of thermodynamics. During FFP the gas temperature within NGVs increased by 45K. This temperature rise stops the charging process before the cylinder be really fulfilled, and consequently reducing the driving range. In this even the cylinder wall temperature was simulated using the lumped system method.

It was also found that even though SSS tanks provided an advantage of low refuel time and high filling ratio, CSS tanks were preferred because of their lower energy consumption (i.e. energy used by compressor and cooler) for refueling.

A similar research as above was carried by (Javad Khadem, 2015) for mathematically modeling fast filling process at CNG refueling stations. The thermodynamic model developed was based on transient flow of ideal gas from high pressure reservoir tanks to an on-board NGV cylinder through the pipe and convergent nozzle. In this model the connecting pipes and nozzle were also modelled congruently with the tanks rather than replacing them with an orifice in the thermal model as done by previous studies. It was identified that the difference in final temperatures of the gas in both buffer and cascade storage system were because of the use of ideal gas model and also due to lack of Joule-Thompson cooling effect during filling. It was also found that the initial reservoir temperature had an effect on pressure variations within the onboard cylinder.

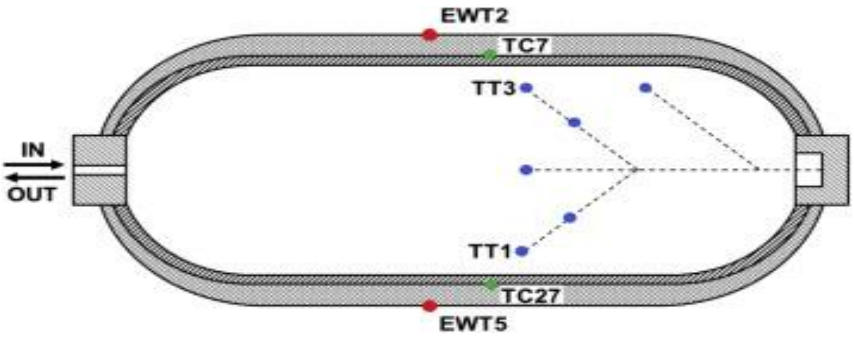

Figure 2-1: Approximate position of the selected tank thermocouples

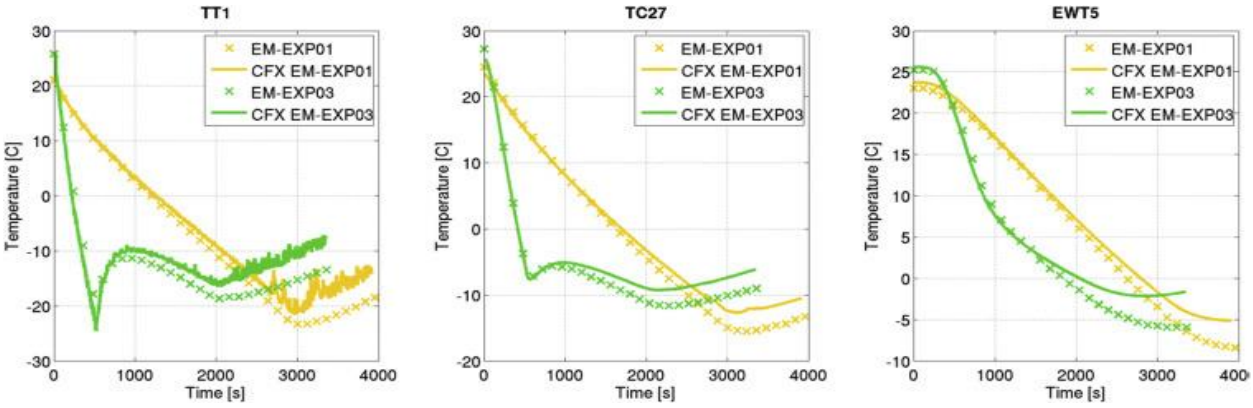

Figure 2-2: Comparison of simulation results and experimental data for the two types of emptying

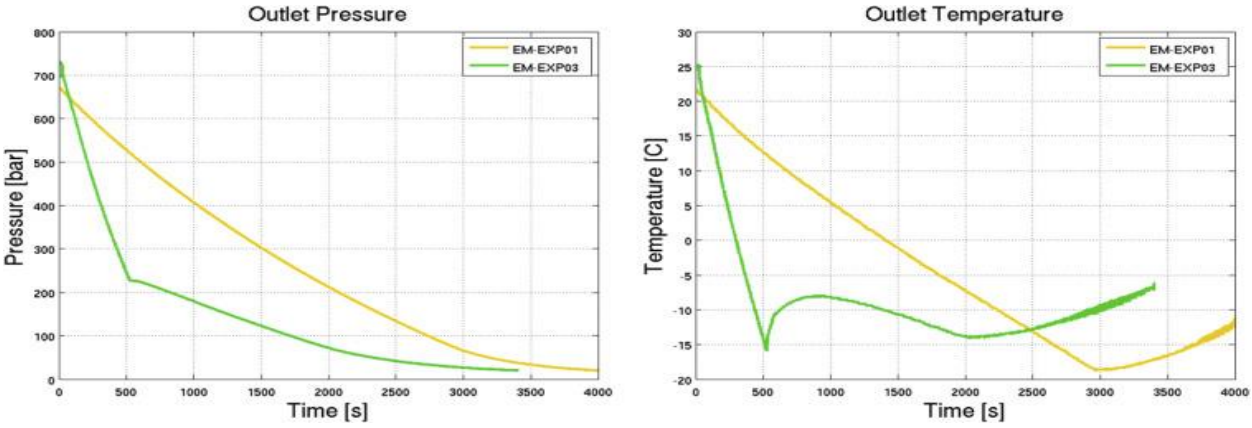

Figure 2-3: Pressure and Temperature profile at the tank inlet for the two emptying tests

Chapter 3 : Mathematical Formulation

GFSSP

GFSSP stands for Generalized Fluid System Simulation Program developed at Marshall Space Flight Center for flow analysis of Rocket Engine Turbo Pump and Propulsion System. GFSSP was initially developed by NASA/Marshall Space Flight Center for analyzing steady state and time dependent flow rate, pressure, temperature and concentrations in a complex flow networks but as its potential was realized its applications got numerous and the program was enhanced to be capable of modelling compressibility, mixture thermodynamics, and external body forces such as gravity and centrifugal (A.K. Majumdar, 2013). It provides an alternative to three dimensional Navier-Stokes computational fluid dynamic (CFD) analysis by constructing a fluid network consisting of a group of flow branches, such as pipes and ducts that are joined together at a number of nodes. The flow network can range from simple system consisting of few nodes and branches to a very complex network containing many flow branches simulating valves, orifices, bends, pumps and turbines.

The analysis of thermo-fluid dynamics in a complex network requires resolution of the system into fluid nodes and branches, solid nodes and conductors. Pressure, temperature, species concentration and residual mass in control volume are calculated at the internal/fluid nodes whereas the flow rate is calculated at branches. Fluid nodes can be either internal nodes where properties are calculated or boundary nodes where properties are specified. Temperatures are calculated at solid nodes and internal nodes but is specified at the boundary node. GFSSSP makes use of conservation of mass and energy equations at internal nodes and branches to calculate fluid properties. For calculating the temperatures at solid nodes GFSSP solves energy equation. The equations are non-linear, coupled and are solved by an iterative numerical scheme.

GFSSP employs a unique numerical scheme known as Simultaneous Adjustment with Successive Substitution (SASS) which is a combination of Newton Raphson and Successive Substitution methods. The mass and momentum conservation equations in GFSSP are solved by Newton Raphson method while the energy and species conservation equations are solved by successive substitution method.

GFSSP provides the table below specifying the type of equation solved to get a respective property.

Table 3-A: Summary of equation solvability in GFSSP

Sl.no	The Unknown variable to be calculated	Available Equations to Solve
1.	Pressure	Mass Conservation Equation
2.	Flowrate	Momentum Conservation Equation
3.	Fluid Temperature	Energy Conservation Equation of Fluid
4.	Solid Temperature	Energy Conservation Equation of Solid
5.	Species Concentrations	Conservation Equation for Species
6.	Fluid Mass (Unsteady Flow)	Thermodynamic Equation of State

3.1.1 Mass Conservation Equation

$$\frac{m_{\tau+\Delta\tau} - m_{\tau}}{\Delta\tau} = -\sum_{j=1}^{j=n} m_{ij}$$

The above requires that for the unsteady formulation, the net mass flow from a given node must equate to the rate of change of mass in the control volume.

3.1.2 Momentum Conservation Equation

The flow rate in a branch is calculated from the momentum conservation equation which represents the balance of fluid forces acting on a given branch. GFSSP momentum conservation equation has a source term S additional to inertia, pressure, gravity, friction and centrifugal forces. This source term has been provided to input pump characteristics or to input power to the pump in a given branch. The source term is set to zero in all the branches without a pump or other external momentum source.

$$\frac{(mu)_{\tau+\Delta\tau} - (mu)_{\tau}}{g_c \Delta\tau} + MAX|m_{ij}, 0|(u_{ij} - u_u) - MAX|-m_{ij}, 0|(u_{ij} - u_u)$$

------Unsteady----- ----------Longitudinal Inertia----------

$$+MAX|\dot{m}_{trans}, 0|(u_{ij} - u_p) - MAX|-\dot{m}_{trans}, 0|(u_{ij} - u_p) =$$

----------Transverse Inertia----------

$$(p_i - p_j)A_{ij} + \frac{\rho g v Cos\theta}{g_c} - K_f \dot{m}_{ij}|\dot{m}_{ij}|A_{ij} + \frac{\rho K_{rot}^2 \omega^2 A}{g_c} + \mu \frac{u_p - u_{ij}}{g_c \delta_{ij,p}} A_s$$

--Pressure-- --Gravity-- --Friction-- --Centrifugal-- --Shear--

$$-\rho A_{norm} u_{norm} \frac{u_{ij}}{g_c} + \left(\mu_d \frac{u_d - u_{ij}}{\delta_{ij,d}} - \mu_u \frac{u_{ij} - u_u}{\delta_{ij,u}}\right) \frac{A_{ij}}{g_c} + S$$

--Moving Boundary-- --Normal Stress-- --Source--

The left side of the momentum equation represents the inertia of the fluid. On the other hand the right side of the equation consists of surface and body forces applied in the control volume. The above equation has eleven terms and there haven't been an occasion recorded where all the eleven terms are active. Users has the ability to include or exclude most of the terms except the pressure term. The pressure term will be active under all the circumstances.

GFSSP also incorporates a simplified momentum equation to compute the flowrate for a compressible flow in an orifice. For the ratio of downstream pressure to upstream pressure:

$$\frac{p_j}{p_i} < p_{cr} ,$$

Where:

$$p_{cr} = \left(\frac{2}{\gamma + 1}\right)^{\frac{\gamma}{\gamma-1}} ,$$

The flowrate in a branch is calculated from:

$$\dot{m}_{ij} = C_{L_{ij}} A \sqrt{p_i \rho_i g_c \frac{2\gamma}{\gamma - 1} (p_{cr})^{\frac{2}{\gamma}} \left[1 - (p_{cr})^{\frac{(\gamma-1)}{\gamma}}\right]}$$

If $\frac{p_j}{p_i} > p_{cr}$ the flowrate in a branch is calculated from:

$$\dot{m}_{ij} = C_{L_{ij}} A \sqrt{p_i \rho_i g_c \frac{2\gamma}{\gamma - 1} \left(\frac{p_j}{p_i}\right)^{\frac{2}{\gamma}} \left[1 - \left(\frac{p_j}{p_i}\right)^{\frac{(\gamma-1)}{\gamma}}\right]}$$

It should be noted that this is special form of momentum equation and no other terms in this equation can be activated when the compressible orifice equation is in use.

3.1.3 Energy Conservation Equation

The energy conservation equation is solved at both the internal fluid nodes and solid nodes to find the temperature at the respective nodal points. For all the ideal gases the equation of state is used to solve for different variables but for real gases energy conservation equation is solved which may or may not include heat transfer phenomenon in conjunction. For conjugate heat transfer, the energy conservation equation for solids is solved along with the energy equation for fluid nodes.

3.1.3-1 Energy Conservation Equation of Single Fluid

Following first or second law of thermodynamics the energy conservation equation for any node i can be written based on two formulations. The first law formulation uses enthalpy as the dependent variable whereas the second law formulation uses entropy as its dependent variable.

The energy conservation equation based on enthalpy formulation is as follows:

$$\frac{\mathrm{m}\left(\mathrm{h}-\frac{\mathrm{p}}{\rho \mathrm{J}}\right)_{\tau+\Delta\tau}-\mathrm{m}\left(\mathrm{h}-\frac{\mathrm{p}}{\rho \mathrm{J}}\right)_{\tau}}{\Delta\tau}$$

$$=\sum_{\mathrm{j}=1}^{\mathrm{j}=\mathrm{n}}\left\{\mathrm{MAX}\left[-\dot{\mathrm{m}}_{\mathrm{ij}},0\right]\mathrm{h}_{\mathrm{j}}-\mathrm{MAX}\left[\dot{\mathrm{m}}_{\mathrm{ij}},0\right]\mathrm{h}_{\mathrm{i}}\right\}+\frac{\mathrm{MAX}\left[-\dot{\mathrm{m}}_{\mathrm{ij}},0\right]}{\left|\dot{\mathrm{m}}_{\mathrm{ıj}}\right|}\left[\left(\mathrm{p}_{\mathrm{i}}-\mathrm{p}_{\mathrm{j}}\right)\right.$$

$$\left.+\mathrm{K}_{\mathrm{ij}}\dot{\mathrm{m}}_{\mathrm{ij}}^{2}\right]\left(\vartheta_{\mathrm{ij}}\mathrm{A}\right)+\mathrm{Q}_{\mathrm{i}}$$

Equation above shows that for transient flow, the rate of increase of internal energy in the control volume is equal to the rate of energy transport into the control volume minus the rate of energy transport from the control volume plus the rate of work done on the fluid by the pressure force plus the rate of work done on the fluid by the viscous force plus the rate of heat transfer into the control volume. The term $\left[\left(\mathrm{p}_{\mathrm{i}}-\mathrm{p}_{\mathrm{j}}\right)+\mathrm{K}_{\mathrm{ij}}\dot{\mathrm{m}}_{\mathrm{ij}}^{2}\right]\left(\vartheta_{\mathrm{ij}}\mathrm{A}\right)$ represents the work input to the fluid due to rotation or pump and viscous work in the upstream branch of node i, where ϑ_{ij} and $A_{ij}$are velocity and area of the upstream branch.

In Navier-Stokes equations the MAX operator has been extensively used for upward differencing scheme in convective heat transfer and fluid flow applications. When the flow direction in not known firsthand, this operator allows the transport of energy from its upstream neighbor.

The conservation of energy equation based on entropy formulation is as follows:

$$\frac{(ms)_{\tau+\Delta\tau}-(ms)_{\tau}}{\Delta\tau}=\sum_{j=1}^{j=n}\{MAX[-\dot{m}_{ij},0]s_j-MAX[\dot{m}_{ij},0]s_i\}+\sum_{j=1}^{j=n}\left\{\frac{MAX[-\dot{m}_{ij},0]}{|\dot{m}_{ij}|}\right\}\dot{s}_{ij,gen}+\frac{Q_i}{T_i}$$

Equation above shows that for unsteady flow, the rate of increase of entropy in the control volume is equal to the rate of entropy transport into the control volume plus the rate of entropy generation in all upstream branches due to fluid friction plus the rate of entropy added to the control volume due to heat transfer. The first term in the right hand side of the equation represents the convective transport of entropy from neighboring nodes. The second term represents the rate of entropy generation in branches connected to the i^{th} node. The third term represents entropy change due to heat transfer.

The rate of entropy generation in a branch due to fluid friction is expressed as

$$\dot{S}_{ij,gen}=\frac{\dot{m}_{ij}\,\Delta p_{ij,viscous}}{\rho_u T_u J}=\frac{K_f\left(|\dot{m}_{ij}|\right)^3}{\rho_u T_u J}$$

3.1.3-2 Energy Conservation Equation of Fluid Species

In GFSSP, modelling of fluid mixtures requires the use of energy conservation equations for fluid species. It assumes the mixture to homogeneous, thus the mass and momentum equations are similar to those of single fluid. GFSSP allows modelling of mixtures in three different ways to calculate the temperature and its thermo-physical properties. The first two options referred to as temperature option and enthalpy-1 option, can be used for a mixture of gas/liquid as long as there is no phase change involved the process.

But if there is an expected phase change involved in the process then the option three has to be chosen which is referred to as enthalpy-2 option. In all the mentioned options the conservation of fluid species equation is solved and they differ only in the way energy equations are handled.

The energy equation is solved in terms of temperature for the first option which is referred as temperature option. For the second option referred as enthalpy-1 option, enthalpies of fluid species are used to calculate mixture enthalpy for the energy conservation equation and temperature is calculated by an iterative method from mixture enthalpy equation. The option three which is referred as enthalpy option-2 handles a mixture of liquid and gas where the liquid or gas may go through a phase change. In this option separate energy equations for each species are solved and the temperature of the mixture is calculated by averaging the thermal mass (product of mass and specific heat) of all the components. It should be noted that work input and viscous work would be neglected in the species energy equation.

In the present study only one of the above mentioned options was used which is the enthalpy-2 option to model phase change in the mixture. In this option the energy equation for individual species, k, can be expressed as follows:

$$\frac{\left(m_i h_{ik} - \frac{p}{\rho_k J}\right)_{\tau+\Delta\tau} - \left(m_i h_{ik} - \frac{p}{\rho_k J}\right)_{\tau}}{\Delta\tau} = \sum_{j=1}^{j=n} \left\{ MAX\left[-\dot{m}_{ij}, 0\right] h_{jk} - MAX\left[\dot{m}_{ij}, 0\right] h_{ik} \right\} + \dot{Q}_{ik}$$

The external heat source term is expressed as:

$$\dot{Q}_{ik} = \overline{C_{ik}} \dot{Q_i},$$

Where, $\dot{Q}_i$=External Heat Source (i.e. Heat from Solid node etc.), and

$\overline{C_{ik}}$ = Molar concentration of Kth species in the ith node.

3.1.3-3 Energy Conservation Equation of Solid Node

The solid node can typically be connected to other solid nodes, ambient node and fluid node with a respective conductor option. The energy conservation equation for solid node i can be expressed as follows:

$$\frac{\partial}{\partial \tau}\left(mC_p T_s^i\right) = \sum_{j_s-1}^{n_{ss}} \dot{q_{ss}} + \sum_{j_f-1}^{n_{sf}} \dot{q_{sf}} + \sum_{j_a-1}^{n_{sa}} \dot{q_{sa}} + \dot{S_ı}$$

The above equation shows that rate of change of temperature of solid node i, is equal to the heat transfer from the neighboring node and heat source or sink.

$$\dot{q_{ss}} = k_{ij_s} A_{ij_s} / \delta_{ij_s} \left(T_s^{j_s} - T_s^i\right)$$

$$\dot{q_{sf}} = h_{ij_f} A_{ij_f} \left(T_f^{j_f} - T_s^i\right)$$

$$\dot{q_{sa}} = h_{ij_a} A_{ij_a} \left(T_a^{j_a} - T_s^i\right)$$

The effective heat transfer coefficients for solid to ambient nodes and solid to fluid nodes are expressed as the sum of the convection and radiation:

$$h_{ij_f} = h_{c,ij_f} + h_{r,ij_f}$$

$$h_{ij_a} = h_{c,ij_a} + h_{r,ij_a}$$

$$h_{r,ij_f} = \frac{\sigma\left[\left(T_f^{j_f}\right)^2 + \left(T_s^i\right)^2\right]\left[T_f^{j_f} + T_s^i\right]}{\frac{1}{\varepsilon_{ij,f}} + \frac{1}{\varepsilon_{ij,f}} - 1}$$

$$h_{r,ij_a} = \frac{\sigma\left[\left(T_a^{j_a}\right)^2 + \left(T_s^i\right)^2\right]\left[T_a^{j_a} + T_s^i\right]}{\frac{1}{\varepsilon_{ij,a}} + \frac{1}{\varepsilon_{ij,s}} - 1}$$

In GFSSP there are four different ways of specifying heat transfer coefficient:

1. User can specify heat transfer coefficient values during the beginning of the analysis
2. GFSSP allows the use of Dittus-Boelter equation for single phase flow where Nusselt number is expressed as follows:

$$\frac{h_c D}{k_f} = 0.023(\mathrm{Re})^{0.8}(\mathrm{Pr})^{0.33}$$

Where $\mathrm{Re} = \frac{\rho u D}{\mu_f}$ and $\mathrm{Pr} = \frac{C_p \mu_f}{k_f}$

3. For the two phase flows modified Miropolsky's correlation is used which is as follows:

$$\mathrm{Nu} = 0.023(\mathrm{Re}_{mix})^{0.8}(\mathrm{Pr}_v)^{0.4}(Y)$$

$$\mathrm{Re}_{mix} = \left(\frac{\rho u D}{\mu_f}\right)\left[x + \left(\frac{\rho_v}{\rho_l}\right)(1-x)\right]$$

$$\mathrm{Pr}_v = \frac{C_p \mu_v}{k_v}$$

$$Y = 1 - 0.1\left(\frac{\rho_l}{\rho_v} - 1\right)^{0.4}(1-x)^{0.4}$$

4. If the has defined a new subroutine rather using the ones provided in the GFSSP data base then GFSSP allows the user to define a new correlation to be used in conjunction with the energy equation for the solid node (mentioned above) to find the temperature of the solid node. The equation for T_s^i would be as follows:

$$T_s^i = \frac{\sum_{j_{s-1}}^{n_{ss}} C_{ij_s} T_s^{j_s} + \sum_{j_{f-1}}^{n_{sf}} C_{ij_f} T_f^{j_f} + \sum_{j_{a-1}}^{n_{sa}} C_{ij_a} T_a^{j_a} + \frac{(mC_p)_m}{\Delta\tau} T_{s,m}^i + \dot{S}}{\frac{mC_p}{\Delta\tau} + \sum_{j_{s-1}}^{n_{ss}} C_{ij_s} + \sum_{j_{f-1}}^{n_{sf}} C_{ij_f} + \sum_{j_{a-1}}^{n_{sa}} C_{ij_a}}$$

3.1.3-4 Fluid Species Conservation Equation

In the present study on Biogas tank decanting, the molar concentration of individual species is specified during the start of the analysis and this stays constant throughout the study. The density of the mixture will be a function of concentrations of individual species. The concentration for any species k can be written as follows:

$$\frac{\left(m_i C_{i,k}\right)_{\tau+\Delta\tau} - \left(m_i C_{i,k}\right)_{\tau}}{\Delta\tau} = \sum_{j=1}^{j=n} \left\{ MAX\left[-\dot{m}_{ij}, 0\right] C_{j,k} - MAX\left[\dot{m}_{ij}, 0\right] C_{i,k} \right\} + \dot{S}_{i,k}$$

Mixture property calculations:

In order to calculate the properties of the mixture at i^{th} node GFSSP makes use of the nodal pressure p_i and molar concentration x_k. We have to calculate the density, ρ_i, temperature, T_i, specific heat, C_p, specific heat ratio, Υ, and viscosity, μ, of the mixture at the i^{th} node.

As mentioned earlier we have suggested the use of enthalpy-2 option for calculating the properties of fluid species in a mixture as this option allows us to model phase change. Temperature of the mixture and individual properties of the species are calculated from nodal pressures and enthalpy of the species:

$$T_{ik} = f(p_i, h_{ik})$$

$$\rho_{ik} = f(p_i, h_{ik})$$

$$\mu_{ik} = f(p_i, h_{ik})$$

$$K_{ik} = f(p_i, h_{ik})$$

$$C_{p_{ik}} = f(p_i, h_{ik})$$

To calculate the nodal properties in the network averaging of the properties of species is incorporated which is done as follows:

$$\mu_i = \sum_{k=1}^{k=n} \overline{x_k}\, \mu_k$$

$$C_{p,i} = \frac{\sum_{k=1}^{k=n} C_{p,k} \overline{x_k}\, M_k}{\sum_{k=1}^{k=n} \overline{x_k} M_k}$$

$$\gamma_i = \sum_{k=1}^{k=n} \overline{x_k}\, \gamma_k$$

After calculating the above properties, the temperature of the node is calculated as follows:

$$T_i = \frac{\sum_{k=1}^{n_f} \overline{c_{ik}} C_{p_{ik}}\, T_{ik}}{C_{p_i}}$$

Chapter 4 : Results for Methane Tank Decanting

This chapter is devoted in studying Methane tank decanting under different system initial conditions and at different decanting rates. The analysis was carried in GFSSP and the liquefaction of Methane during decanting was predicted by plotting pressure-temperature of the Methane during decanting against the saturation curve of Methane.

Below is the general Schematic for the fuel tank which is made of three important parts: high density polyethylene liner, the carbon epoxy fiber wrapping and the flow regulator. The composite tank wall will be divided into 10 solid nodes in GFSSP details of which will be explained in the coming paragraphs.

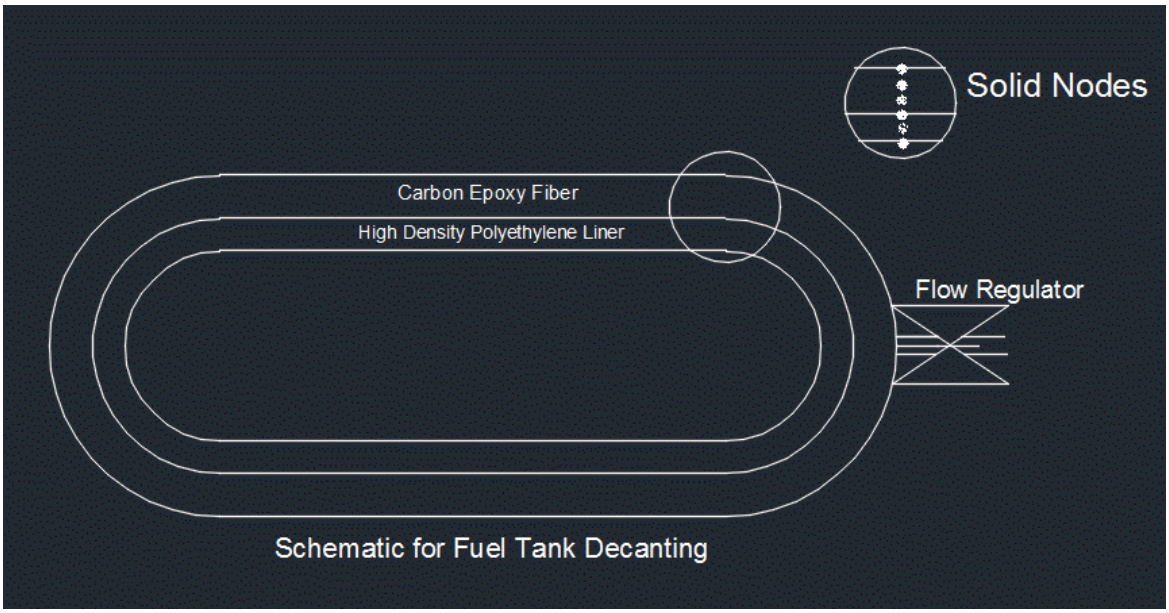

Figure 4-1 shows the GFSSP flow network for Methane tank decanting. It consists of 1 ambient node, 10 solid nodes, 1 boundary node, 1 internal node and 1 compressible orifice all connected with each other with respective conductors. The ambient node represents the external atmosphere where the user is required to specify the temperature of the surroundings.

The ambient node is followed by 10 solid nodes (elements numbered 2-11) which represents the tank wall thickness and the weight of the tank wall is equally divided in these 10 solid nodes. The choice of number of solid nodes has no significant effect on the overall simulation and 10 solid nodes were chosen to simplify the division of weight and also if two different materials were chosen to build the cylinder wall, even number of nodes would better divide the overall thickness of wall in equal intervals. The ambient node and the solid node are connected by a fluid-solid conductor where the user has to specify the surface area of contact between the two nodes and their heat transfer coefficient. Solid nodes represent the tank wall so the user has to define its thermal properties like thermal conductivity and specific heat values (**Table 4-A** below) at different ranges of temperature in the back ground of the program. The values for required temperature are then interpolated by using the data provided in the program background. The user also has to specify the temperature, mass and also the material to be used for wall thermal properties. The material can be chosen from the list of material data base provided with GFSSP or it can be specified by the user as explained above. The two solid nodes are connected by solid-solid conductor where the user has to specify the surface area of the conductor and distance between the two solid nodes.

After the tank wall has been specified by all the 10 solid nodes, the next element in the flow network represents the inner volume of the Methane tank called as the interior node (element numbered 12). The interior node represents the inner volume of the Methane tank and its thermodynamic states during the start as well as during the tank decanting. The solid node and the interior node are connected by convection fluid-solid conductor where the user has to input its surface area and heat transfer coefficient values. The interior node is the place where Methane properties are simulated during decanting. The interior node is given an initial pressure, temperature and volume for the fluid selected from the list of fluids provided in the GFSSP data base.

The fluid in the interior node is decanted through a compressible orifice (element labelled 1213) which is one of the component offered in the GFSSP data base. The compressible orifice is made to act as a flow regulator, where for present simulations the flow rate through the orifice is fixed and the area of the orifice is allowed to vary to attain the required flow rate as the pressure in the interior node decreases as time progresses. The initial and allowed range of areas for the compressible orifice are given as initial input to the system. Also, user is required to specify the flow coefficient for the compressible orifice (typically the flow coefficient is taken to be '1' and for all the simulations presented in this study this remains constant). As the fluid flows through the compressible orifice it is rejected to a boundary node (element numbered 13). The boundary node is pseudo representation of surroundings as it does not have any thermal effect on simulations to be carried in compressible orifice or interior node. As we know any flow of fluid requires pressure difference and for this boundary node is set to atmospheric pressure to allow a well-defined pressure difference between interior node and boundary node for fluid flow through compressible orifice.

Table 4-A below indicates the values of different variable used in defining the flow simulation model in GFSSP. The values defined are kept constant throughout the study of Methane tank decanting and also serves as a standard for comparing different decanting conditions.

Table 4-A: Input values to GFSSP used in all the simulations

Sl.no	Property	Value defined
1.	Specific heat of tank wall material (Carbon epoxy fiber)	850 J/Kg-K
2.	Thermal conductivity	10.46 W/m-K
3.	Weight of the tank	2268 kg
4.	Inner surface area of the tank	32.7 m^2
5.	External surface area of the tank	36.1671 m^2
6.	Tank interior heat transfer coefficient (Cole, June 12, 2015)	19.33 W/m^2/K
7.	Tank exterior heat transfer coefficient (Cole, June 12, 2015)	10 W/m^2/K
8.	Volume of the tank	8.5m^3

Figure 4-2 shows saturation curve for Methane with temperature on X-axis and pressure on Y-axis. The saturation line separates liquid phase of Methane with its vapor counterpart. The critical temperature of Methane is -82.59°C which means below this temperature the gaseous Methane starts to condense and forms liquid Methane. Also critical pressure of Methane is 4599kPa which means that a minimum pressure of 4599kPa would be required at critical temperature to convert Methane into liquid form completely. Any pressure below the critical pressure at below critical temperatures would partially convert the Methane in liquid form and thus resulting in Methane vapor formation. The saturation curve data was obtained using REFPROP (Reference Fluid Thermodynamic and Transport Properties Database) which is a program developed by NIST (National Institute of Standards and Technology) (Eric W. Lemmon, 2007). It calculates the thermodynamic and transport properties of industrially important fluids and their mixtures. REFPROP is based on the most accurate pure fluid and mixture models currently available. It implements three models for the thermodynamic properties of pure fluids: equations of state explicit in Helmholtz energy, the modified Benedict-Webb-Rubin equation of state, and an extended corresponding states (ECS) model. Mixture calculations employ a model that applies mixing rules to the Helmholtz energy of the mixture components; it uses a departure function to account for the departure from ideal mixing. Viscosity and thermal conductivity are modeled with either fluid-specific correlations, an ECS method, or in some cases the friction theory method.

4.1 Decanting Flow Rate Selected is 0.064kg/s

Figure 4-3, Figure 4-4 shows the pressure and temperature histories for tank decanting respectively, for which the valve closed after reaching a preset safe pressure. The starting conditions for **Figure 4-3** are full tank at 218.2 bar and 0°C decanted at 0.064kg/s. The valve closes after 24927 seconds when the tank reaches the safe operating pressure of 14bar. As it is observed the minimum temperature of the Methane in decanting was -42.1°C when the pressure in the tank was 47.3bar which is 19909 seconds after the decanting has started. Methane is still in gaseous phase in these conditions.

Figure 4-5 shows the comparison of Pressure-Temperature (P-T) curve for Methane tank decanting with the saturation curve of Methane under the decanting conditions mentioned above. As it can be seen from the **Figure 4-5** that the temperature of the Methane in the tank never fell below the critical temperature and hence there is no possibility of liquid Methane formation within the tank in the specified decanting conditions.

Figure 4-6 shows the temperature histories for tank wall temperature where TS2 curve represent temperature values for the solid node (element #2) closest to ambient surroundings and representing the exterior surface of the tank and TS11 temperature curve for solid node (element #11) representing interior surface of the tank wall. The cylinder pressure is not allowed to go below 14 bar in order to ensure the stability of the cylinder liner and this is the reason to stop the analysis at 14bar. It has been seen from above mentioned graphs that favorable conditions for liquid Methane formation were not developed within the cylinder which might have damaged the cylinder liner. Also as can be seen there is considerable temperature difference between the two solid node temperatures which is expected. The solid node (element #11) which is in contact with the interior node (element #12) would cool more effectively than the solid node (element #2) which is in contact with ambient surroundings.

Figure 4-7 draws a comparison between the fluid and wall temperature when decanting was done at a flow rate of 0.064kg/s with initial system temperature, pressure of 0°C, 218.2 bar respectively. It is observed that even though the fluid and tank wall starts at the same temperature before decanting, the temperature of the fluid falls more rapidly than the wall temperature. The cooling in the tank is partially explained by an effect called the Joule-Thomson effect or Joule-Kelvin effect. As the gas in the tank expands during the decanting process it does positive work and thus its temperature decreases. The initial temperature of the system i.e. the fluid and wall temperature are same but the high specific heat and mass of the wall does not allow it to get as cold as the fluid it is in contact. As a result, the wall pumps heat into the tank and the temperature of the fluid recorded is more than the temperature we would observe if the process was an adiabatic expansion carried in a tank with insulated interior surface. Also the temperature of the tank wall eventually falls as it loses its heat to the fluid within the tank.

Figure 4-8, Figure 4-9 shows the pressure and temperature histories for tank decanting when the tank is full at 112.3bar and initial system temperature of -50°C at a decanting rate of 0.064kg/s. It takes about 24344 seconds for the tank pressure to reach 14 bar. But before the tank has reached to 14 bar it is observed that at about 42.6 bar i.e. 15353 seconds after the decanting has started, the Methane in the tank has reached its critical temperature and undergone a phase transformation where a mixture of two phased Methane exists in the tank from that point onwards. After the tank has reached to 14bar the valve was closed but the simulations were continued for another 15656 seconds to study the behavior of the tank wall heating characteristics. It has been observed that even after the tank valve has been closed the wall continues to pump heat into the system and the temperature of the remaining Methane in the tank rises from -83.5°C to -54.8°C in 15656 seconds. Also during this period, the pressure of the system increases from 14bar to 16.7bar due to heating of Methane inside the tank by the tank walls.

Figure 4-10 shows the comparison of Pressure-Temperature curve for Methane tank decanting with the saturation curve of Methane under the decanting conditions mentioned above. As it can be seen from **Figure 4-10** that the temperature of the Methane in the tank falls below the critical temperature and gaseous Methane starts to condense and Methane vapors are formed in the tank. Though it can be seen that favorable conditions were not developed in the tank for liquid Methane formation, it is advised to stop the decanting at the point where Methane has crossed its critical temperature i.e. 15353 seconds after the start of decanting process.

Figure 4-11 shows the temperature histories for tank wall temperature under the initial conditions suggested above. It is observed that the minimum temperature of the tank wall was -72.3°C which happens 22848sec after the tank decanting has started. The tank liner would be in danger if the decanting is continued after the tank reaches 42.6 bar as two phased Methane exists at this point and this would induce additional thermal stresses in the tank wall.

Figure 4-12 draws a comparison between fluid and wall temperatures during decanting process. As it is observed the minimum temperatures of fluid and wall were -85°C and -72.3°C respectively. Also it can be seen that as the decanting has stopped the tank wall pumps heat into the tank and the temperature of Methane rises rapidly. The temperature of the tank wall also rises as it is taking heat from the surroundings but its temperatures does not rise as rapidly as that of Methane because the tank is not just taking in heat from the surroundings but also pumping a part of that heat into tank to heat Methane.

Figure 4-13 shows a cumulative pressure plot for different system initial conditions with a decanting flow rate of 0.064kg/s. In all the decanting iterations the final pressure was set to be 14bar and the decanting was stopped as the pressure in the tank reached 14bar.

Figure 4-14 shows a cumulative temperature plot for different system initial conditions with a decanting flow rate of 0.064kg/s. As it can be observed there is only instance when the temperature in the tank went below the critical temperature of Methane i.e. when the initial temperature of the system was -50°C. And also it can be seen from **Figure 4-10** that Methane never crosses the saturation line and thus stays in vapor phase once it crosses its critical temperature. The decanting process was safe in all the occasions when the decanting rate was 0.064kg/s as necessary conditions for Methane liquefaction were not formed within the tank. But as Methane reaches it critical temperature when the initial system temperature was -50°C it is advised to stop the decanting in this iteration at the critical point in order to protect the tank liner material from experiencing any other additional thermal stress.

4.2 Decanting Flow Rate Selected is 0.11975kg/s

Figure 4-15, Figure 4-16 shows the pressure and temperature histories for tank decanting with starting conditions of full tank at 154.5 bar and initial system temperature of -30°C and flow rate of 0.11975kg/s. It takes 13047s for the tank pressure to reach 14bar and the temperature in the tank does fall below critical temperature of Methane. Methane in the tank reaches its critical temperature 10715 seconds after the decanting has started when the pressure in the tank was 33.3bar. The minimum observed temperature in the tank is -84.2°C and it occurs 12451s after the decanting has started when the pressure in the tank is 20bar.

Figure 4-17 shows the comparison of Pressure-Temperature curve for Methane tank decanting with the saturation curve of Methane under the decanting conditions mentioned above. It is evident from the figure below that the temperature of Methane in the tank falls below its critical temperature but favorable conditions for liquid Methane formation are not developed within the tank. But it is advised to stop the decanting after 10715 seconds as Methane reaches its critical temperature and Methane vapor starts forming after this point.

Figure 4-18 shows the temperature histories for tank wall temperatures under the initial conditions suggested above. It is observed that the minimum temperature experienced by the tank wall is -62.9°C which happens 13047seconds after decanting has started and the pressure in the tank has reached the preset limit of 14bar.

As can be seen from **Figure 4-19** the minimum observed wall and fluid temperatures are -62.9°C and -84.2°C respectively. **Figure 4-20** shows the cumulative pressure histories for different tank decanting conditions with flow rate of 0.11975kg/s as summarized in **Table 4-B**.

Figure 4-21 shows a cumulative plot for temperature histories for different tank decanting conditions with flow rate of 0.11975kg/s. As can be seen most of the temperature plots seem linear with no sudden changes except the temperature plot with initial system temperature as -50°C. The behavior of this particular plot will be explained with a pressure-temperature vs saturation curve plot (**Figure 4-22**).

Figure 4-22 shows the Pressure-Temperature curve for Methane Vs saturation curve when the system initial temperature was -50°C at 112.3bar with decanting flow rate of 0.11975kg/s. As can be seen that the temperature of Methane falls below the critical temperature at about 5761 seconds after the decanting process has started when the pressure in the tank was 45.6bar. At this point the pressure in the tank is little less than the critical pressure of Methane and thus Methane vapor starts forming in the tank. As the decanting process is continued at about 6044 seconds after the decanting has started the pressure-temperature curve intersects the saturation curve and at this point liquid Methane is formed. If the decanting process is continued it is observed that the P-T curve traces the saturation curve until the pressure in the tank falls to 24.7bar. After this point the pressure in the tank is no longer sufficient to liquefy Methane and hence Methane vapors are formed in the tank until the pressure in tank goes to 14bar where the simulations are stopped as the tank pressure has reached a preset critical point. The two distinctive times where Methane liquefies and Methane vapors forms can be identified from the **Figure 4-21** as deviations in the temperature curve is observed.

4.3 Decanting Flowrate Selected is 0.3kg/s

Figure 4-23, Figure 4-24 shows pressure and temperature histories for tank decanting when the initial pressure in the tank was 218.2bar at 0°C with decanting rate of 0.3kg/s. It takes about 5188seconds for the tank pressure to reach 14bar. It is observed that the temperature of the Methane falls below the critical temperature and the minimum observed temperature in the tank was -89.6°C.

Figure 4-25 shows the comparison of Pressure-Temperature curve for Methane tank decanting with the saturation curve of Methane when the system initial temperature and pressure were 0°C and 218.2bar respectively at a decanting rate of 0.3kg/s. As it can be seen that the temperature in the tank falls below the critical point at about 4488 seconds after the decanting has started and at this point the pressure in the tank is about 30bar. The pressure in the tank is below the critical pressure of Methane i.e. 46bar and thus liquid Methane is not formed at this point but Methane is no more in gaseous phase rather Methane is in vapor phase and continues to be in vapor phase until the simulation is stopped at tank pressure of 14bar.

Figure 4-26 shows temperature histories for tank wall temperature under the decanting conditions mentioned above. As can be seen the minimum observed wall temperature is -41°C when the pressure in the tank was 14bar.

In **Figure 4-27** it can be observed that the minimum temperature of Methane was -89.6°C where the minimum temperature of wall is -41°C and both occur when the pressure in the tank was 14bar.

Figure 4-28, Figure 4-29 shows cumulative pressure and temperature plots for Methane tank decanting at different system initial temperatures and pressures at a decanting rate of 0.3kg/s. It can be observed that the pressure and temperature plots for starting conditions of -30°C, -40°C and -50°C shows some discrepancies. The Methane in the tank changes its phase in the above mentioned conditions and the details of which would be explained with the respective pressure-temperature and saturation curve plots.

Figure 4-30 shows the comparison of Pressure-Temperature curve for Methane tank decanting with the saturation curve of Methane when the system initial temperature and pressure were -30°C and 175.7bar respectively at a decanting rate of 0.3kg/s. It is observed that as the temperature in the tank goes below the critical temperature of Methane at about 2919seconds after the decanting has started but the pressure in the tank is below its critical pressure. Hence the Methane doesn't convert in liquid Methane at this point but vapor Methane is formed. As the decanting is continued favorable conditions are formed for liquid Methane formation at about 3211seconds after the decanting has started when the pressure in the tank is around 40bar. The liquid Methane continues to form until the pressure in the tank falls to 18bar where the pressure in the tank is no longer enough to liquefy Methane and thus Methane vapor starts forming until the pressure reaches the preset limit of 14bar.

Similarly, **Figure 4-31, Figure 4-32** shows the comparison of Pressure-Temperature curve for Methane tank decanting with the saturation curve of Methane when the system initial temperature and pressure were -40°C and 133.3bar, -50°C and 112.3bar respectively at a decanting rate of 0.3kg/s. As it can be seen in both the cases favorable conditions for liquid Methane formation are developed within the tank and the details of which are summarized in **Table 4-B**.

Table 4-B provides a summary of results obtained by GFSSP analysis for different tank decanting conditions. Flow rates of 0.064kg/s, 0.11975kg/s and 0.3 kg/s were selected for analyzing the tank decanting with initial system temperature varying from -50°C to 20°C in steps of 10°C. When the flow rate selected was 0.064kg/s it is observed that tank decanting to 14 bar was safe until the initial system temperature was down to -50°C when the Methane reaches its critical point where the gaseous phase, liquid phase exists in equilibrium.

When the flow rate of 0.11975 kg/s was chosen with the respective pressures and temperatures suggested in the **Table 4-B**. It was found that at many instances favorable conditions were developed for liquid Methane formation. The tank decanting has to be stopped before the critical pressure of 46 bar is reached in order to avoid liquid Methane formation.

When the flow rate was chosen to be 0.3kg/s it was found that in only one case where initial system temperatures was 20°C liquid Methane was not formed during Methane decanting. But in the rest of the cases liquid Methane was formed and tank decanting has to be stopped before the critical point of Methane is reached.

Table 4-B: Summary of results for Methane tank decanting at varying flow rates and different initial temperatures for the system.

Sl.no	Flow Rate (kg/s)	Initial Pressure during start of tank decanting (bar)	Initial Temp (°C)	Pressure corresponding to Min Temp (kPa) **(Min Pressure)**	Min Fluid Temp (°C) **(M)**	Time at Min Temp occurs (sec) **(I)**	Minimum observed Wall Temp(°**C)**	Time where phase transformation starts (Sec)	Pressure at which phase transformation occurs (kPa)	Time taken to empty the tank (Sec)
1.	0.064	250	20	5156.4	-24.4	19368	-8.3	None	none	24288
2.		250	10	5297.4	-4.0	20170	-18.1	None	none	25764
3.		218.2	0	4733.3	-42.1	19909	-26.8	None	none	24927
4.		197	-10	4361.8	-50.7	20096	-35.9	None	none	24860
5.		175.7	-20	4034.9	-59.3	20199	-45.0	None	none	24767
6.		154.5	-30	3704.5	-67.9	20327	-54.1	None	none	24662
7.		133.3	-40	3373.8	-76.5	20459	-63.2	None	none	24518
8.		112.3	-50	3042.9	-85.1	20620	-72.2	15353	4266.5	24344
9.	0.11975	250	20	2239.9	-43.4	12304	-18.8	None	none	12894
10.		250	10	2525.5	-52.7	12810	-28.7	None	none	13673
11.		218.2	0	2281.3	-60.1	12513	-36.8	None	none	13220
12.		197	-10	2198.2	-68.1	12491	-45.5	None	none	13176
13.		175.7	-20	2092.8	-76.1	12477	-54.2	None	none	13116
14.		154.5	-30	1995.1	-84.2	12451	-62.9	10715	3326.2	13047
15.		133.3	-40	1888.0	-92.2	12418	-71.5	7858	4339.7	12954
16.		112.3	-50	2469.9	-101.5	11183	-79.9	5761	4558.0	12842
17.	0.3	250	20	1402.4	-74.7	5073	-23.1	None	none	5073
18.		250	10	1401.2	-83.7	5374	-33.6	5218	1817.9	5374
19.		218.2	0	1400.9	-89.6	5188	-41.0	4488	2996.2	5188
20.		197	-10	1400.8	-96.6	5161	-49.3	3497	3745.9	5161
21.		175.7	-20	1401.2	-103.4	5125	-57.6	3428	4185.8	5125
22.		154.5	-30	1401.1	-111.2	5075	-65.3	2919	4427.1	5075
23.		133.3	-40	1401.1	-116.4	4995	-71.1	2402	4545.4	4995
24.		112.3	-50	1400.7	-116.4	4922	-76.5	1869	4591.0	4922

4.4 Chapter Conclusions

Throughout **Chapter 4** efforts were made to identify the point where phase transformation of Methane is observed and **Table 4-B** summarizes the technical findings. It was observed that, at many instances the temperature of Methane went below the critical temperature, out of which tank decanting even provided ideal pressure for Methane liquefaction. **Table 4-C** gives the overview of the fluid phase observed at the end of tank decanting under respective flow rates and corresponding system initial conditions. As the decanting flow rate is increased, the chances of Methane phase transformation increased. The reason behind this trend is that as more and more gas is emptied from the tank, the remainder of the gas present in the tank has more volume available to occupy and thus as it expands the gas is cooled. If the cooling effect is sufficient enough accompanied by the available pressure in the tank, the chances of liquefaction increases. Also as the decanting flow rate increases the tank wall doesn't have enough time to pump heat into the system and the balance between the cooling effect provided by gas expansion and heating effect provided by the wall is lost, resulting in Methane liquefaction.

As the system initial temperature is decreased the Methane in the tank has to cool relatively lower to reach the critical temperature of -82.59°C. With the decreasing initial temperature even the amount of heat the tank wall can supply decreases as the range of temperature difference between the tank wall and the fluid within decreases.

The provided results act as a guide line for the tank decanting industry to watch for the fluid liquefaction and take appropriate measures to avoid such circumstances. If the possibility of liquefaction is neglected, then life expectancy of the tank will decrease which would be a huge loss to the industry. Most importantly the safety of the personnel working around the tank during decanting is at risk as the possibility of liner failure and leaking provides risk for fire.

Methane being a greenhouse gas would even have an environmental effect and the climatic impact of Methane is considered to be more than 25 times higher than carbon dioxide. The possible solution to avoid liquefaction other than stopping the decanting process would be to reduce the decanting flow rate before the point where the possibility of liquefaction was observed through decanting simulations. By doing this we would provide additional time for the tank wall to pump enough heat into the system to avoid liquefaction. Another possible solution is by providing gradual heating to the tank walls during decanting so as such the tank wall can provide additional heat input to the fuel in the tank than it was capable without the heat input. But before doing this, proper thermodynamic calculations should be made so as that the heating provided doesn't add to the thermal stresses experienced by the tank walls.

Table 4-C: Final Phase of fluid after decanting to 14bar

System Initial Pressure (bar)	System Initial Temperature (°C)	Decanting Flow rate (Kg/s)		
		F1=0.064	F2=0.11975	F3=0.3
250	20	Gas	Gas	Gas
250	10	Gas	Gas	Vapor
218.2	0	Gas	Gas	Vapor
197	-10	Gas	Gas	Vapor
175.7	-20	Gas	Gas	Vapor
154.5	-30	Gas	Vapor	Liquid
133.3	-40	Gas	Vapor	Liquid
112.3	-50	Vapor	Liquid	Liquid

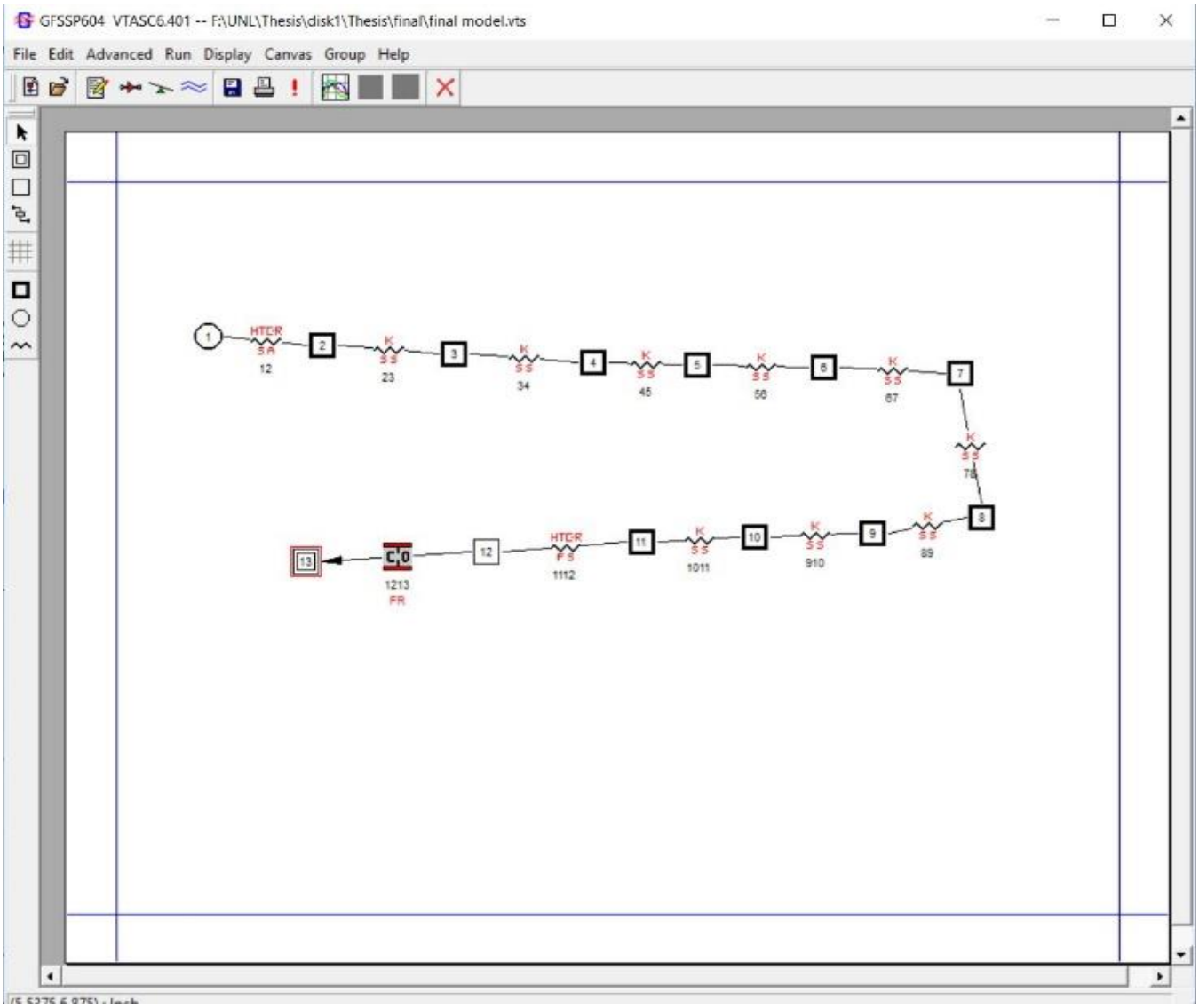

Figure 4-1: GFSSP Flow Network for Pressurized Tank Decanting consisting of one ambient node, ten solid nodes, one interior node, one boundary node, one flow regulator and respective connecting conductors.

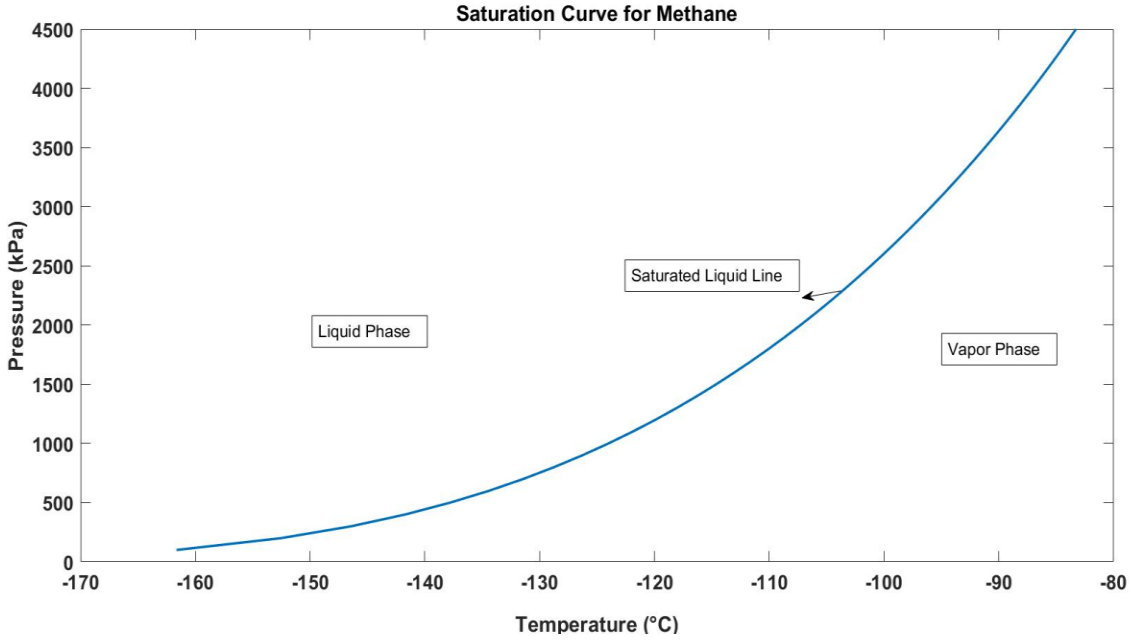

Figure 4-2: Saturation Curve for Methane

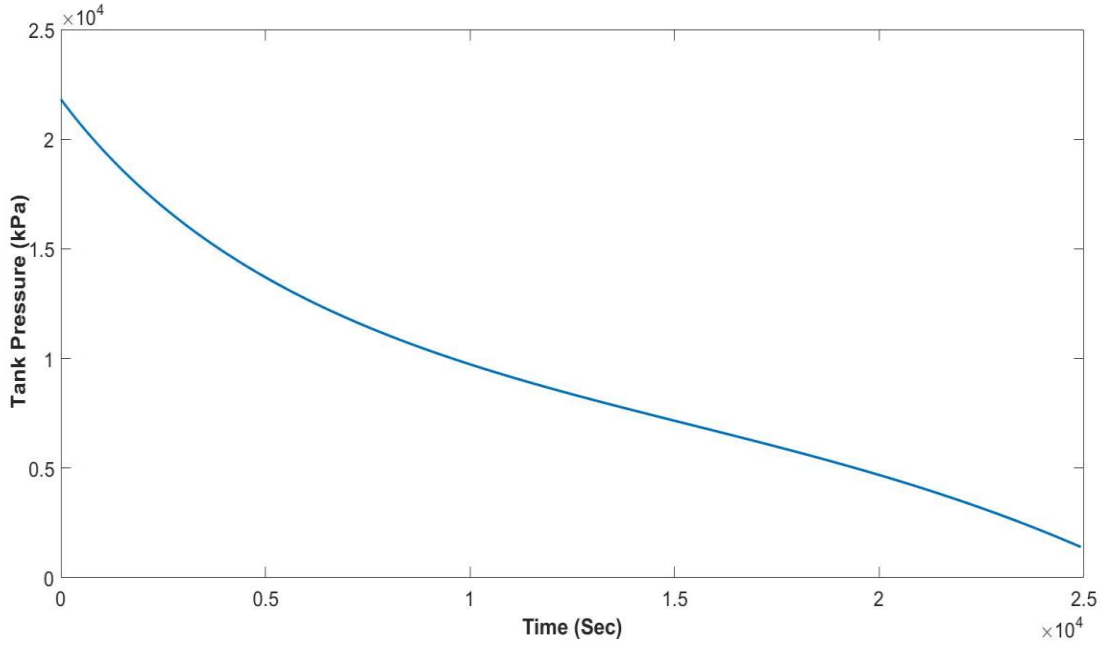

Figure 4-3: Tank Pressure Vs Time plot when the initial temperature of the system is 0°C and tank decanting rate is 0.064kg/s. Time taken to reach 14bar=24927s

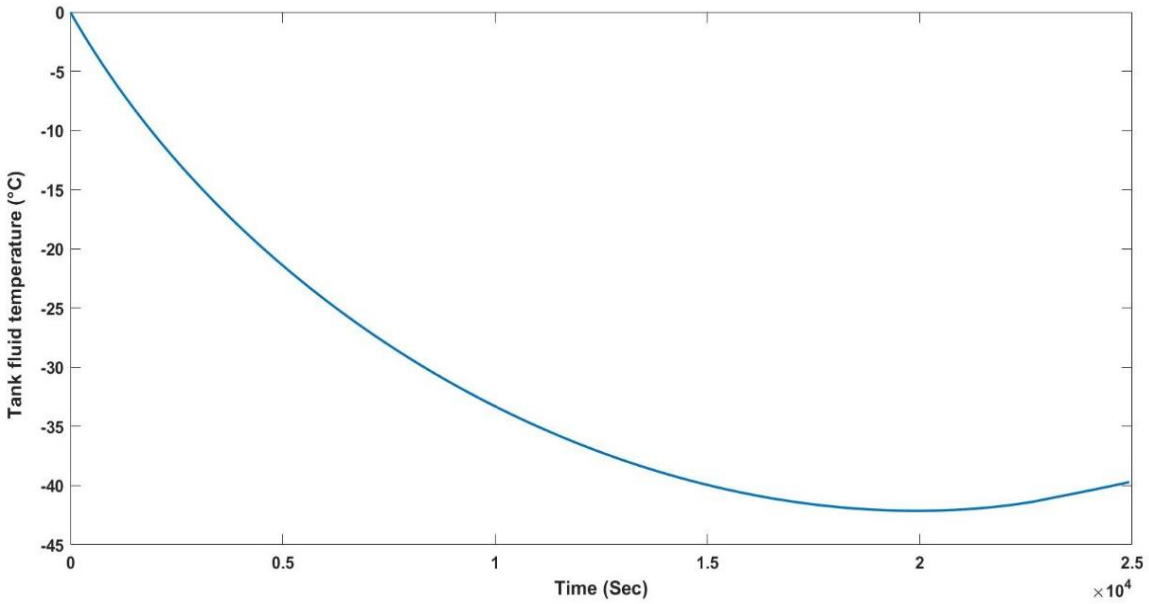

Figure 4-4: Tank Fluid (Methane) Temperature Vs time plot when initial temperature of the system is 0°C and tank decanting rate is 0.064kg/s. Minimum observed temperature of the fluid is -42.1°C.

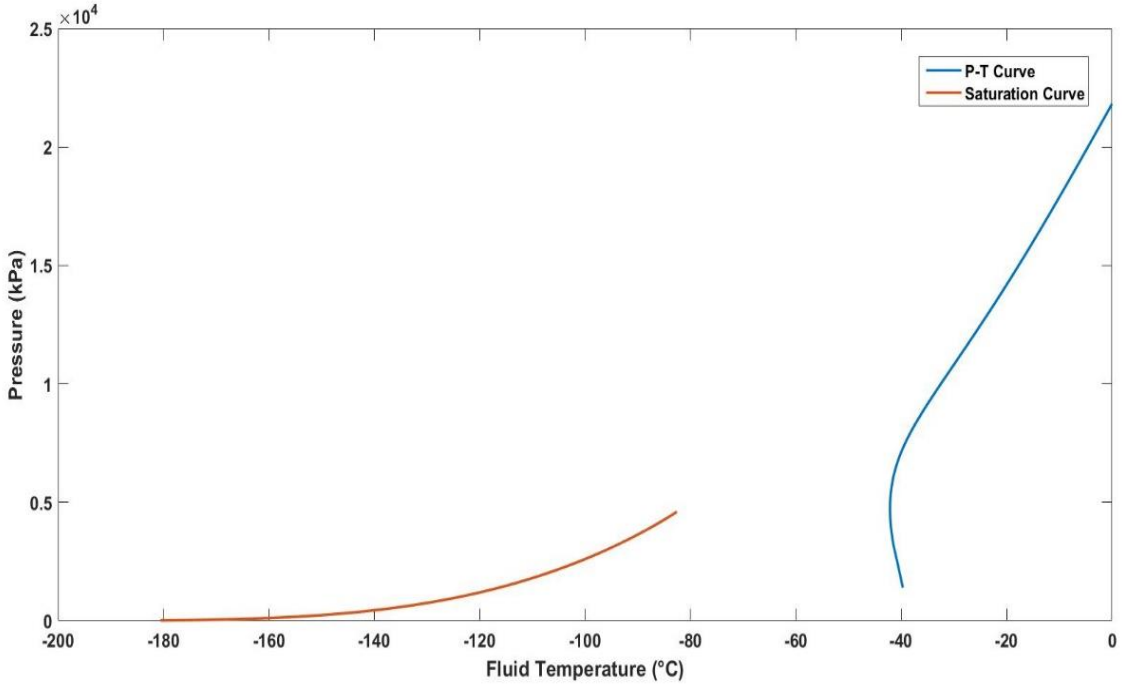

Figure 4-5: Pressure (kPa)-Temperature (°C) Vs Saturation Curve plot for Methane decanting at 0.064kg/s where the system initial conditions are at 218.2 bar and 0°C.

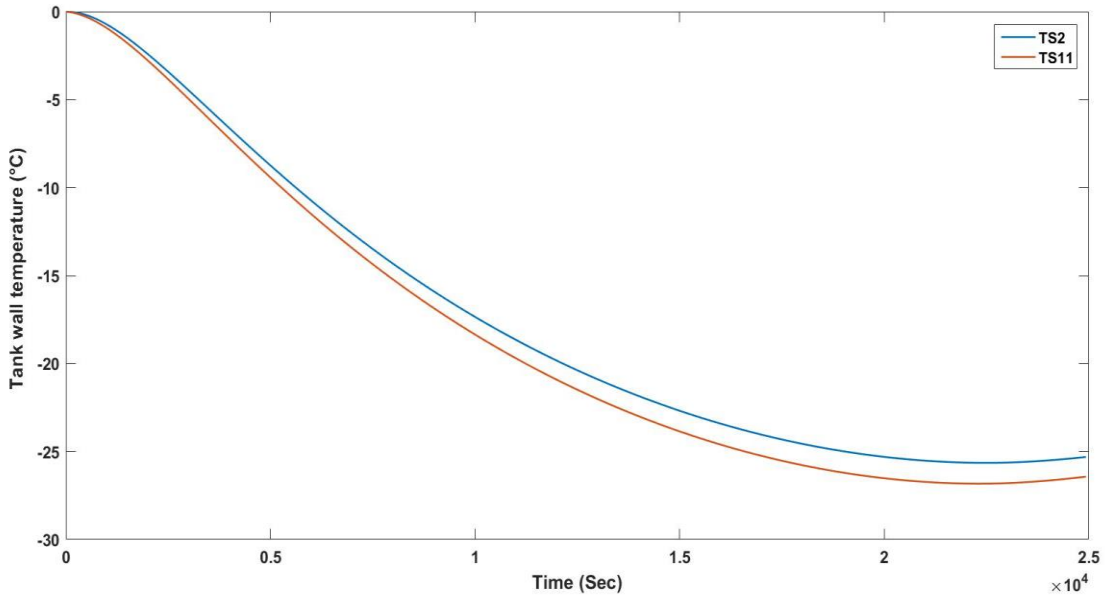

Figure 4-6: Tank wall Temperature (°C) Vs Time plot when the initial temperature of the system is 0°C and tank decanting rate is 0.064kg/s. Minimum observed temperature of the wall is -26.8°C where TS2 is the node closest to surroundings and TS11 is the node adjacent to inner tank wall surface

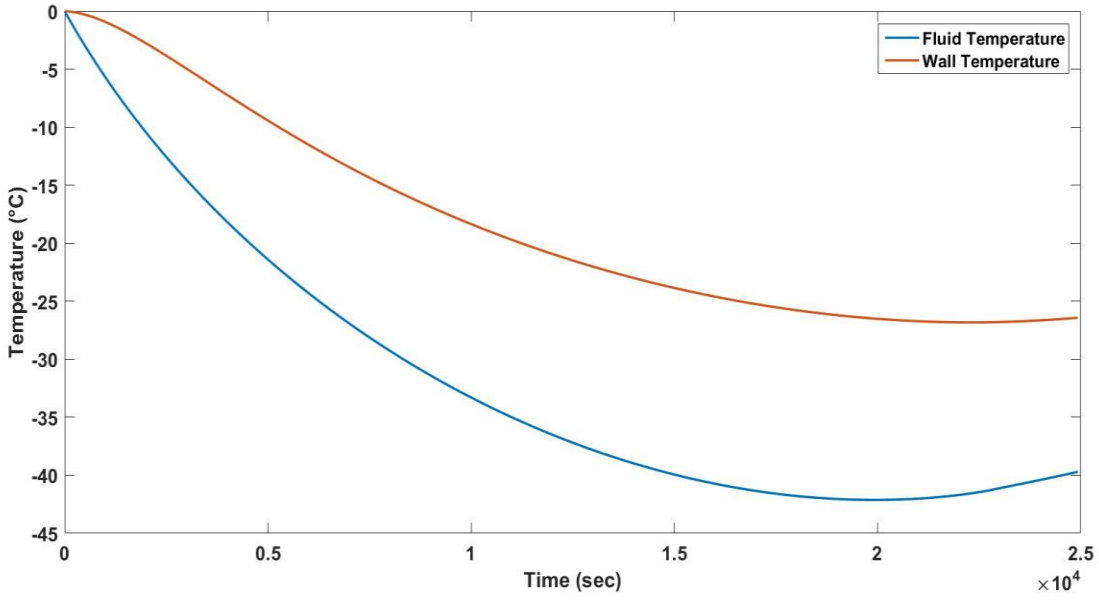

Figure 4-7: Wall Temperature (°C) Vs Fluid temperature (°C) when the initial temperature of the system is 0°C and tank decanting rate is 0.064kg/s. Minimum observed fluid and wall temperatures are -42.1°C and -26.8°C respectively.

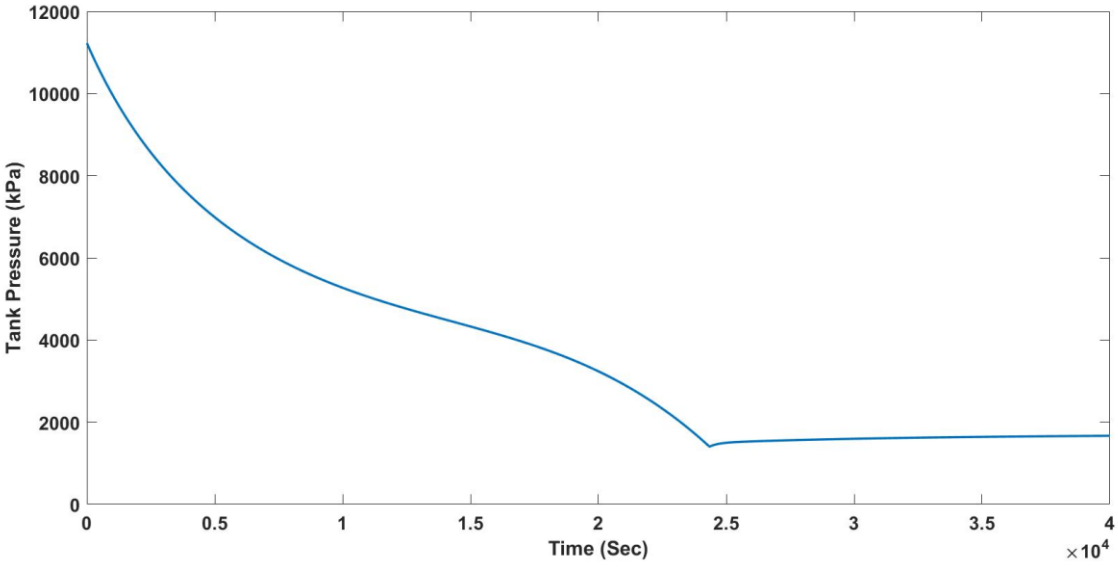

Figure 4-8:Tank Pressure Vs Time plot when the initial temperature of the system is -50°C and tank decanting rate is 0.064kg/s. Time taken to reach 14bar=24344s

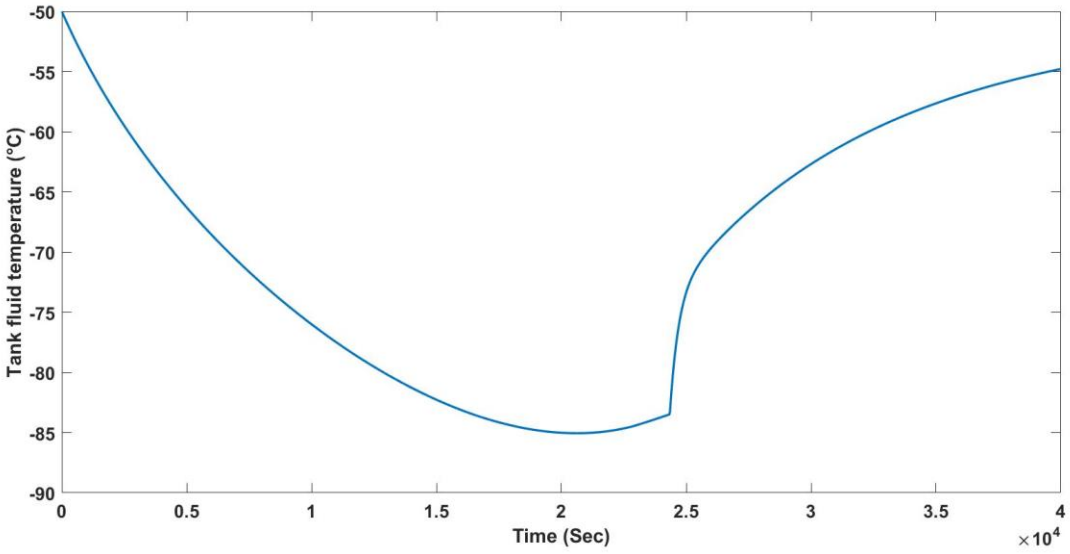

Figure 4-9:Tank Fluid (Methane) Temperature Vs time plot when initial temperature of the system is -50°C and tank decanting rate is 0.064kg/s. Minimum observed temperature of the fluid is -85°C

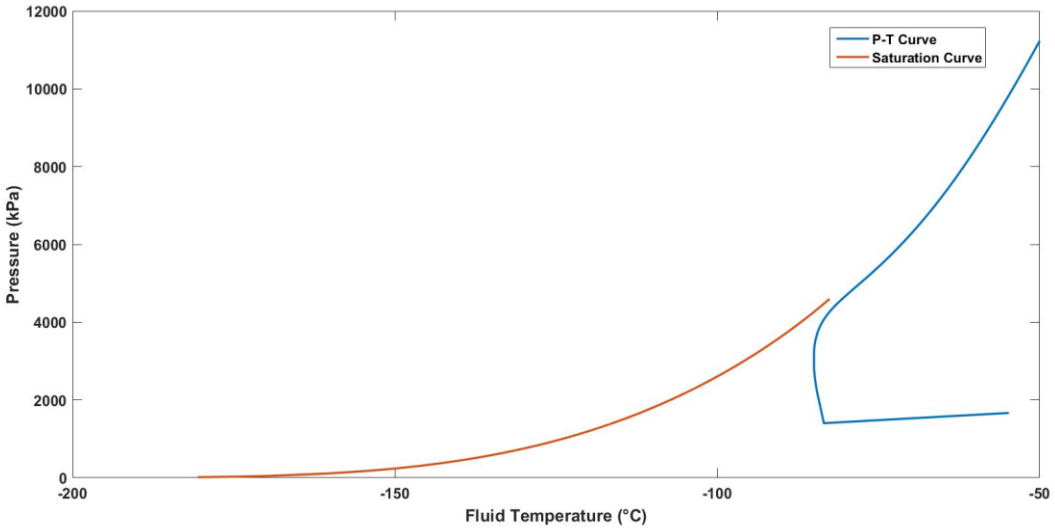

Figure 4-10: Pressure (kPa)-Temperature (°C) Vs Saturation Curve plot for Methane decanting at 0.064kg/s where the system initial conditions are at 112.3 bar and -50°C.

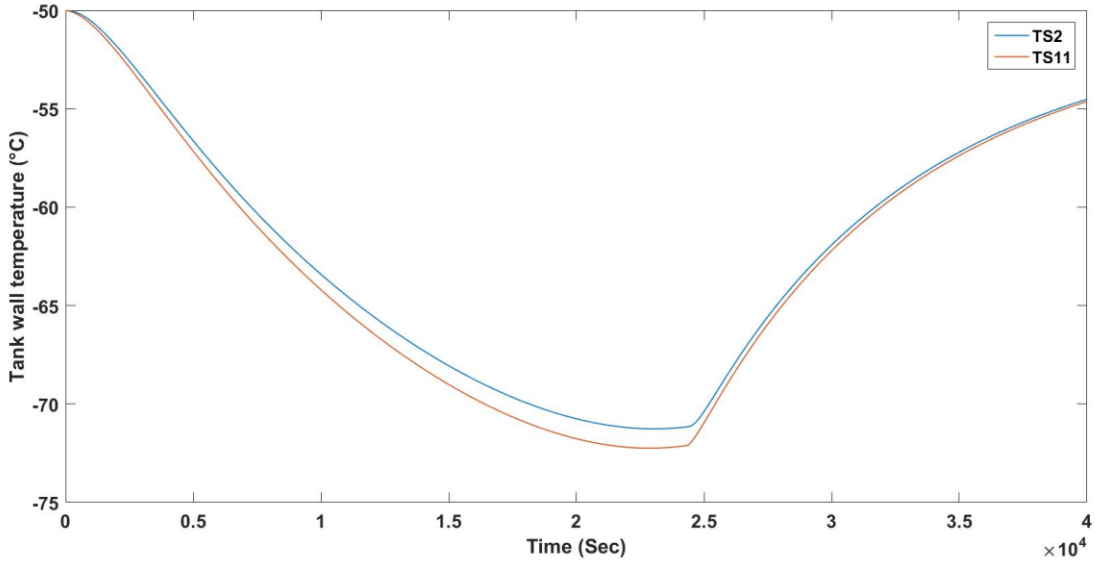

Figure 4-11: Tank wall Temperature (C) Vs Time plot when the initial temperature of the system is -50°C and tank decanting rate is 0.064kg/s. Minimum observed temperature of the wall is -72.3°C

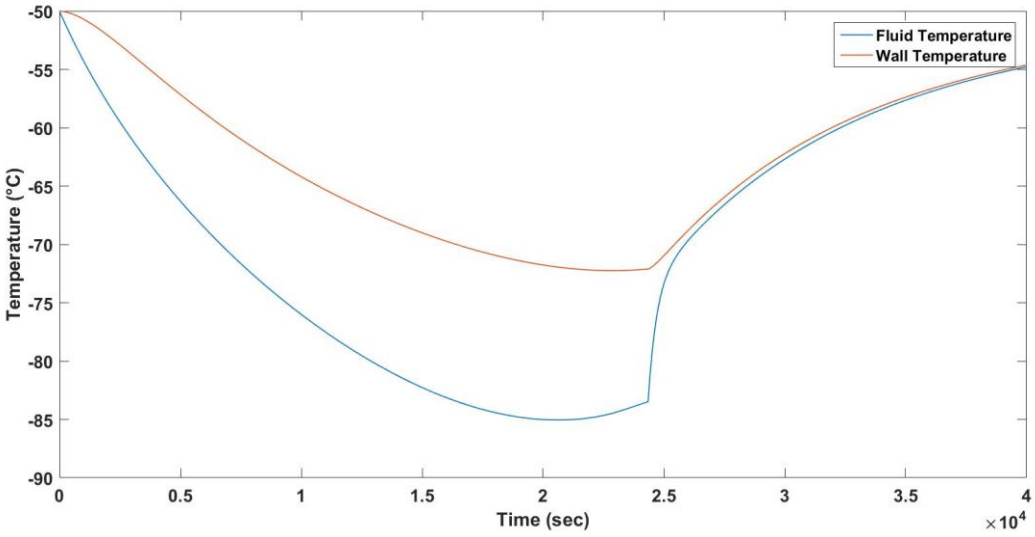

Figure 4-12: Wall Temperature (°C) Vs Fluid temperature (°C) when the initial temperature of the system is -50°C and tank decanting rate is 0.064kg/s. Minimum observed fluid and wall temperatures are -85.0°C and -72.3°C respectively.

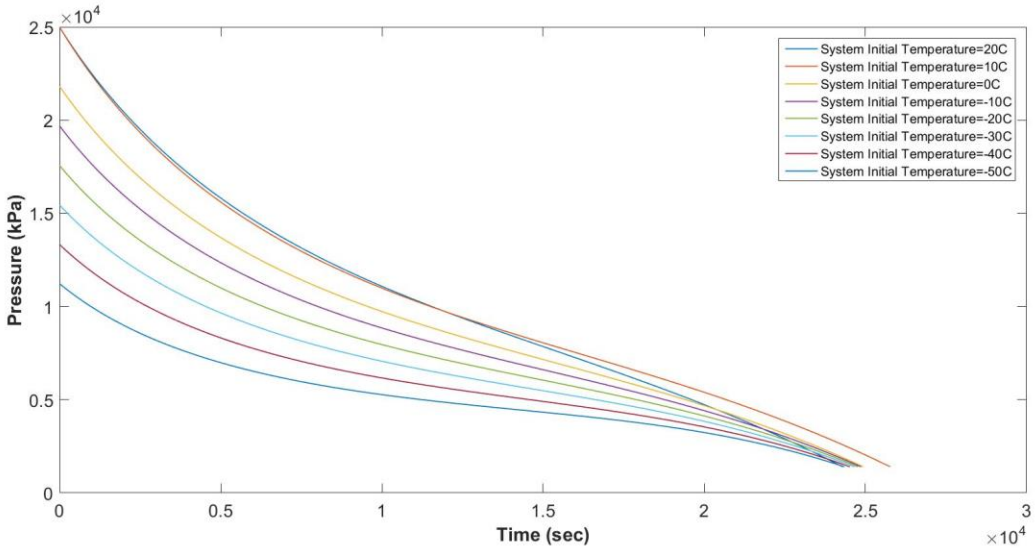

Figure 4-13: Cumulative Tank Pressure (kPa) vs Time (sec) plot for different system initial conditions with decanting rate of 0.064kg/s.

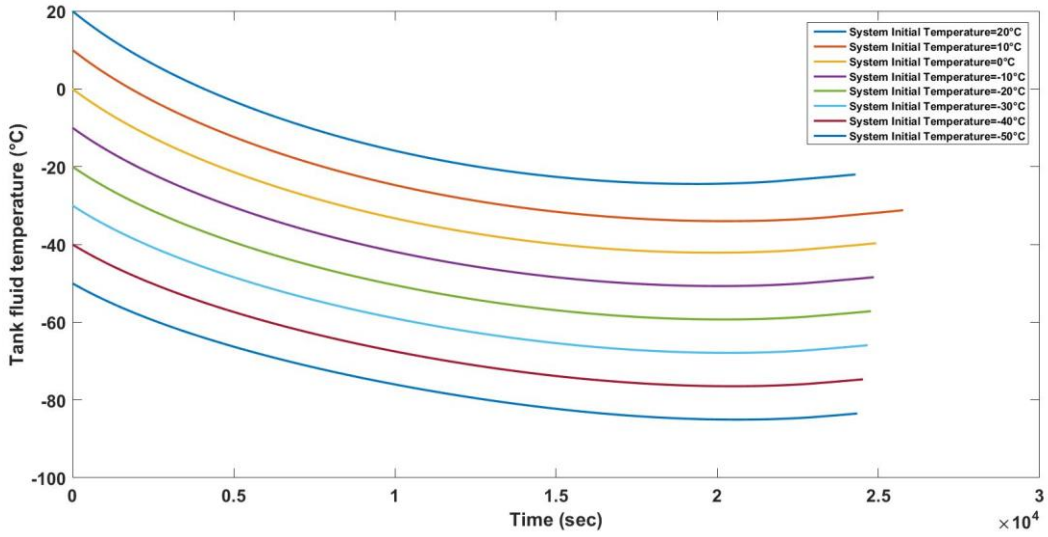

Figure 4-14: Cumulative Fluid temperature (°C) vs Time (sec) plot for different system initial temperatures with decanting rate of 0.064kg/s

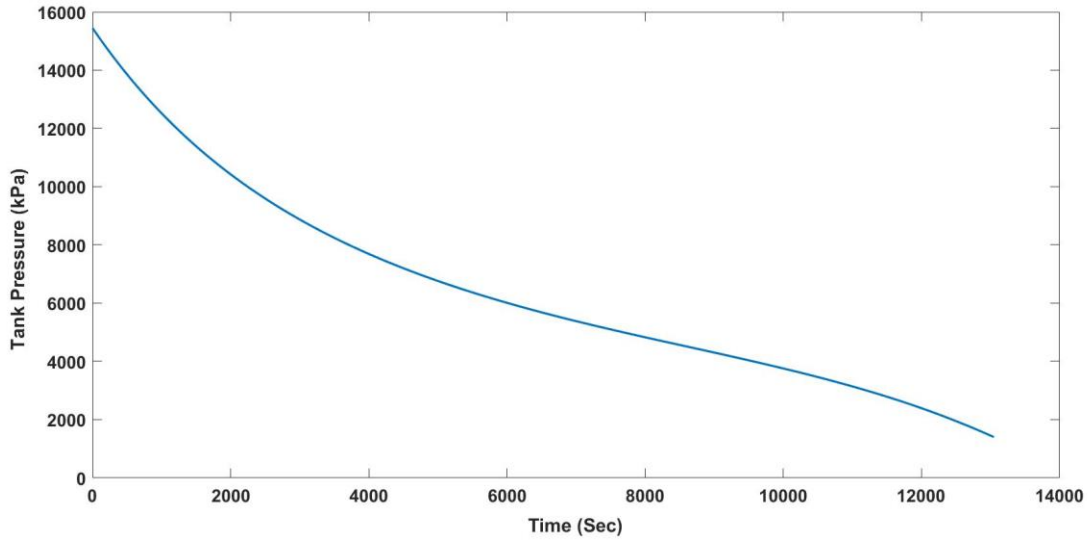

Figure 4-15: Tank Pressure Vs Time plot when the initial temperature of the system is -30°C and tank decanting rate is 0.11975kg/s. Time taken to reach 14bar=13047s

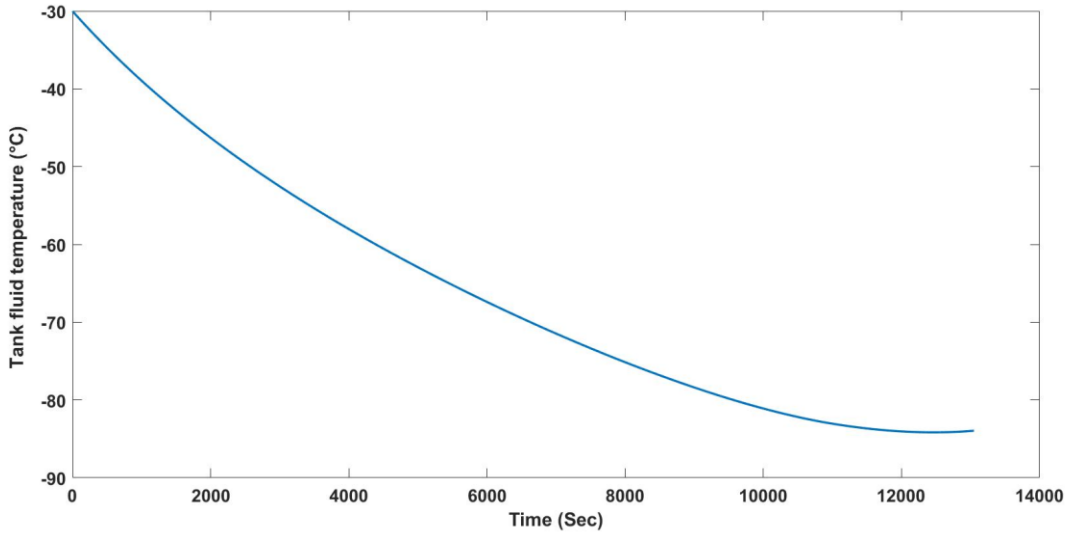

Figure 4-16: Tank Fluid (Methane) Temperature Vs time plot when initial temperature of the system is -30°C and tank decanting rate is 0.11975kg/s. Minimum observed temperature of the fluid is -84.2°C

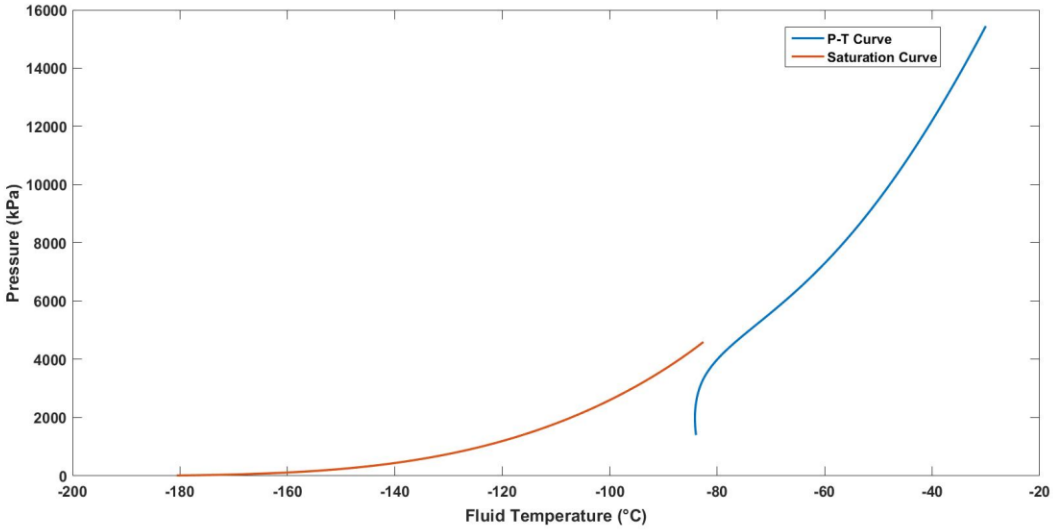

Figure 4-17: Pressure (kPa)-Temperature (°C) Vs Saturation Curve plot for Methane decanting at 0.11975kg/s where the system initial conditions are at 154.5 bar and -30°C

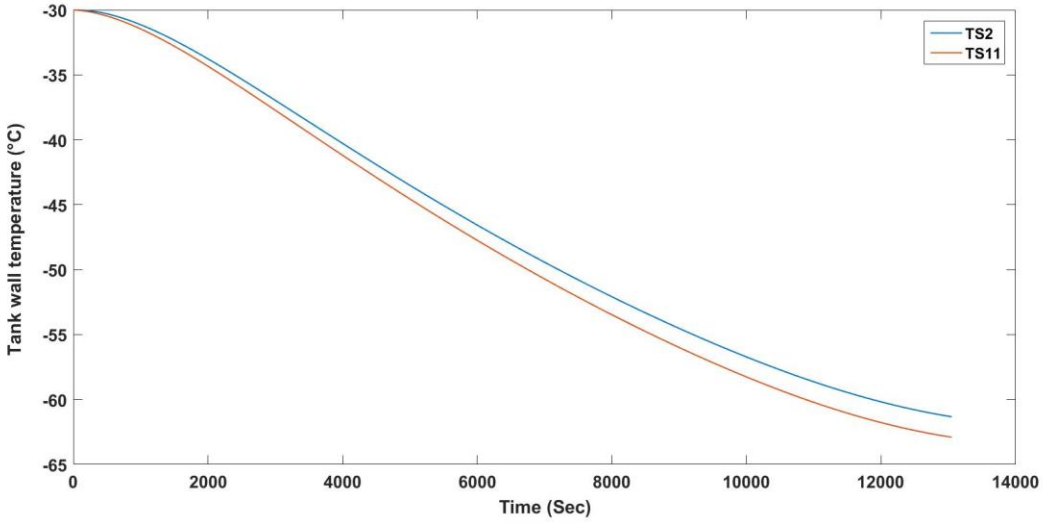

Figure 4-18: Tank wall Temperature (°C) Vs Time plot when the initial temperature of the system is -30°C and tank decanting rate is 0.11975kg/s. Minimum observed temperature of the wall is -62.9°C

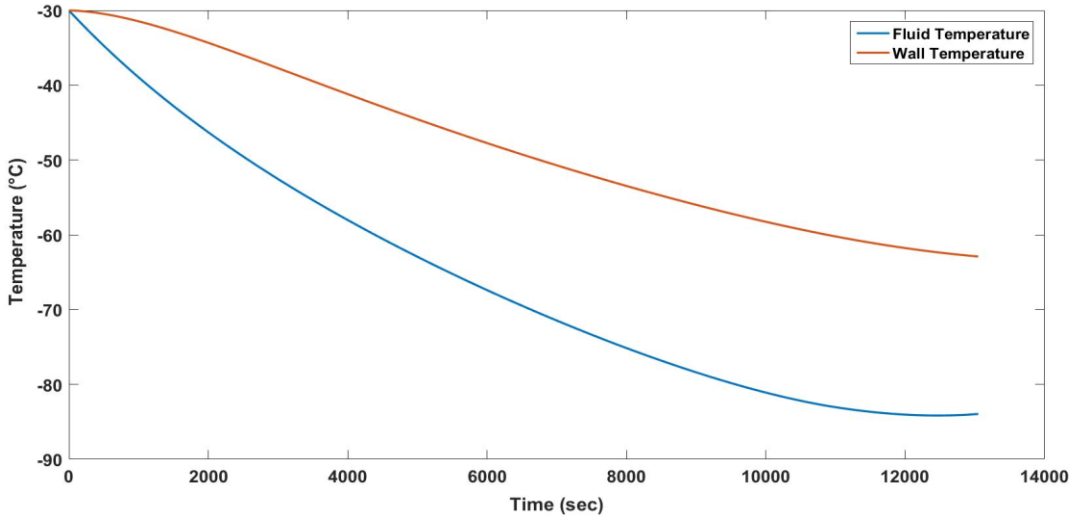

Figure 4-19: Wall Temperature (°C) Vs Fluid temperature (°C) when the initial temperature of the system is -30°C and tank decanting rate is 0.11975kg/s. Minimum observed fluid and wall temperatures are -84.2°C and -62.9°C respectively

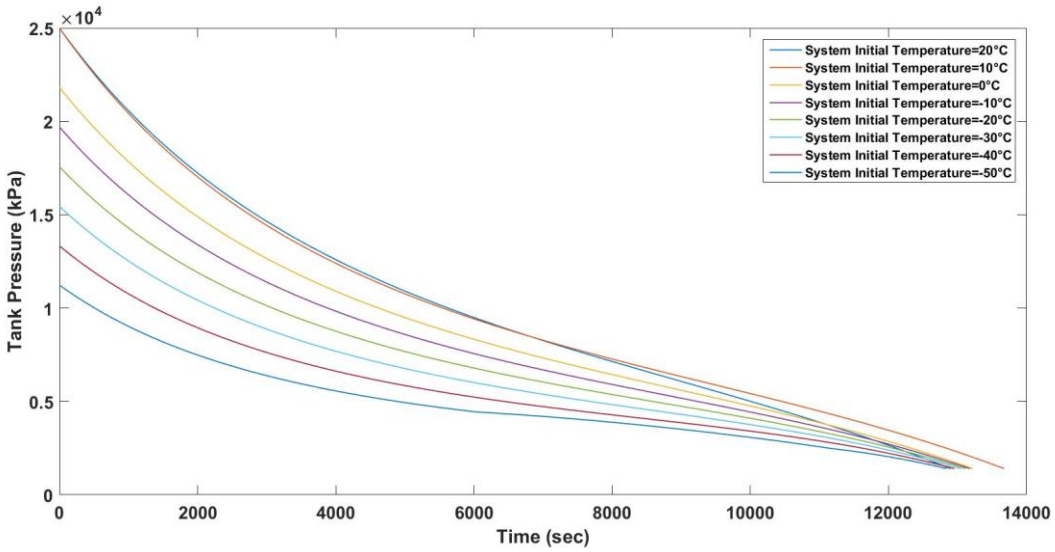

Figure 4-20: Cumulative Tank Pressure (kPa) vs Time (sec) plot for different system initial temperatures with decanting rate of 0.11975kg/s

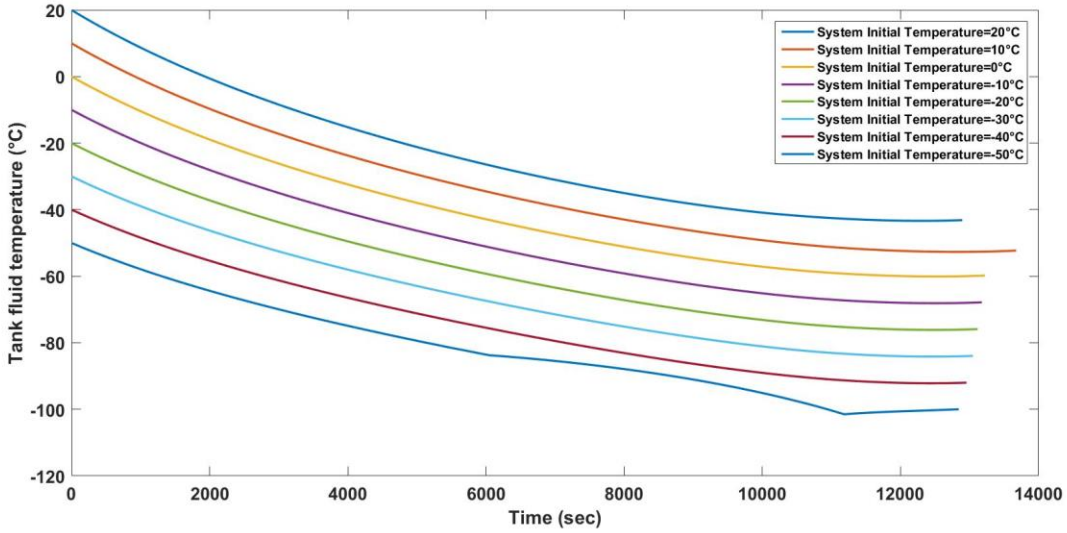

Figure 4-21: Cumulative Fluid temperature (°C) vs Time (sec) plot for different system initial temperatures with decanting rate of 0.11975kg/s

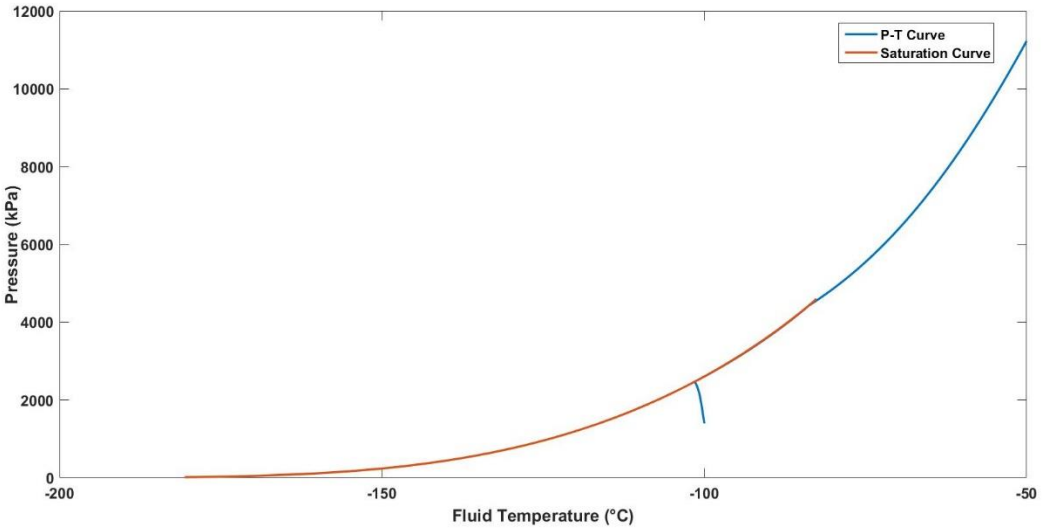

Figure 4-22: Pressure (kPa)-Temperature (°C) Vs Saturation Curve plot for Methane decanting at 0.11975kg/s where the system initial conditions are at 112.3 bar and -50°C

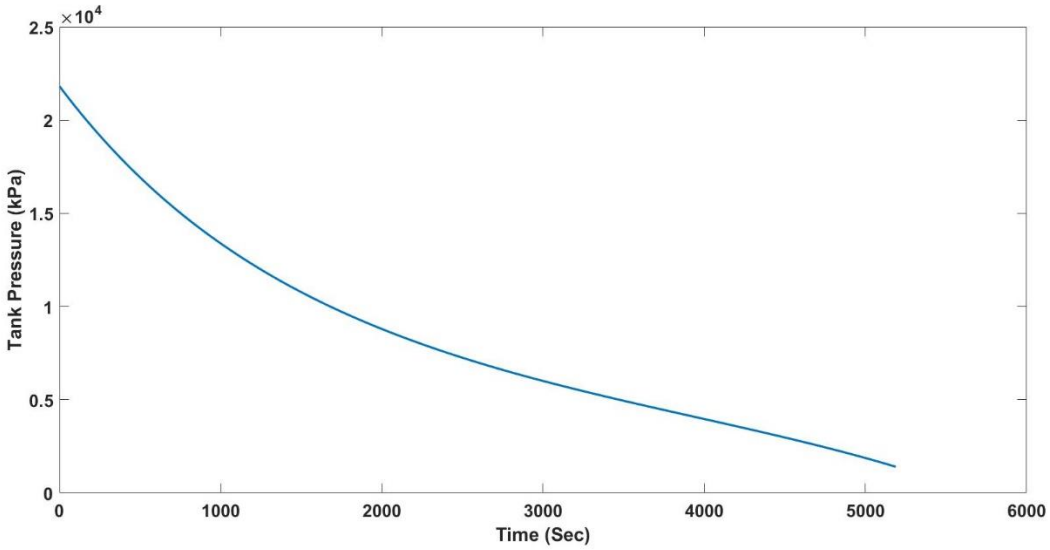

Figure 4-23: Tank Pressure Vs Time plot when the initial temperature of the system is 0°C and tank decanting rate is 0.3kg/s. Time taken to reach 14bar=5188s

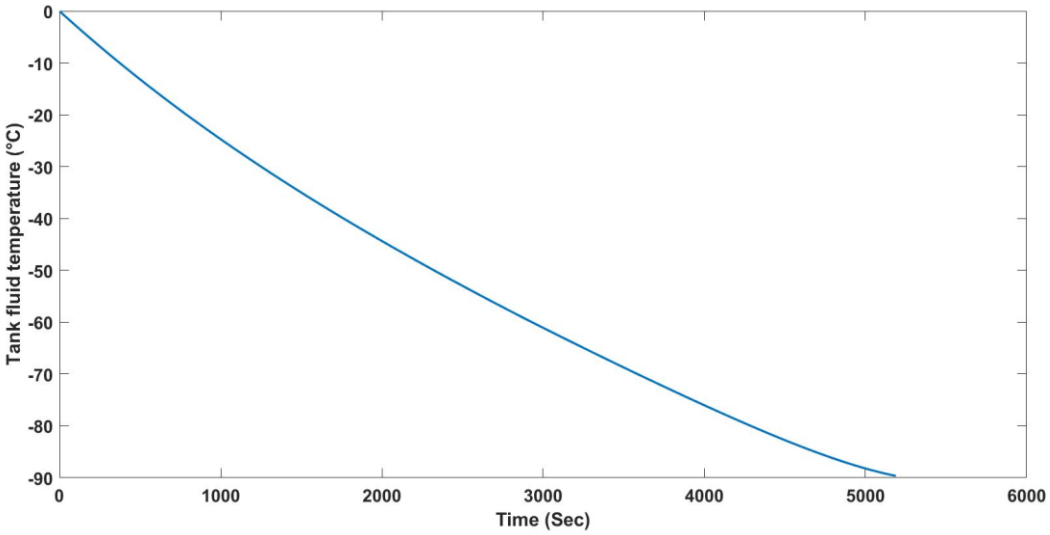

Figure 4-24: Tank Fluid (Methane) Temperature Vs time plot when initial temperature of the system is 0°C and tank decanting rate is 0.3kg/s. Minimum observed temperature of the fluid is -89.6°C

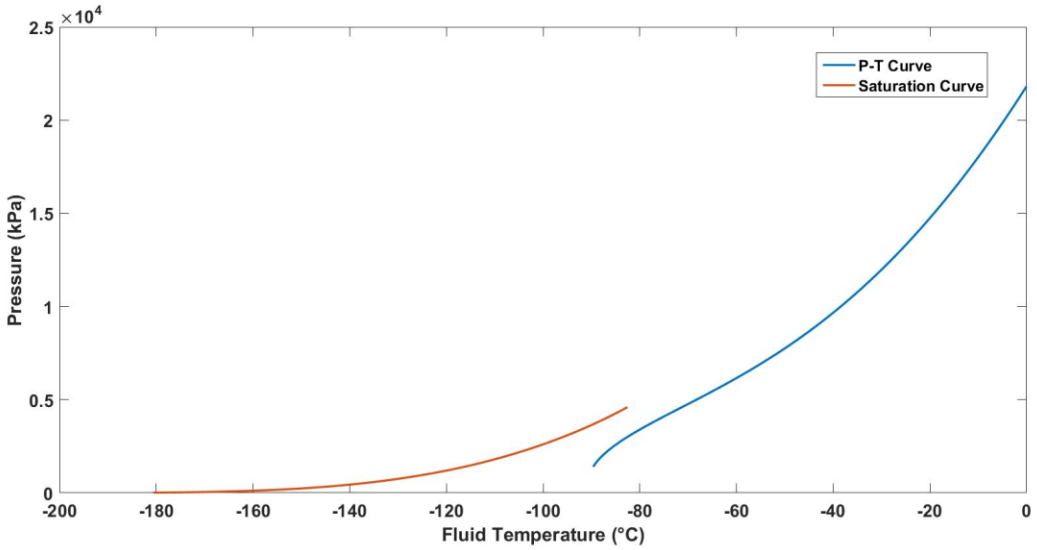

Figure 4-25: Pressure (kPa)-Temperature (°C) Vs Saturation Curve plot for Methane decanting at 0.3kg/s where the system initial conditions are at 218.2 bar and 0°C

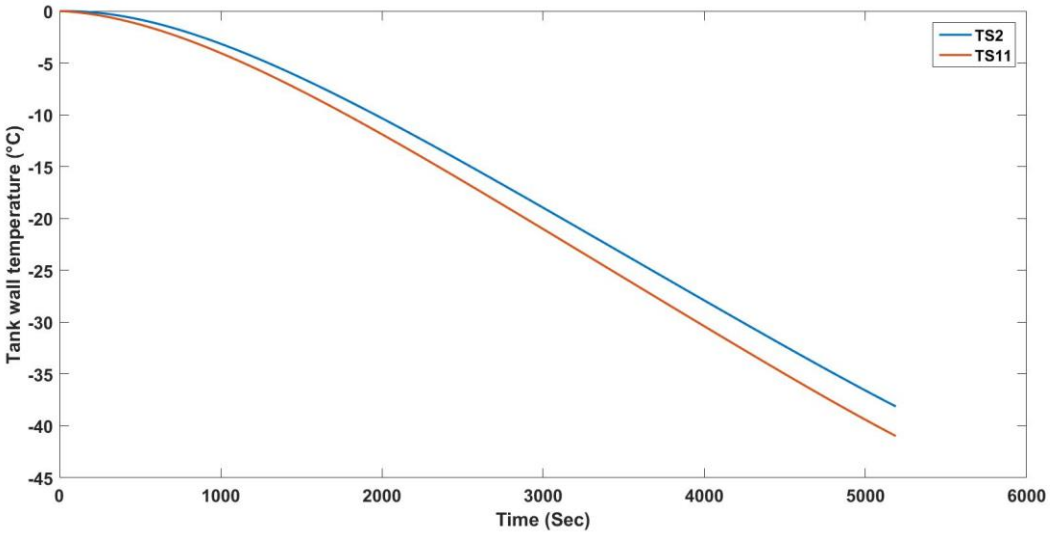

Figure 4-26: Tank wall Temperature (°C) Vs Time plot when the initial temperature of the system is 0°C and tank decanting rate is 0.3kg/s. Minimum observed temperature of the wall is -41°C

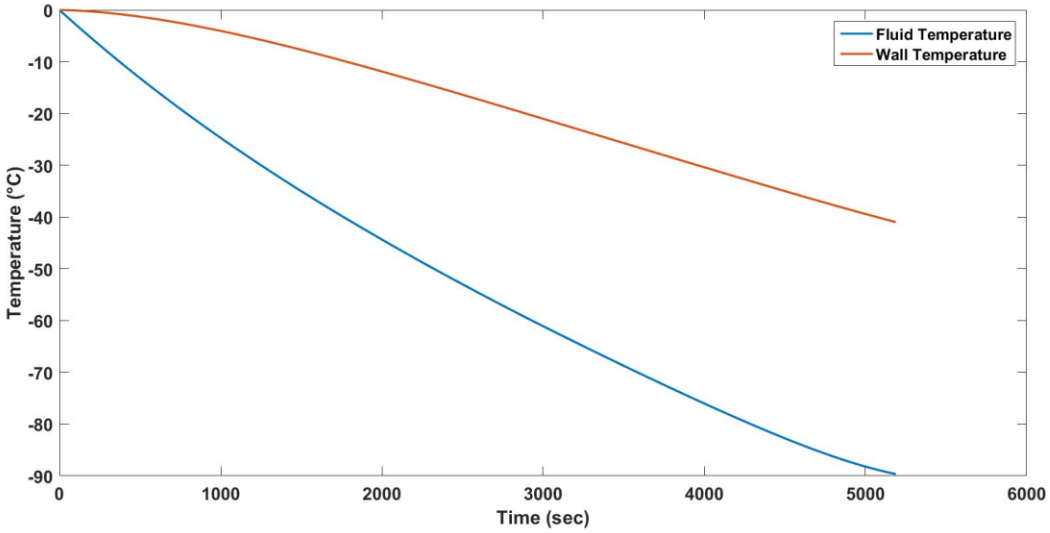

Figure 4-27: Wall Temperature (°C) Vs Fluid temperature (°C) when the initial temperature of the system is 0°C and tank decanting rate is 0.3kg/s. Minimum observed fluid and wall temperatures are -89.6°C and -41°C respectively

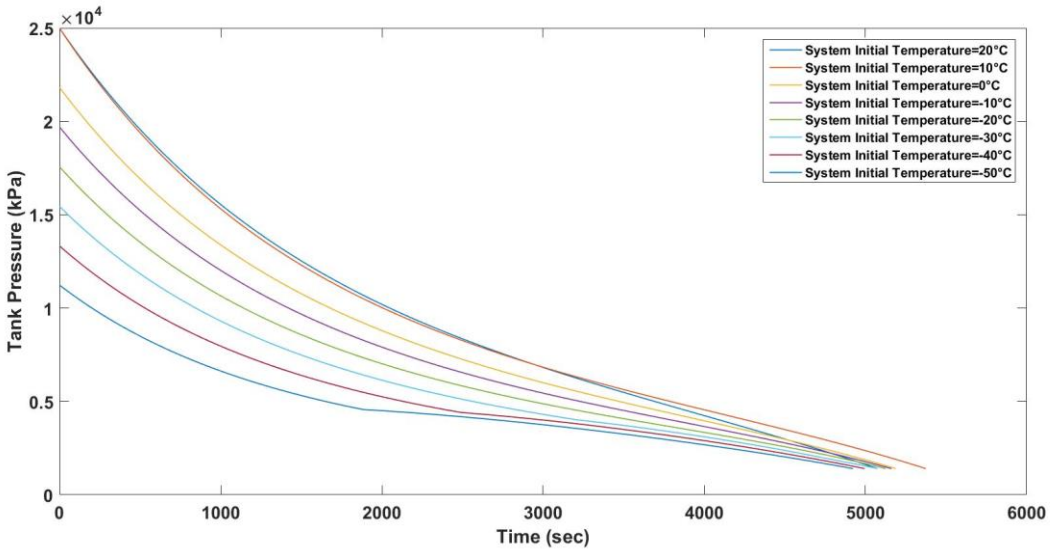

Figure 4-28: Cumulative Tank Pressure (kPa) vs Time (sec) plot for different system initial temperatures with decanting rate of 0.3kg/s

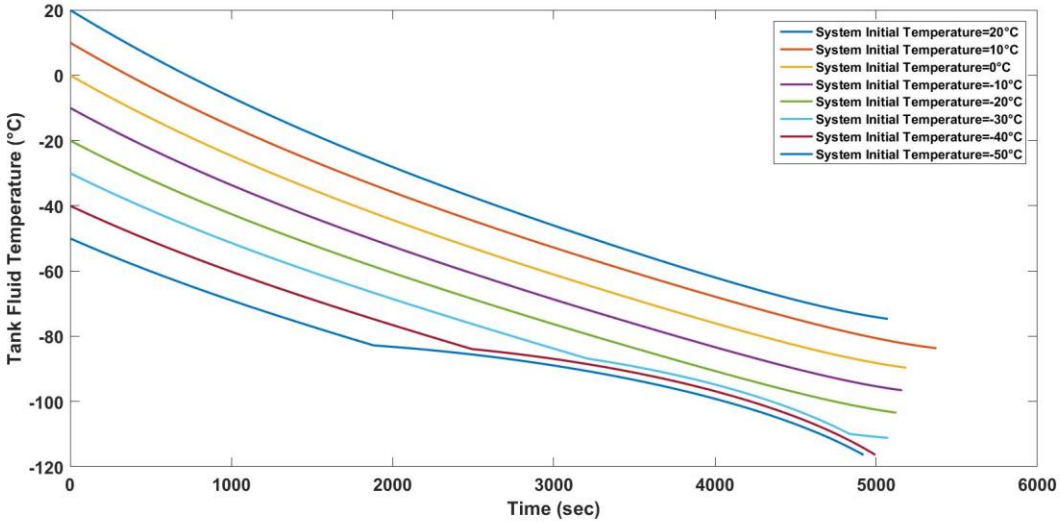

Figure 4-29: Cumulative Fluid temperature (°C) vs Time (sec) plot for different system initial temperatures with decanting rate of 0.3kg/s

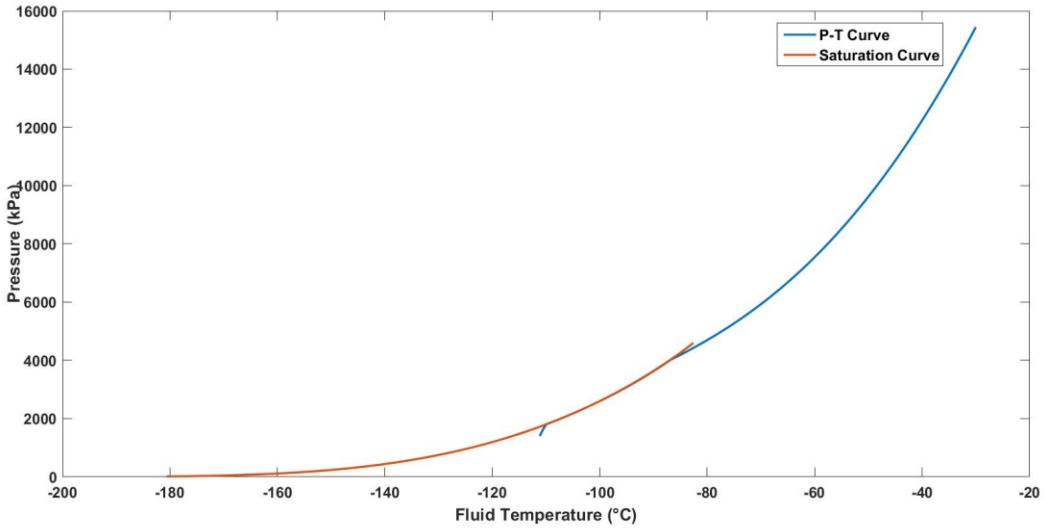

Figure 4-30: Pressure (kPa)-Temperature (°C) Vs Saturation Curve plot for Methane decanting at 0.3kg/s where the system initial conditions are at 154.5 bar and -30°C

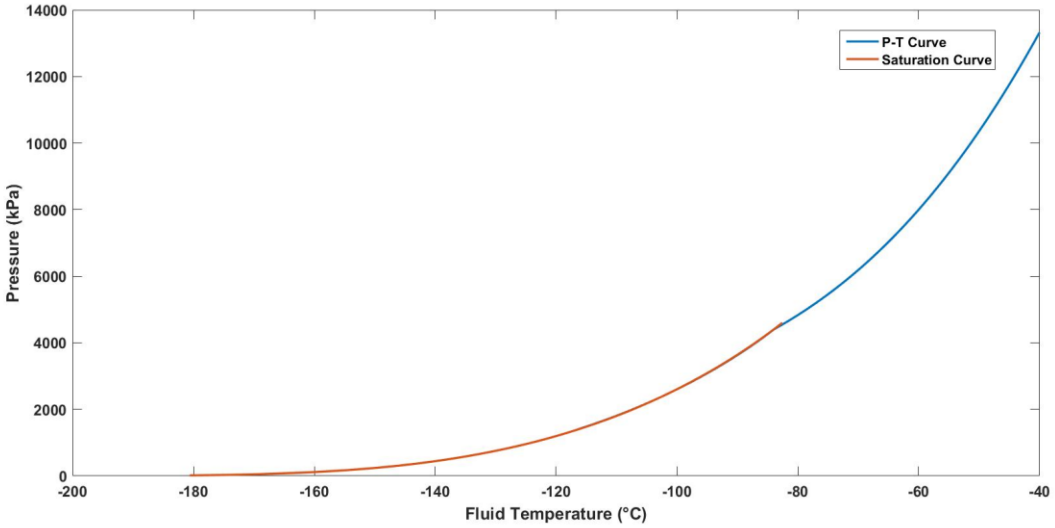

Figure 4-31: Pressure (kPa)-Temperature (°C) Vs Saturation Curve plot for Methane decanting at 0.3kg/s where the system initial conditions are at 133.3 bar and -40°C

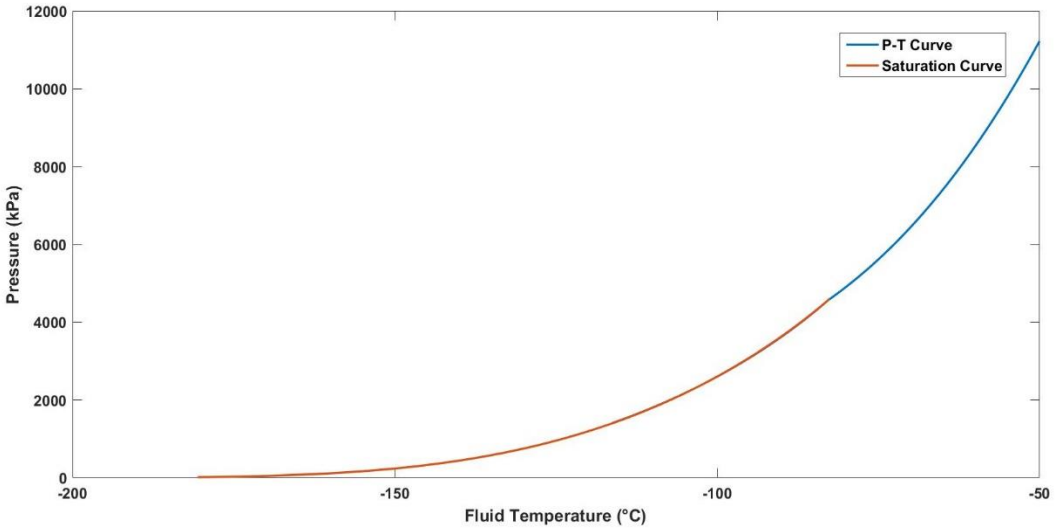

Figure 4-32: Pressure (kPa)-Temperature (°C) Vs Saturation Curve plot for Methane decanting at 0.3kg/s where the system initial conditions are at 112.3 bar and -50°C

Chapter 5 : Results for Biogas Tank Decanting

This chapter is dedicated for studying the decanting of Biogas. Different decanting flow rates of 0.064kg/s, 0.11975kg/s and 0.3kg/s were chosen in conjunction with varying initial system temperatures from -50°C to 20°C in steps of 10°C increments.

Table 5-A shows the molar composition of Biogas. The respective critical pressures and critical temperatures of the individual components are also mentioned in the table whose values are derived from REFPROP (Eric W. Lemmon, 2007) as mentioned above.

Table 5-A: Biogas Critical Properties and related mole fractions of the constituent gases

Sl.no	Fluid	Mole Fraction (%)	Critical Pressure (kPa)	Critical Temperature (°C)
1.	Methane	22	4599.2	-82.6
2.	Carbon monoxide	24	3493.5	-140.1
3.	Carbon dioxide	10.4	7384.3	31.0
4.	Hydrogen	28.5	1296.7	-240.0
5.	Nitrogen	14.6	3399.1	-146.9
6.	Oxygen	0.5	5043	-118.6

Figure 5-1 shows the saturation curve for Biogas. As it can be seen from the graph the critical temperature of the mixture is identified to be as -63.1°C and critical pressure is 9200kPa. As the temperature of the mixture falls below the critical temperature, the gaseous phase of the mixture starts to condense and vapor formation takes place in the tank. The vapor continues to form and converts into liquid once the pressure and temperature in the tank lies in line with the saturation curve.

5.1 Decanting Flow Rate Selected is 0.064kg/s

Figure 5-2, Figure 5-3 shows the pressure and temperature histories for Biogas tank decanting with a flow rate of 0.064kg/s when the initial pressure and temperature were 218.2 bar and 0°C respectively. It is observed that the decanting takes 6018 seconds for the pressure in the tank to fall to 14bar with minimum temperature of fluid as -106.4°C. The critical temperature of Biogas is identified as -63.1°C and it is observed that the temperature in the tank falls well below -63.1°C and thus phase transformation does takes place in the mixture. The mixture temperature reaches the critical temperature 6018seconds after the decanting has started when the pressure in the tank is 66.4bar which is lower than the critical pressure of 92bar. At this moment it is difficult to predict the exact phase of the mixture because each individual gas behaves differently under different conditions. But the mixture crosses the saturation line when the pressure in the tank is 63.8bar where the mixture when considered as a single entity would be in liquid phase defined by the saturation line obtained from **REFPROP**. The mixture continues to stay behind the saturation line till the pressure in the tank reaches the preset limit of 14bar. In **Figure 5-3** a distinctive change in the curve flow is observed when the temperature in the tank falls below -84°C i.e. 4859seconds after the start of the decanting. This change is found to be caused by a component of the mixture 'Methane' as at this point the pressure and temperature of the Methane crosses the saturation line.

Figure 5-4 shows the comparison of Pressure-Temperature curve for Biogas tank decanting with the saturation curve of Biogas when the system initial temperature and pressure are 0°C and 218.2bar respectively. As explained above the mixture crosses the saturation line when the pressure in the tank is 63.8bar and temperature is -64.7°C. It is advised to stop the decanting at this point to avoid any possible damage to tank liner material.

Figure 5-5 shows the temperature histories for tank wall temperatures under the above mentioned decanting conditions. The minimum observed wall temperature was -45.5°C which is observed when the pressure in the tank was 14bar.

Figure 5-6 draws a comparison between fluid and wall temperature during decanting under the conditions mentioned above. It can be seen that the minimum fluid and wall temperatures observed during the decanting process are -106.4°C and -45.5°C respectively.

Figure 5-7 shows the cumulative plot for tank pressure during decanting at different system initial conditions with a flow rate of 0.064kg/s. In all the decanting simulations the final pressure was set to 14bar and the decanting was stopped when this preset pressure was reached.

Figure 5-8 shows a cumulative plot for fluid temperatures during tank decanting at different tank initial conditions at a decanting flow rate of 0.064kg/s. As it can be observed that the temperature in the tank went below the critical mixture temperature of -63.1°C in all the decanting iterations and thus it is suggested to stop the tank decanting as the pressure-temperature curve for individual iterration crosses the saturation line for the mixture. But it is observed that in three particular iterations when the initial system temperature was 10°C, -40°C and -50°C there is a distinctive change in the mixture temperature curve. The reason for these changes will be better explained below with pressure-temperature vs saturation curve plots.

Figure 5-9 shows pressure-temperature vs saturation curve plots for Biogas decanting when the system initial temperature and pressure are 10°C and 250bar with a decanting rate of 0.064kg/s. The temperature in the tank falls below the critical temperature when the pressure in the tank reaches 63.6 bar which is 4471 seconds after the decanting has started but at this point the pressure is below the critical pressure and thus liquefaction of the mixture is not observed at this point.

As the decanting is continued the pressure-temperature crosses the saturation line when the pressure in the tank falls to 60.3 bar. At this point favorable conditions are formed within the tank for liquefaction of the mixture. But as the decanting is continued beyond this point when the pressure falls to 50.2 bar fluctuations in the pressure-temperature plot can be observed and at this point it is unsure what might have caused the fluctuation as the fluid is a mixture of gases whose thermal behavior is very different from each other.

Figure 5-10 shows the pressure-temperature vs saturation curve plot for Biogas decanting when the initial system temperature and pressure are -40°C and 133.3bar with a decanting flowrate of 0.064kg/s. It is observed that the temperature in the tank falls below the critical temperature 1372seconds after the decanting process has started when the pressure in the tank was 84.2bar. This is also the point at which the pressure-temperature curve crosses the saturation line. The phase transformation of the mixture starts beyond this point and continues until the decanting is stopped at tank pressure of 14bar. It is also observed that as the decanting is continued beyond 84.2bar at about 2764seconds after the start of the decanting process the pressure and temperature in the tank forms favorable conditions for Methane liquefaction where the pressure and temperature in the tank are 45.6bar and -83.8°C. This point can be clearly observed from the sharp change in pressure-temperature curve shown in the figure.

Figure 5-11 shows the pressure-temperature vs saturation curve for Biogas tank decanting with an initial system pressure and temperature as 112.3bar and -50°C with a decanting flow rate of 0.064kg/s. It is observed that the temperature of the fluid mixture falls below the critical temperature when the pressure in the tank is 86.3bar i.e. 751seconds after the decanting has started. As seen in **Figure 5-10** that favorable conditions for Methane liquefaction are formed, similarly the pressure and temperature in the tank favors liquid Methane formation after 2172seconds into the decanting process and thus a sharp change in the P-T curve is observed.

5.2 Decanting Flow Rate Selected is 0.11975kg/s

Figure 5-12, Figure 5-13 shows the pressure and temperature histories for tank decanting when the system initial pressure and temperature are 218.2bar and 0°C with a decanting flow rate of 0.11975kg/s. It can be seen that the minimum observed temperature in the tank is -116.6°C when the pressure in the tank was 14bar. It is evident that the phase transformation is observed in the tank, details of which will be explained with the pressure-temperature vs saturation curve in **Figure 5-14**.

Figure 5-14 shows the P-T vs saturation curve for Biogas. The temperature in the tank falls below the critical temperature 1920seconds after the decanting has started when the pressure in the tank was 70.5bar. At this point the pressure in the tank is not sufficient for the mixture phase transformation and as the decanting is continued phase transformation is observed when the pressure in the tank is 68.8bar and this transformation continues till the tank pressure reaches the preset final pressure of 14bar.

Figure 5-15 shows the temperature histories for tank wall temperatures during decanting under the conditions mentioned above. The minimum wall temperature is observed to be -36.3°C which occurs when the pressure in the tank is 14bar i.e. 3182seconds after the start of the decanting process.

Figure 5-16 draws a comparison between fluid and wall temperatures during decanting process. The minimum observed fluid and wall temperatures are -116.6°C and -36.3°C respectively.

Figure 5-17, Figure 5-18 shows cumulative pressure and temperature plots for Biogas tank decanting at different system initial pressures and temperatures at a decanting rate of 0.11975kg/s. It can be seen from **Figure 5-18** that there is a sharp change in the temperature plots when the system initial temperatures were -30°C, -40°C and -50°C.

The reason for this change will be studied using the P-T vs saturation curve plots. In all the cases mentioned the temperature in the tank falls below the critical temperature of the mixture and it is suggested to stop the decanting process at a point where the P-T curve intersects the saturation curve to prevent any damage to the cylinder liner material.

Figure 5-19 shows the comparison of Pressure-Temperature curve for Biogas tank decanting with the saturation curve when the system initial temperature and pressure were -30°C and 175.7bar respectively at a decanting rate of 0.11975kg/s. The temperature in the tank goes below the critical temperature when the pressure in the tank is 82.3bar i.e. 1032seconds after the start of the decanting process. But the P-T curve crosses the saturation line a little further into the decanting when the pressure in the tank is 82bar and continues to stay behind the saturation line until the preset final pressure of 14bar is reached. A little discrepancy in the P-T plot can be observed when the pressure in the tank is 45.1bar and temperature in the tank is -85°C which are favorable conditions for Methane liquefaction.

Similarly **Figure 5-20, Figure 5-21** shows the comparison of P-T curve for Biogas tank decanting with the saturation curve when the system initial temperatures and pressures were -40°C, -50°C and 133.3bar and 112.3bar respectively at a decanting rate of 0.11975kg/s. A similar discrepancy as mentioned above can be seen in both the figures and it happens to be that similar favorable conditions are formed within the tank for Methane liquefaction.

5.3 Decanting Flow Rate Selected is 0.3kg/s

Figure 5-22, Figure 5-23 shows the pressure and temperature histories for Biogas tank decanting with a flow rate of 0.3kg/s when the initial pressure and temperature were 218.2 bar and 0°C respectively. The temperature in the tank crosses the critical temperature when the pressure in the tank falls to 73.5bar i.e. 736seconds after the start of the decanting process. The phase transformation in the tank is observed as the P-T curve crosses the saturation curve as shows in **Figure 5-24**.

Figure 5-24 shows P-T vs saturation curve for Biogas tank decanting under the decanting conditions mentioned above. It is seen that the temperature in the tank falls below the critical temperature as the pressure in the tank falls to 73.5bar but the phase transformation is observed when the pressure in the tank falls to 72.4bar when the P-T curve crosses the saturation curve. The phase transformation continues to happen until the preset final pressure of 14bar is reached.

Figure 5-25 shows the tank wall temperature histories during tank decanting. It can be seen that the minimum observed temperature of the tank wall is -21.2°C which happens when the pressure in the tank is 14bar. It can be seen that the temperature of the tank wall has increased when compared to decanting at lower flowrate of 0.11975kg/s and 0.064kg/s because the time of decanting has decreased and thus there is less time available with the tank to catchup with the fluid mixture temperature and thus the minimum observed temperature of the wall increases with the flowrate.

Figure 5-26 shows a comparison between the wall temperature and fluid mixture temperature during decanting under the conditions mentioned above. The minimum observed fluid and wall temperatures are -126.3°C and -21.2°C and as explained above the huge difference between fluid mixture temperature and wall temperature is due to high flow rate which cools the fluid rapidly and does not give enough time for the tank wall to catchup with the fluid temperature.

Figure 5-27 shows the cumulative plot for tank pressure during decanting at different system initial conditions with a flowrate of 0.3kg/s. In all the decanting simulations performed the final pressure was set to be 14bar and decanting was stopped as this pressure was reached.

Figure 5-28 shows a cumulative plot for fluid mixture temperature during decanting at different tank initial conditions at a decanting flowrate of 0.3kg/s. It can be seen that in all the decanting simulations the temperature of the fluid mixture went below the critical temperature of the mixture and it is suggested to stop the decanting as the P-T curve crosses the saturation curve for each simulation in order to protect the tank liner material from any damage. Also it can be seen that during decanting with system initial temperatures of -20°C, -30°C, -40°C and -50°C discrepancies in the temperature curve are observed. In all these cases it is observed that the point of discrepancy happens to be a point where favorable conditions for Methane liquefaction is formed within the tank and hence the sudden projection in the temperature curve.

Table 5-B provides a summary of results obtained by GFSSP analysis for different tank decanting conditions. The system initial conditions for each simulation were kept consistent with the conditions used for Methane tank decanting as described above in **Chapter 4**. When the flow rate of 0.064kg/s was used the temperature of the fluid mixture went below the critical temperature in all the instances and it is suggested to stop the tank decanting when the P-T curve crosses the saturation curve in all the cases to prevent the cylinder liner material from any damage.

Also when the flowrates of 0.11975kg/s and 0.3kg/s were used the temperature of the fluid mixture went below the critical temperature in all the cases and thus as suggested above tank decanting has to be stopped at the point where P-T curve intersects the saturation curve.

Table 5-B: Summary of results for Biogas tank decanting at varying flow rates and different initial temperatures for the system

Sl.no	Flow Rate (kg/s)	Initial Temp(°C)	Pressure corresponding to Min Temp (kPa) **(Min Pressure)**	Min Fluid Temp (°C) **(M)**	Time at Min Temp occurs (sec) **(I)**	Min observed Wall Temp(°**C)**	Time where phase transformation starts (Sec)	Pressure at which phase transformation occurs (kPa)	Time taken to empty the tank (Sec)
1	0.064	20	1400.8	-98.5	6382	-31.7	4699	5343.1	6382
2.		10	1399.7	-103.9	6596	-40.3	4471	6363	6596
3.		0	1400.2	-106.4	6018	-45.5	3783	6639.6	6018
4.		-10	1400.3	-109.7	5662	-51.65	3216	7147.8	5662
5.		-20	1400.4	-112.8	5262	-57.6	2620	7631.7	5262
6.		-30	1399.8	-115.9	4818	-63.5	2002	8074.3	4818
7.		-40	1401.1	-119	4317	-69.1	1372	8425.6	4317
8.		-50	1401.1	-121.6	3758	-74.6	751	8628.6	3758
9.	0.11975	20	1399.9	-110.2	3376	-21.9	2363	5934.2	3376
10.		10	1399.6	-115	3489	-30.9	2262	6871	3489
11.		0	1399.2	-116.5	3182	-36.3	1920	7046.7	3182
12.		-10	1401.7	-119	2992	-42.8	1639	7469.6	2992
13.		-20	1398.9	-121.5	2780	-49.2	1342	7869.4	2780
14.		-30	1398.7	-124	2544	-55.5	1032	8230.6	2544
15.		-40	1400.2	-126.2	2278	-61.8	713	8510.3	2278
16.		-50	1398.7	-128	1982	-68	395	8654.6	1982
17.	0.3	20	1403.8	-121.2	1331	-4.8	899	6373.8	1331
18.		10	1399.9	-125.6	1376	-14.2	865	7248.7	1376
19.		0	1402.8	-126.3	1254	-21.2	736	7351.1	1254
20.		-10	1402.8	-128	1179	-29	631	7702.1	1179
21.		-20	1401.4	-129	1095	-36.7	519	8036.7	1095
22.		-30	1398.9	-131.4	1002	-44.4	401	8342.3	1002
23.		-40	1399.6	-132.8	897	-52	279	8567.1	897
24.		-50	1399.8	-133.7	780	-60	156	8670.3	780

5.4 Chapter Conclusions

Chapter 5 was dedicated to study the tank decanting of Biogas. Thermodynamic behavior of mixture of gases is complex and finding the point where phase transformation takes place during decanting is an even more complex task requiring to make numerous assumptions. In this study initial liquefaction was predicted by using the saturation curve generated by REFPROP for the given mixture. It was found that fuel liquefaction was observed in all the decanting cases studied and the minimum temperatures observed were much lower than that observed for Methane. **Table 5-C** gives the overview of the fluid mixture phase observed at the end of tank decanting under respective flow rates and corresponding system initial conditions.

The study shows that the tank walls would experience immense thermal stresses during fuel mixture decanting. If the decanting is continued until the preset final pressure of 14bar the possibility of tank liner failure is imminent in all the decanting cases and there is a need to avoid it under any circumstances. Similar approach as suggested in **Chapter 4** has to be incorporated to avoid liquefaction of mixture within the tank. The point where liquefaction starts has been identified in all the cases through GFSSP simulations (summarized in **Table 5-B**) and it should be treated as a guiding point to apply appropriate approach to avoid liquefaction.

Table 5-C: Final Phase of fluid mixture after decanting to 14bar

System Initial Pressure (bar)	System Initial Temperature (°C)	Decanting Flow rate (Kg/s)		
		F1=0.064	F2=0.11975	F3=0.3
250	20	Liquid	Liquid	Liquid
250	10	Liquid	Liquid	Liquid
218.2	0	Liquid	Liquid	Liquid
197	-10	Liquid	Liquid	Liquid
175.7	-20	Liquid	Liquid	Liquid
154.5	-30	Liquid	Liquid	Liquid
133.3	-40	Liquid	Liquid	Liquid
112.3	-50	Liquid	Liquid	Liquid

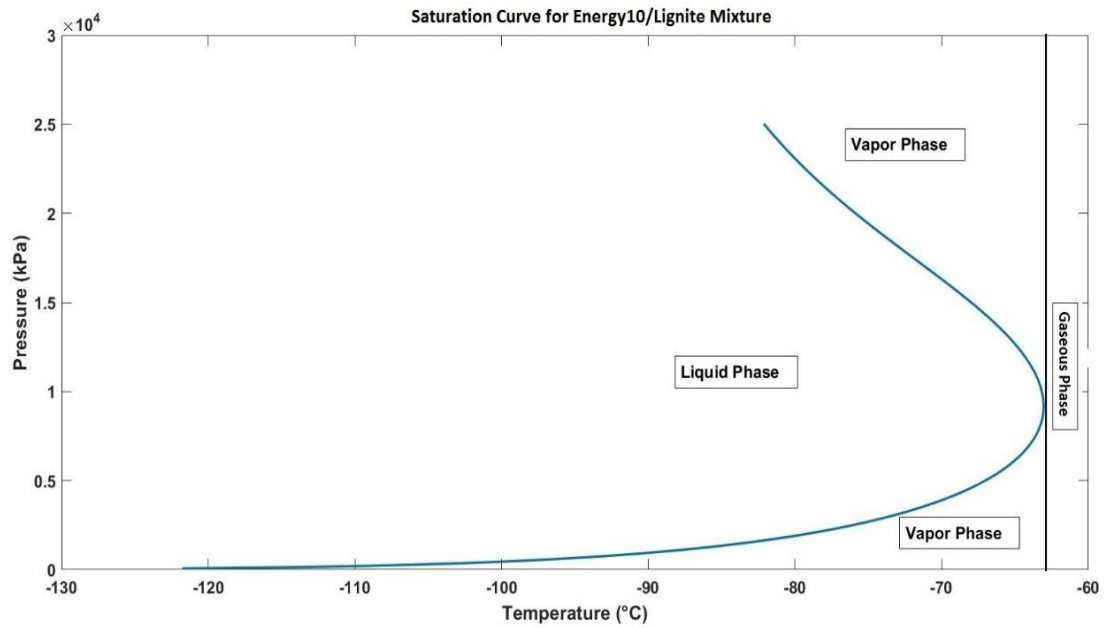

Figure 5-1: Saturation Curve for Biogas

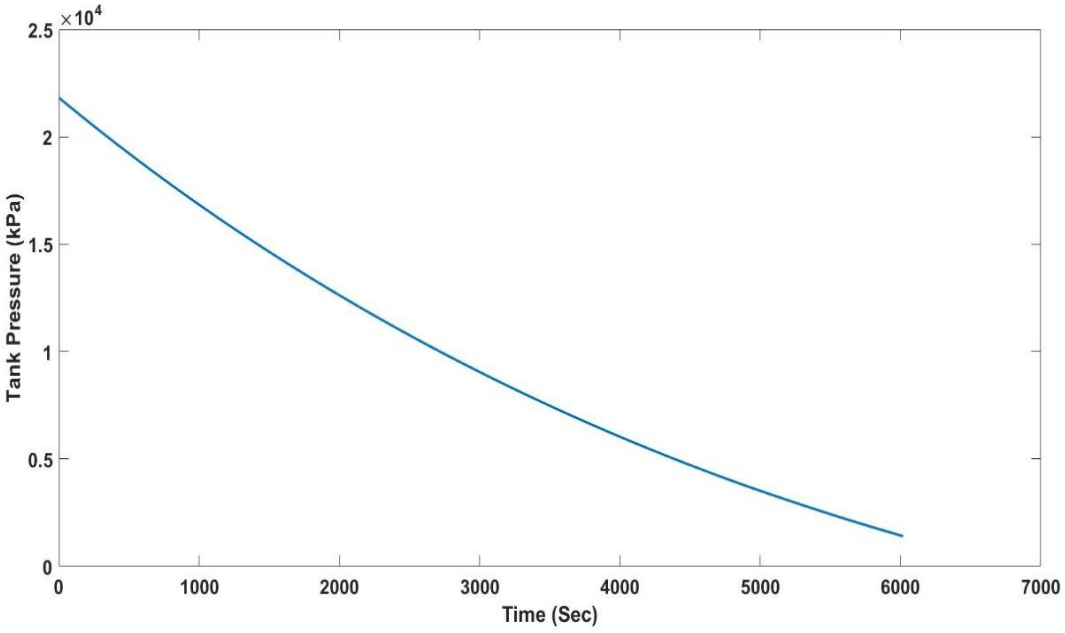

Figure 5-2: Tank Pressure Vs Time plot when the initial temperature of the system is 0°C and tank decanting rate is 0.064kg/s. Time taken to reach 14bar=6018s

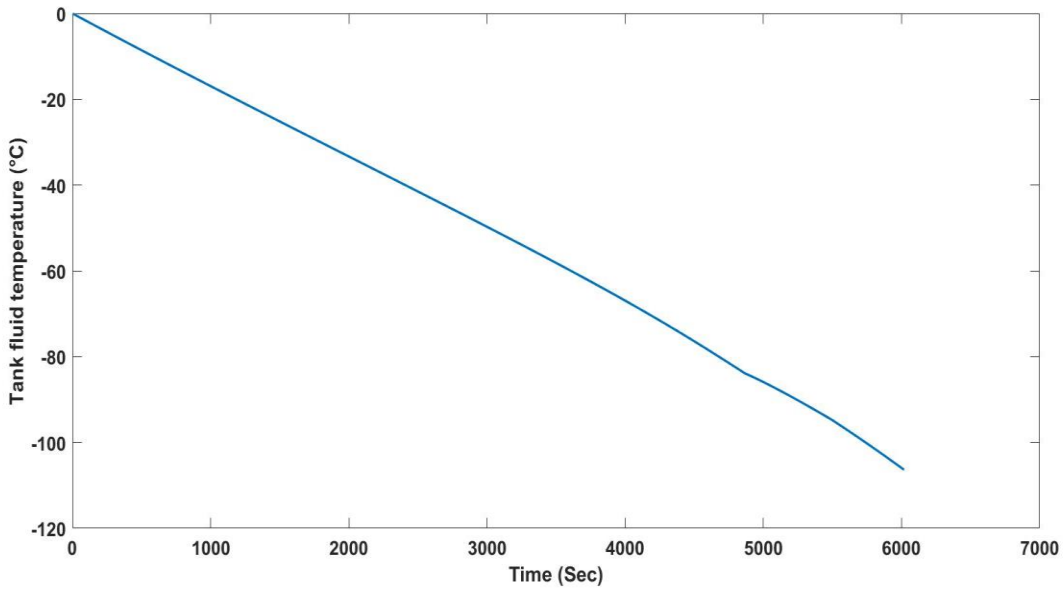

Figure 5-3: Tank Fluid (Biogas) Temperature Vs time plot when initial temperature of the system is 0°C and tank decanting rate is 0.064kg/s. Minimum observed temperature of the fluid is -106.4°C.

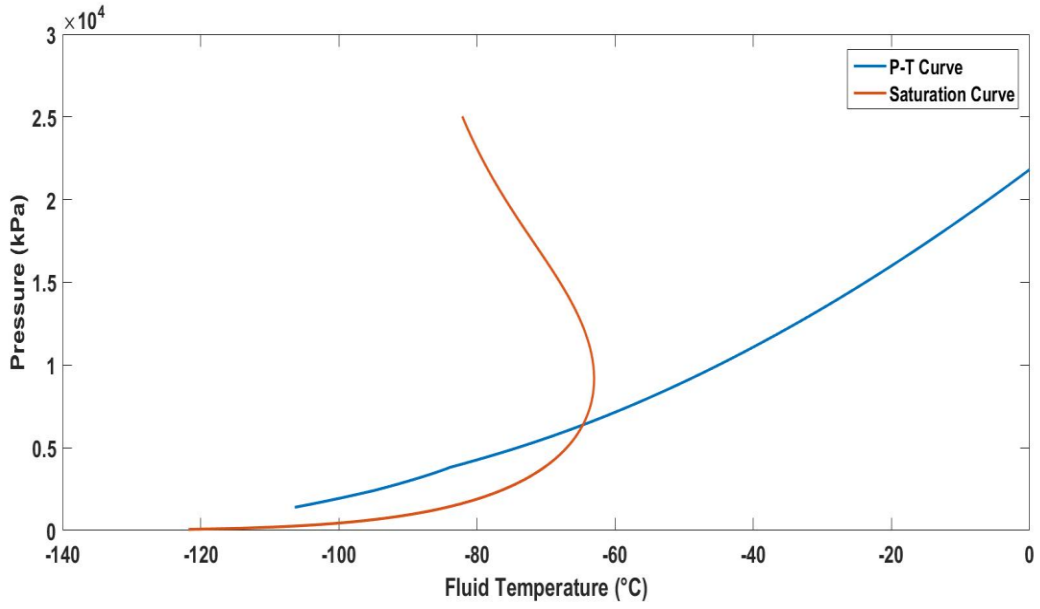

Figure 5-4: Pressure (kPa)-Temperature (°C) Vs Saturation Curve plot for Biogas mixture decanting at 0.064kg/s where the system initial conditions are at 218.2 bar and 0°C

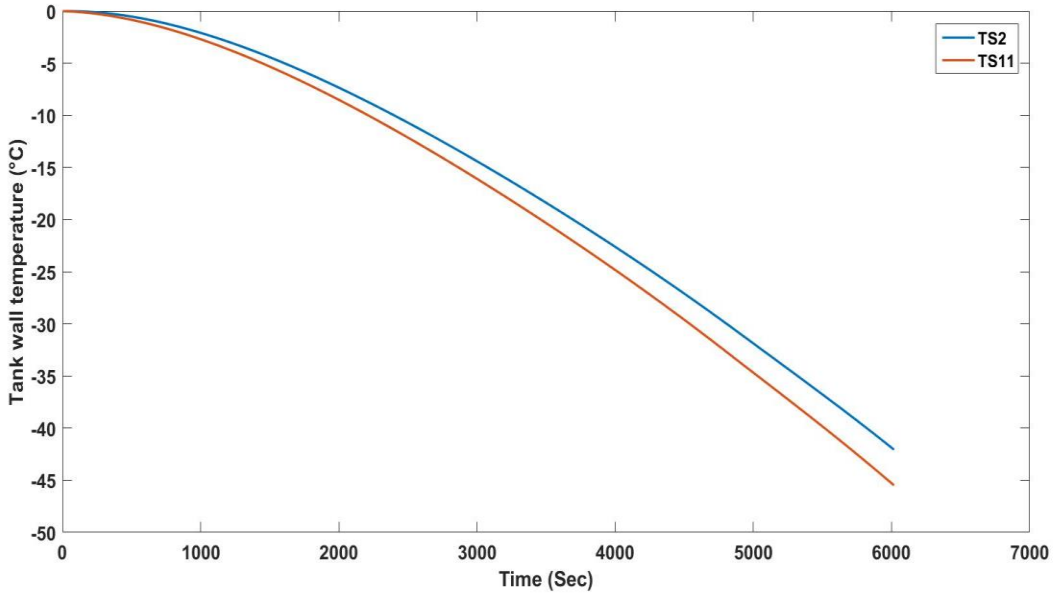

Figure 5-5: Tank wall Temperature (°C) Vs Time plot when the initial temperature of the system is 0°C and tank decanting rate is 0.064kg/s. Minimum observed temperature of the wall is -45.5°C

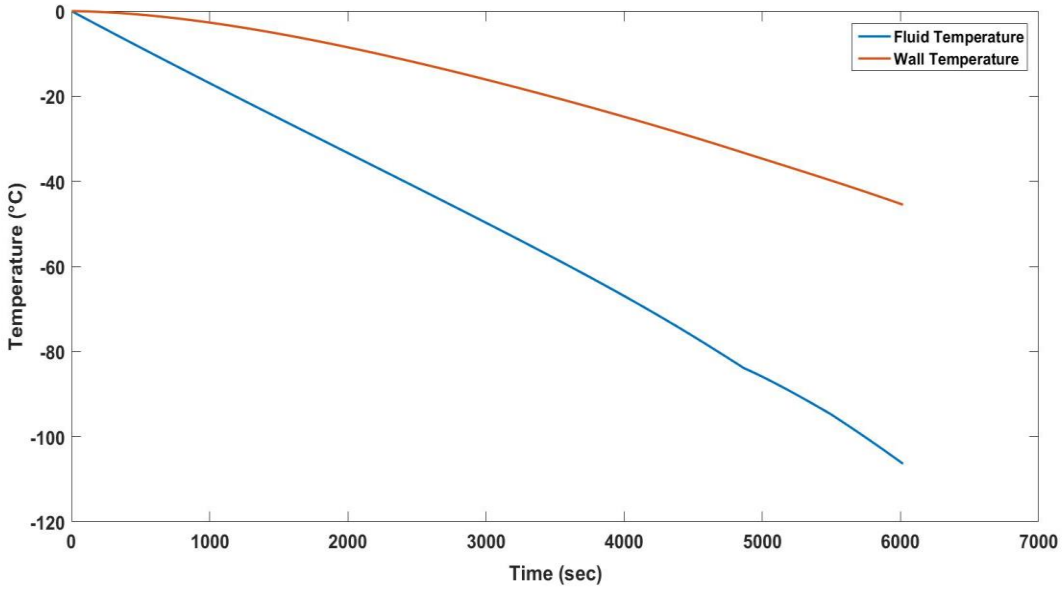

Figure 5-6: Wall Temperature (°C) Vs Fluid temperature (°C) when the initial temperature of the system is 0°C and tank decanting rate is 0.064kg/s. Minimum observed fluid and wall temperatures are -106.4°C and -45.5°C respectively

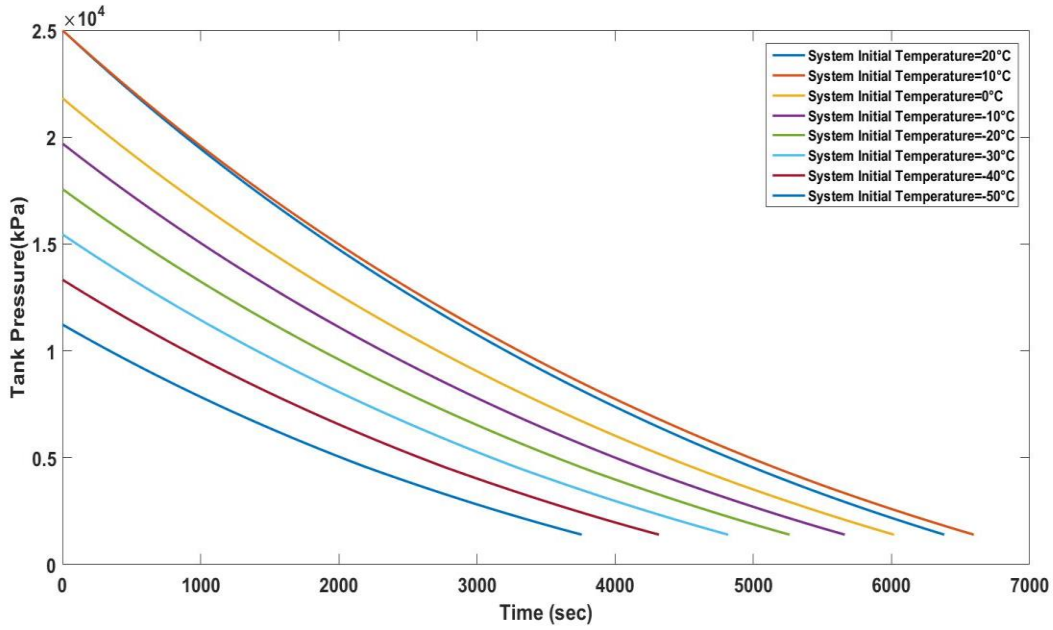

Figure 5-7: Cumulative Tank Pressure (kPa) vs Time (sec) plot for different system initial temperatures with decanting rate of 0.064kg/s

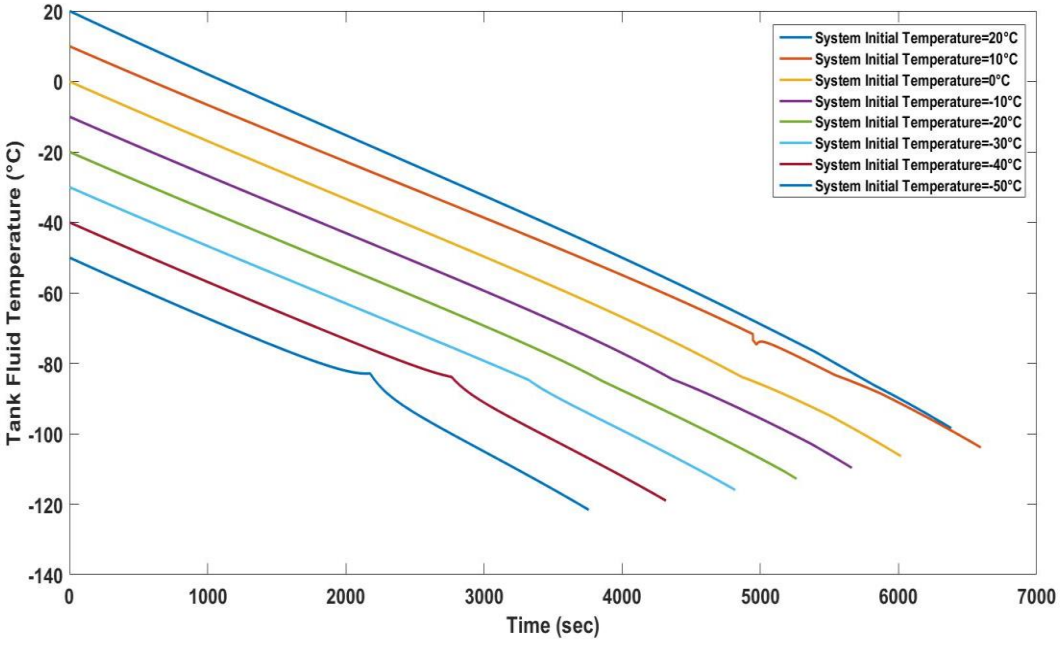

Figure 5-8: Cumulative Fluid temperature (°C) (Biogas) vs Time (sec) plot for different system initial temperatures with decanting rate of 0.064kg/s

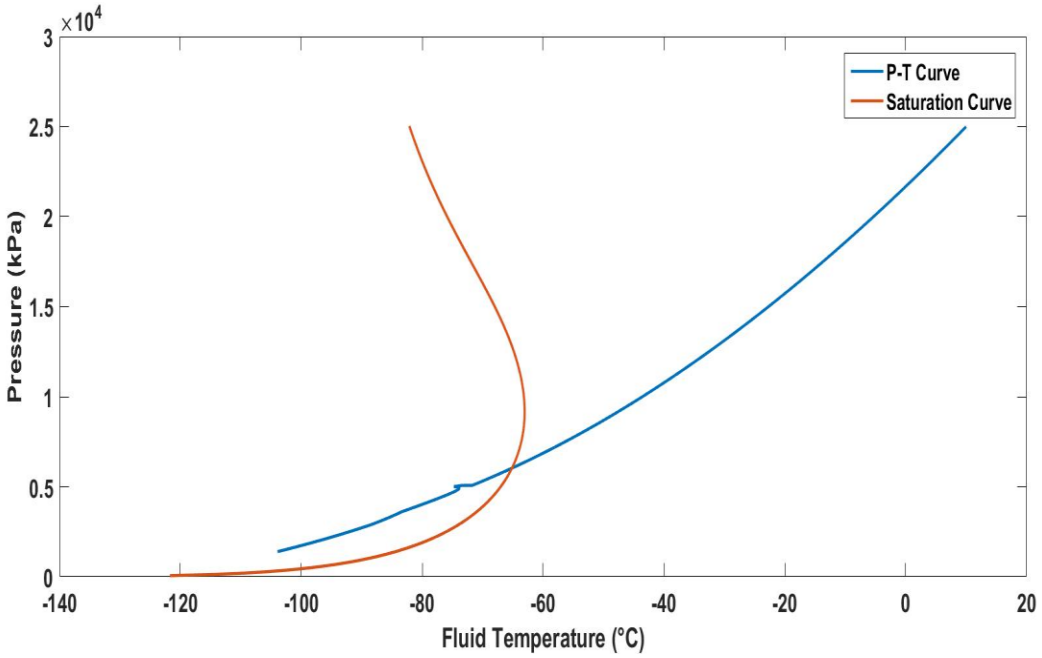

Figure 5-9: Pressure (kPa)-Temperature (°C) Vs Saturation Curve plot for Biogas mixture decanting at 0.064kg/s where the system initial conditions are at 250 bar and 10°C

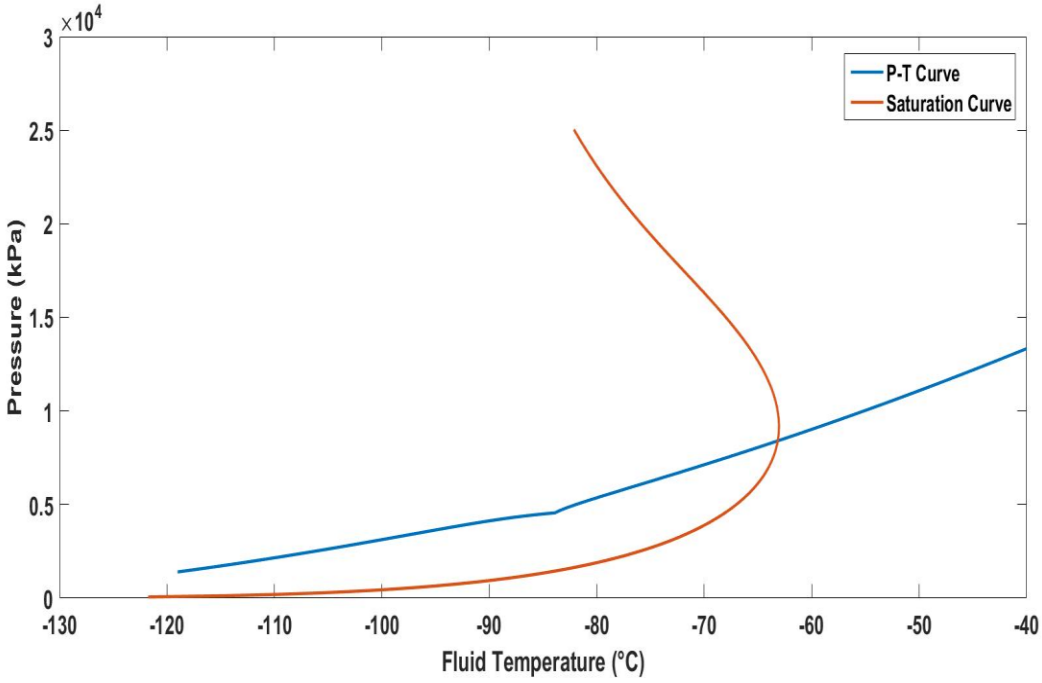

Figure 5-10: Pressure (kPa)-Temperature (°C) Vs Saturation Curve plot for Biogas mixture decanting at 0.064kg/s where the system initial conditions are at 133.3 bar and -40°C

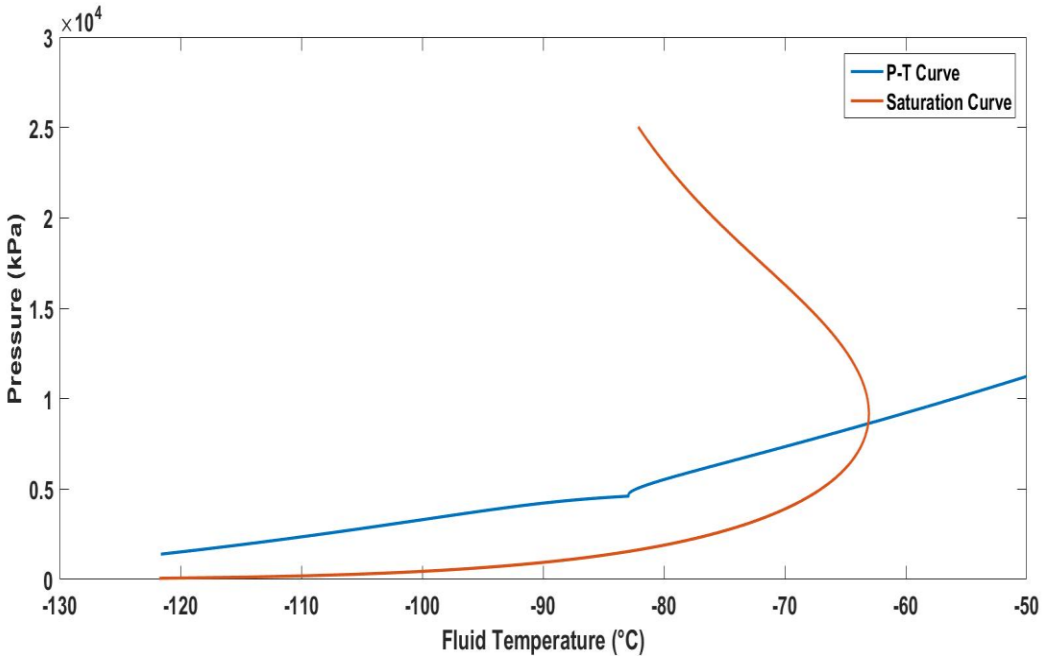

Figure 5-11: Pressure (kPa)-Temperature (°C) Vs Saturation Curve plot for Biogas mixture decanting at 0.064kg/s where the system initial conditions are at 112.3 bar and -50°C

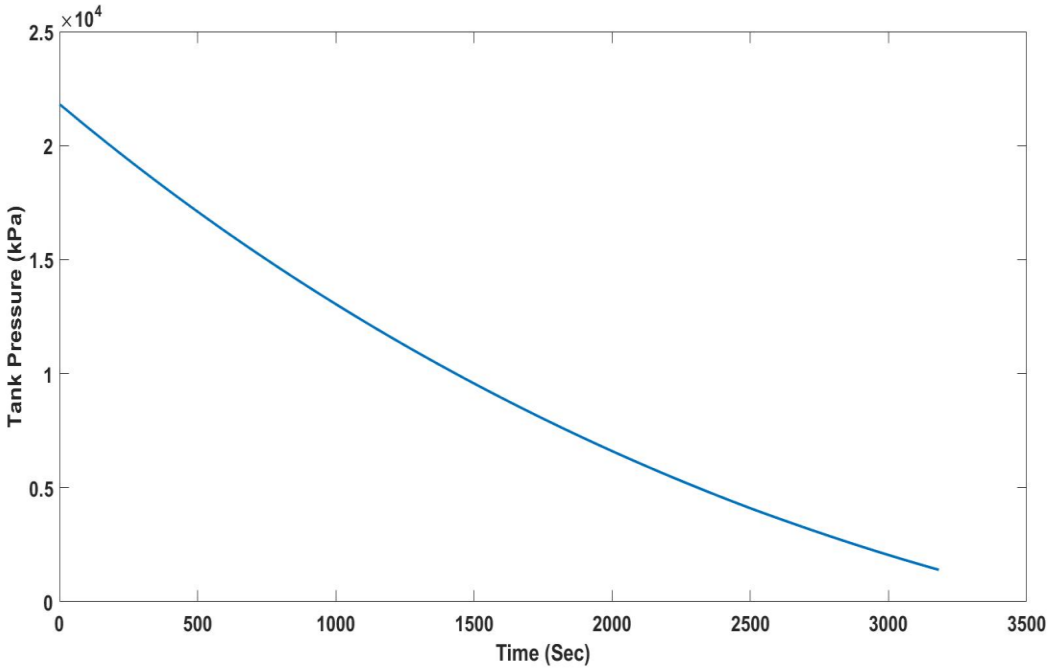

Figure 5-12: Tank Pressure Vs Time plot when the initial temperature of the system is 0°C and tank decanting rate is 0.11975kg/s. Time taken to reach 14bar=3182s

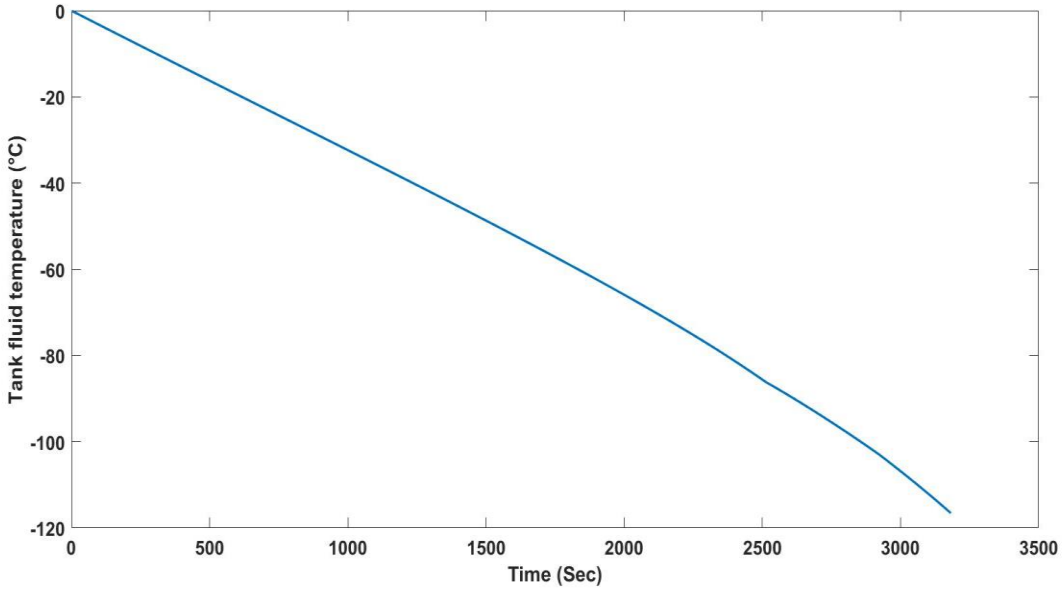

Figure 5-13: Tank Fluid (Biogas) Temperature Vs time plot when initial temperature of the system is 0°C and tank decanting rate is 0.11975kg/s. Minimum observed temperature of the fluid is -116.6°C

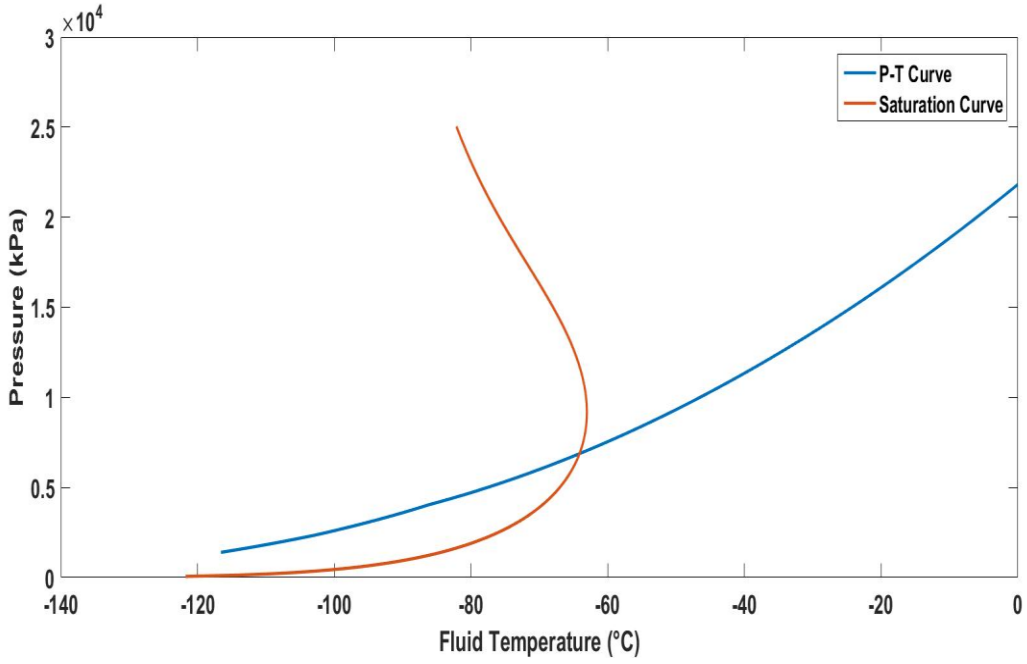

Figure 5-14: Pressure (kPa)-Temperature (°C) Vs Saturation Curve plot for Biogas mixture decanting at 0.11975kg/s where the system initial conditions are at 218.2 bar and 0°C

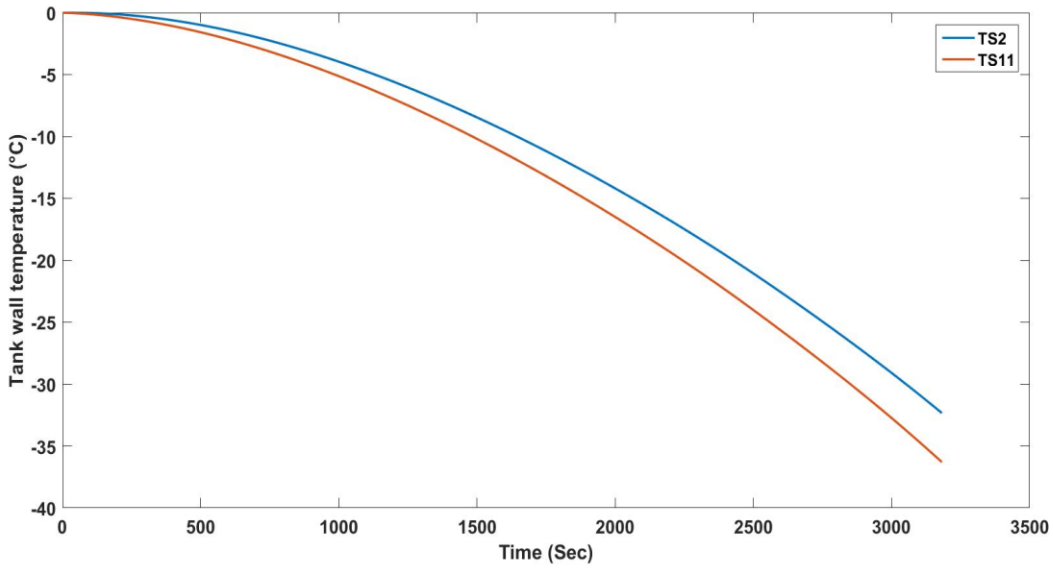

Figure 5-15: Tank wall Temperature (°C) Vs Time plot when the initial temperature of the system is 0°C and tank decanting rate is 0.11975kg/s. Minimum observed temperature of the wall is -36.3°C

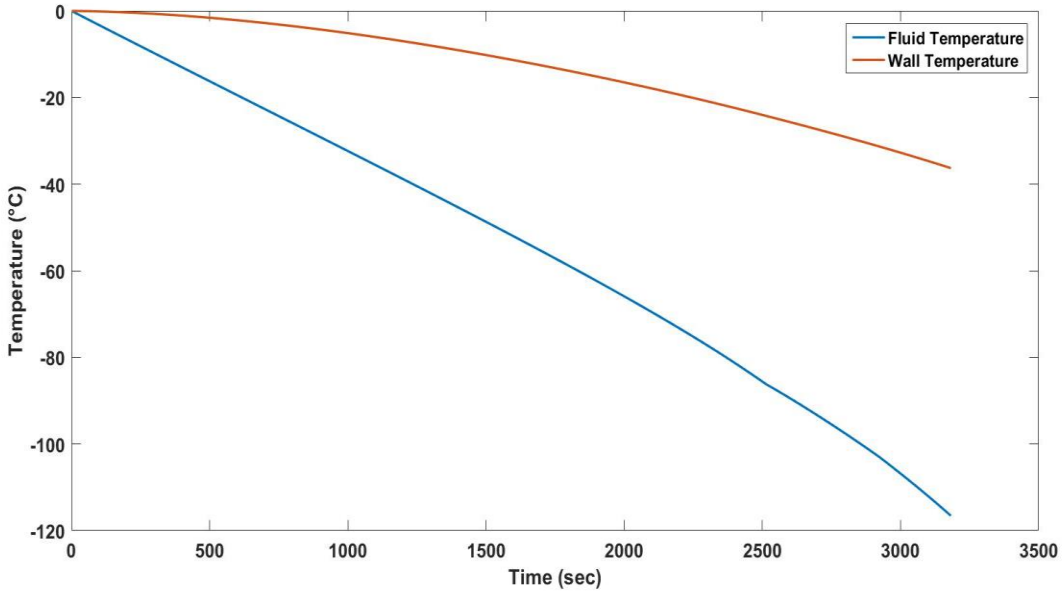

Figure 5-16: Wall Temperature (°C) Vs Fluid temperature (°C) when the initial temperature of the system is 0°C and tank decanting rate is 0.11975kg/s. Minimum observed fluid and wall temperatures are -116.6°C and -36.3°C respectively

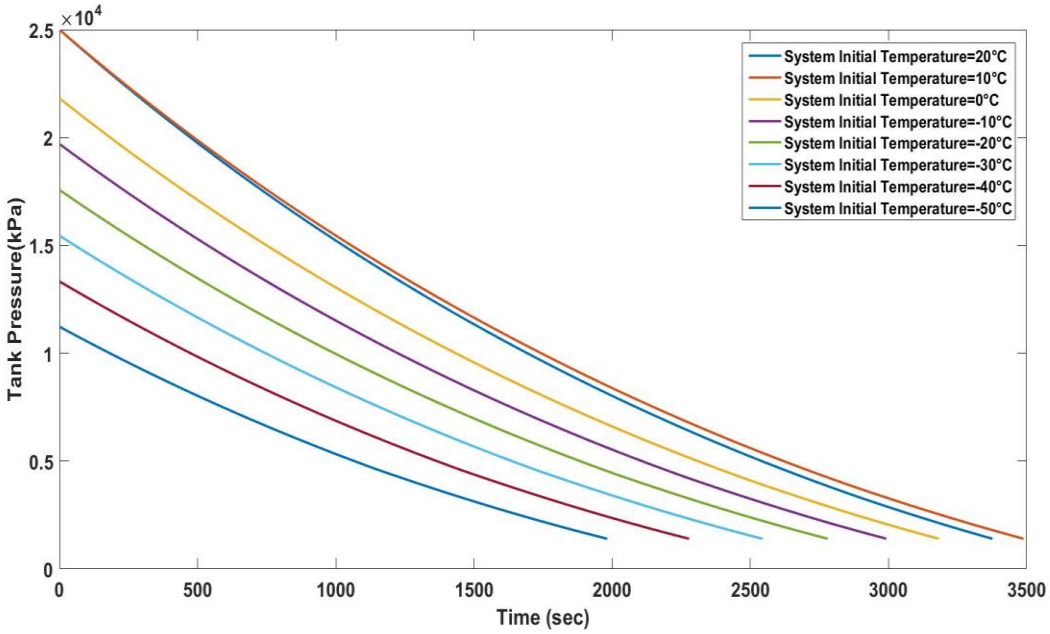

Figure 5-17: Cumulative Tank Pressure (kPa) vs Time (sec) plot for different system initial temperatures with decanting rate of 0.11975kg/s

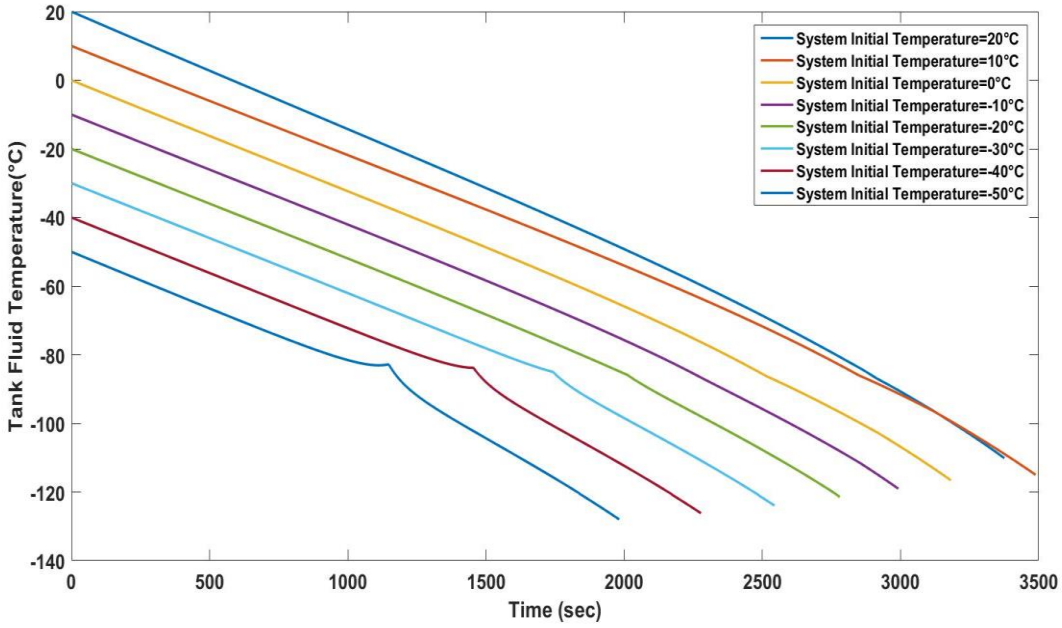

Figure 5-18: Cumulative Fluid temperature (°C) (Biogas) vs Time (sec) plot for different system initial temperatures with decanting rate of 0.11975kg/s

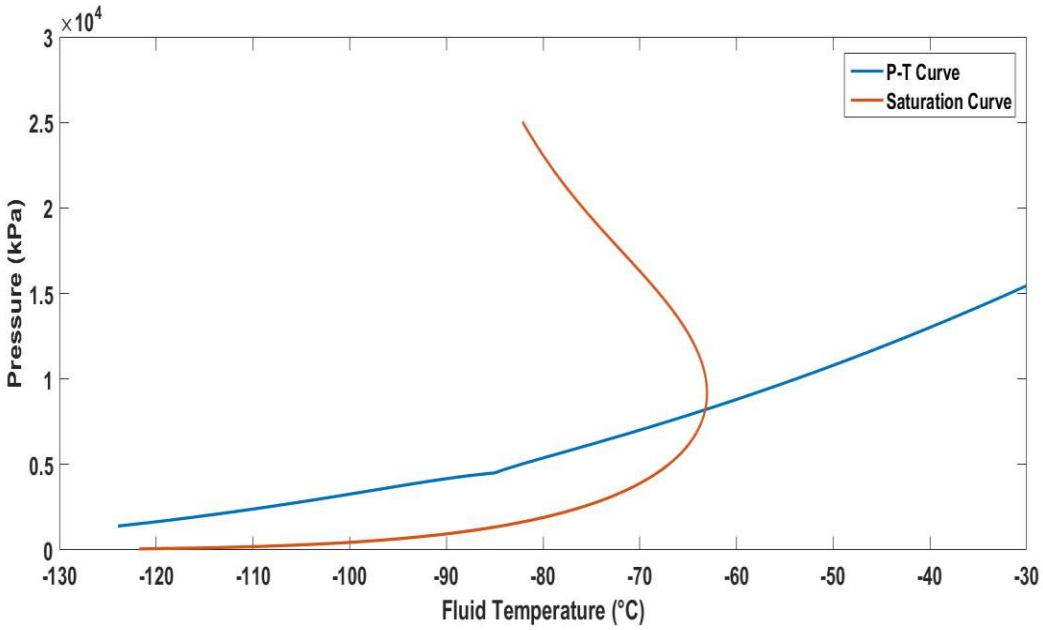

Figure 5-19: Pressure (kPa)-Temperature (°C) Vs Saturation Curve plot for Biogas mixture decanting at 0.11975kg/s where the system initial conditions are at 154.5 bar and -30°C

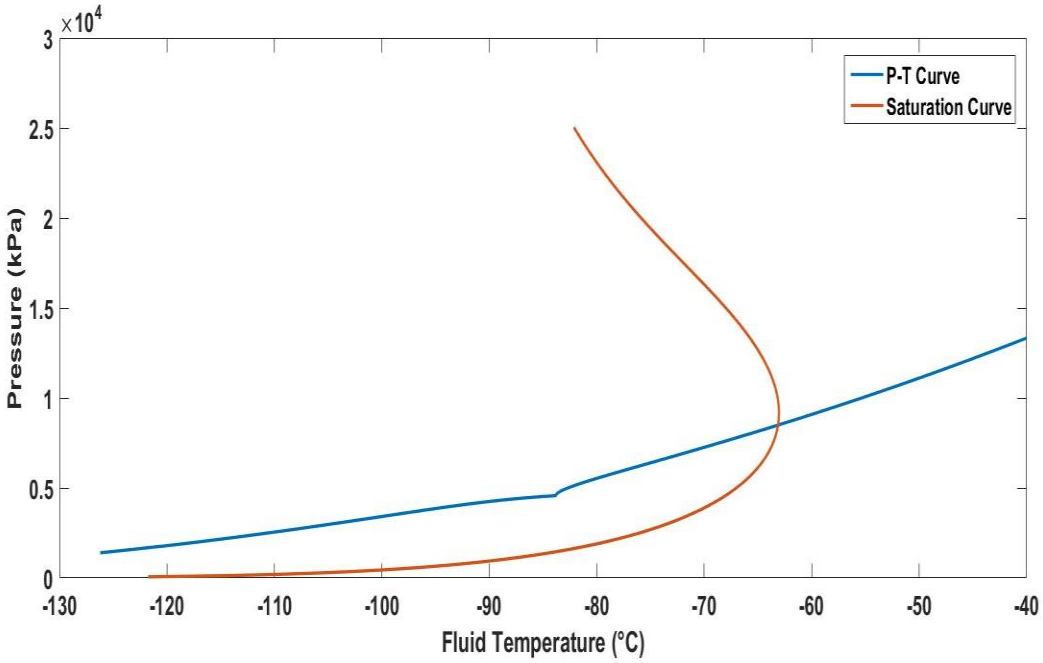

Figure 5-20: Pressure (kPa)-Temperature (°C) Vs Saturation Curve plot for Biogas mixture decanting at 0.11975kg/s where the system initial conditions are at 133.3 bar and -40°C

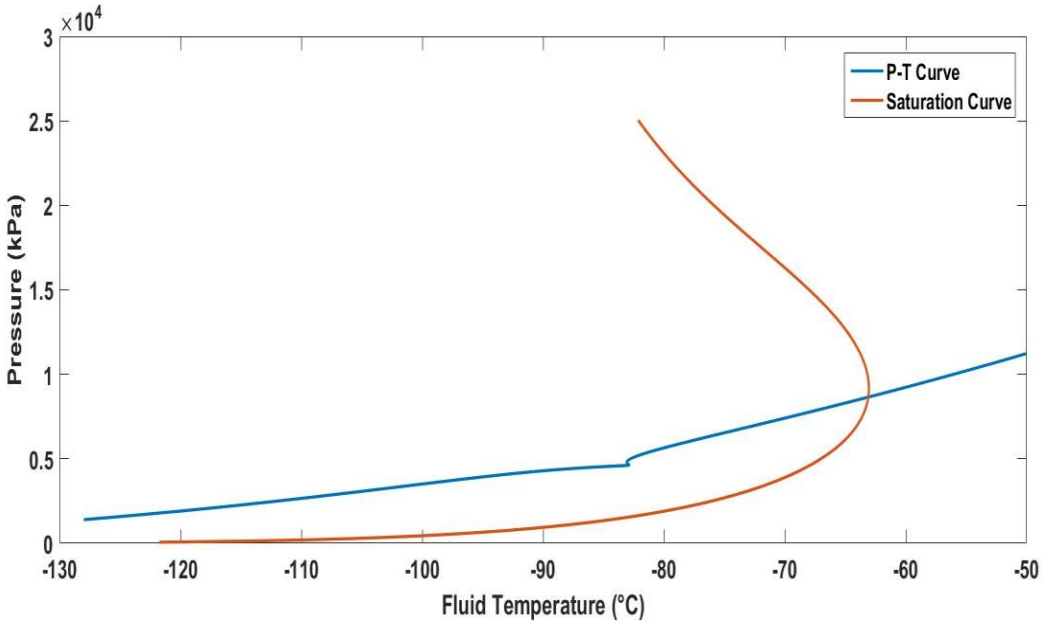

Figure 5-21: Pressure (kPa)-Temperature (°C) Vs Saturation Curve plot for Biogas mixture decanting at 0.11975kg/s where the system initial conditions are at 112.3 bar and -50°C

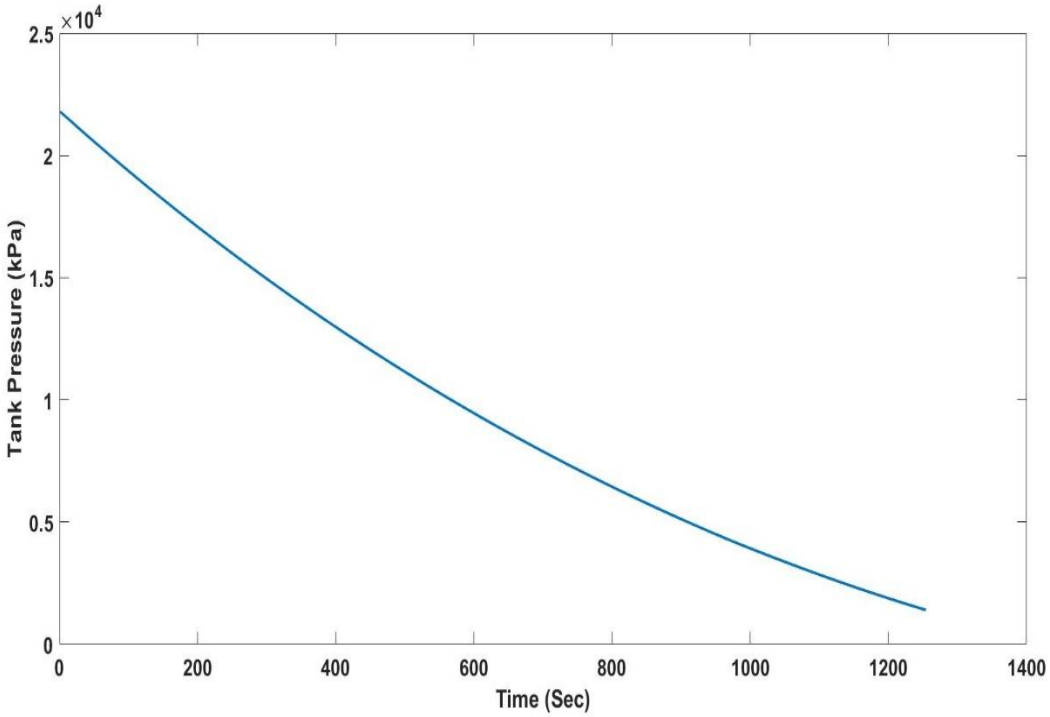

Figure 5-22: Tank Pressure Vs Time plot when the initial temperature of the system is 0°C and tank decanting rate is 0.3kg/s. Time taken to reach 14bar=1254s

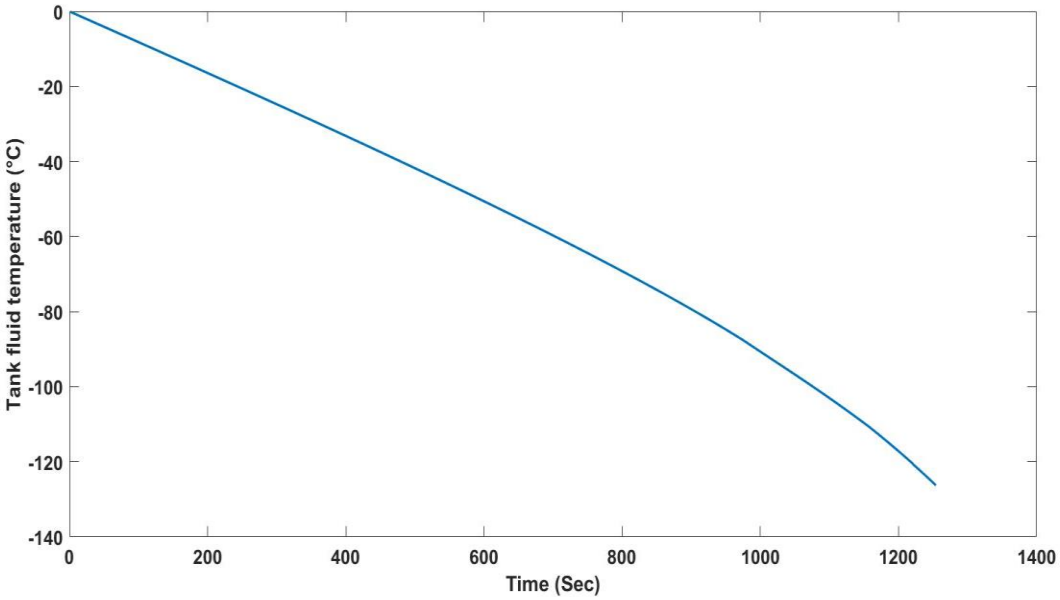

Figure 5-23: Tank Fluid (Biogas) Temperature Vs time plot when initial temperature of the system is 0°C and tank decanting rate is 0.3kg/s. Minimum observed temperature of the fluid is -126.3°C

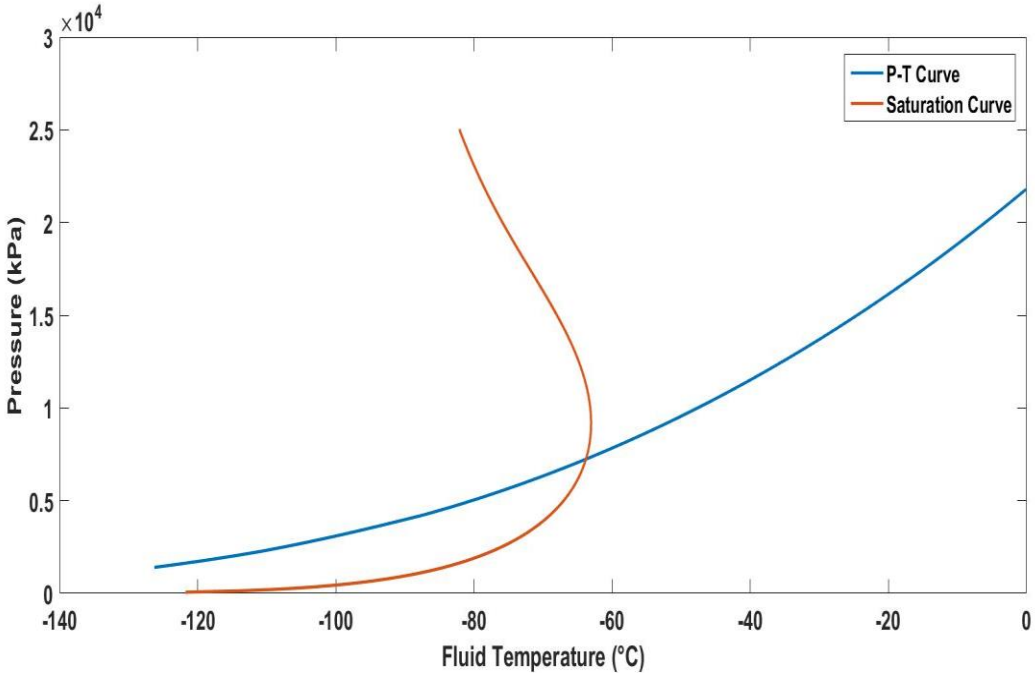

Figure 5-24: Pressure (kPa)-Temperature (°C) Vs Saturation Curve plot for Biogas decanting at 0.3kg/s where the system initial conditions are at 218.2 bar and 0°C

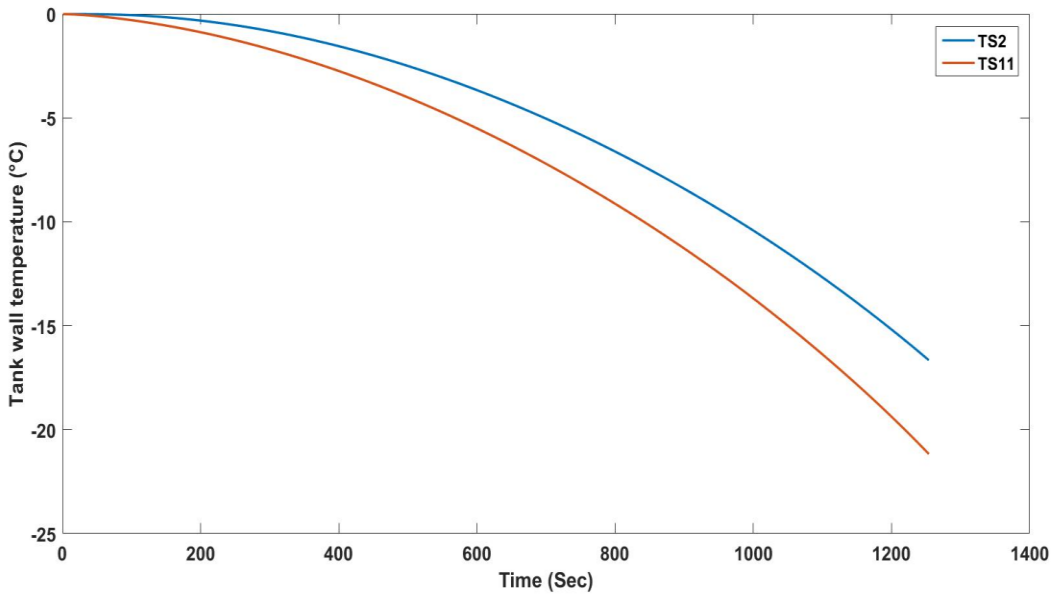

Figure 5-25: Tank wall Temperature (C) Vs Time plot when the initial temperature of the system is 0°C and tank decanting rate is 0.3kg/s. Minimum observed temperature of the wall is -21.2°C

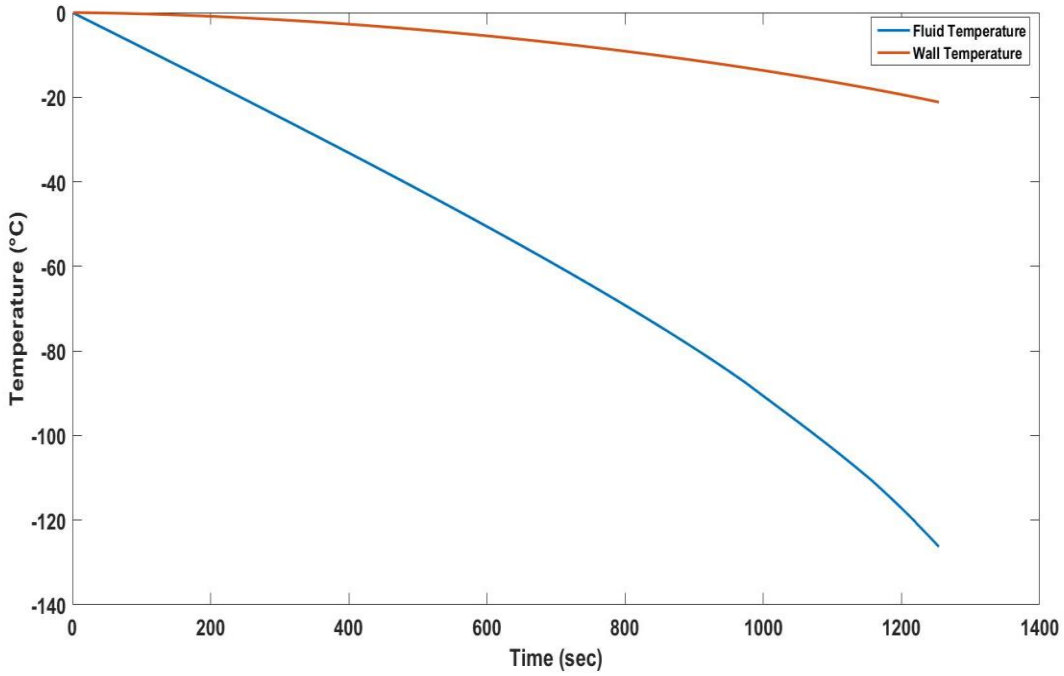

Figure 5-26: Wall Temperature (°C) Vs Fluid temperature (°C) when the initial temperature of the system is 0°C and tank decanting rate is 0.3kg/s. Minimum observed fluid and wall temperatures are -126.3°C and -21.2°C respectively

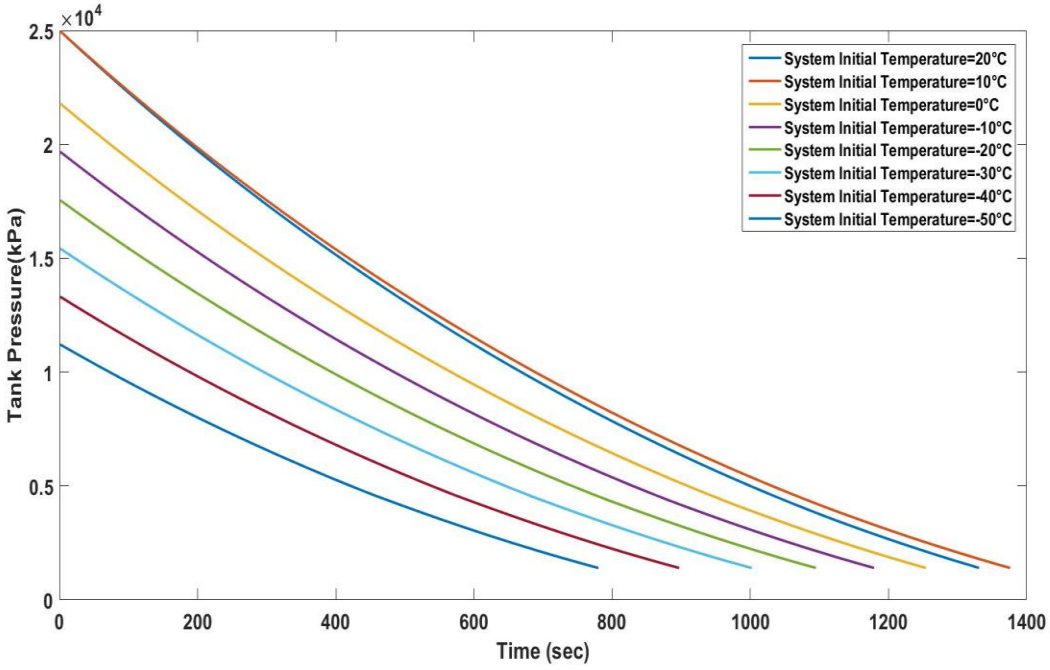

Figure 5-27: Cumulative Tank Pressure (kPa) vs Time (sec) plot for different system initial temperatures with decanting rate of 0.3kg/s

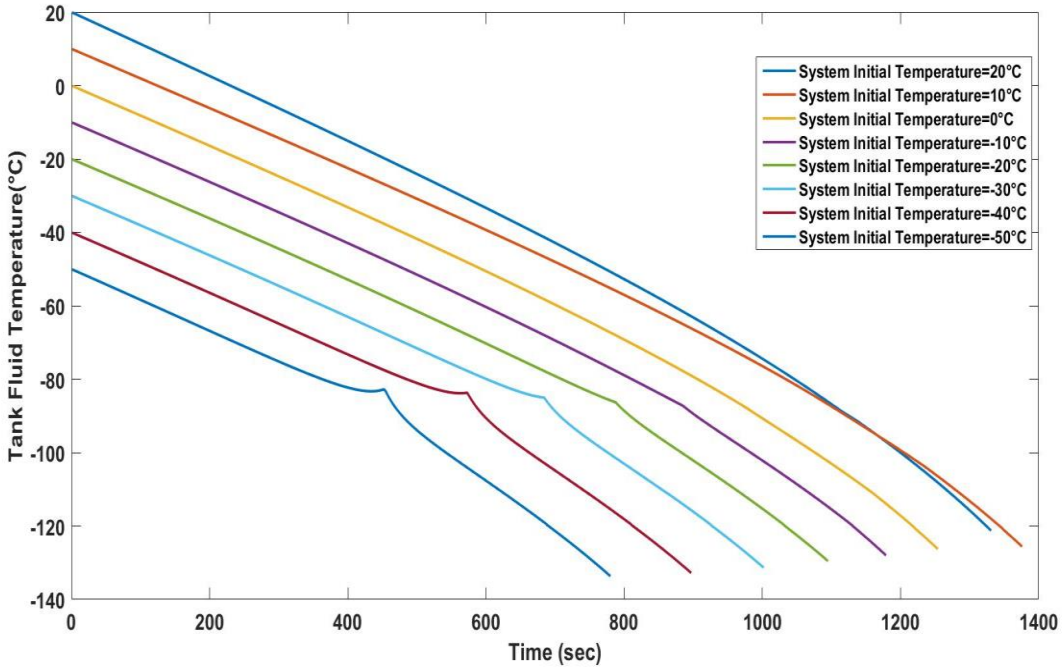

Figure 5-28: Cumulative Fluid temperature (°C) (Biogas) vs Time (sec) plot for different system initial temperatures with decanting rate of 0.3kg/s

Chapter 6 : Results of Methane Tank Decanting using ASPEN Plus

ASPEN stands for Advanced System for Process Engineering, it is one of the markets leading chemical process optimization software used by the bulk, fine, specialty, & biochemical industries, as well as the polymers industry for the design, operation, and optimization of safe, profitable manufacturing facilities. ASPEN can perform many types of thermodynamic calculations, or to retrieve and/or correlate thermodynamic and transport data. In the present study ASPEN Plus software was utilized to study Methane tank decanting simulations under the conditions described in **Chapter 4**.

Figure 6-1 shows the Methane Tank Decanting flow network in Aspen Plus in static environment. In Aspen plus first the flow network has to be sketched in static environment and all the initial properties has to be specified in this domain. Once the sketch has been generated in the static environment it is then exported into the Dynamic simulation domain where flow controllers are added which give a definite flow path for the fluid flow. The static flow network consists of three valves and a central drum. Valve ‘v1’ is the feed valve from which Methane at required pressure and temperature is filled in the central drum. The valve ‘v1’ is cutoff once the central drum reaches the required starting tank capacity for decanting. The central drum is then connected to two valves ‘v2’ and ‘v3’ which are initially closed. The valve ‘v2’ is the vapor valve and only vapor from the tank is allowed to flow through this valve. The valve ‘v3’ is the liquid valve and only liquid is allowed to flow through the valve. During initial stages of the decanting process, Methane vapors flow through the valve ‘v2’ whose exit flow rate is manually specified as per user requirements. As the decanting is continued if there is any liquid Methane formation it would be evident from the increased flow rate in valve ‘v3’ whose flow rate until that point is zero. The decanting will be stopped at this point to avoid any damage to the tank wall.

Aspen Plus doesn't allow the user to specify the tank material properties like thermal conductivity or tank physical properties such as length or thickness but it allows to specify the surface area of the tank, mass of the tank and heat capacity of the tank material. Also all Aspen plus offers is to hypothetically create a boundary around the required control volume and allow the boundary to have a non-varying single starting temperature which wouldn't change throughout the tank decanting process i.e. it considers a wall to be a single node of certain mass and heat capacity held at a constant temperature. Hence the wall effects which were simulated in GFSSP will not be seen in the present simulations with Aspen Plus. In all the previous studies with GFSSP we have seen that tank wall was pumping heat in the tank and the temperature of the fluid within the tank was getting effected with this heat input and in conjunction the tank wall was getting colder due to the expansion of the fluid within the tank. But in Aspen plus simulations due to unavailability of a method to include the wall effects a single constant temperature boundary was selected to act as the tank wall and hence the results obtained for tank decanting will be relatively different from what was obtained with GFSSP but the trends of the results will be the similar.

Figure 6-2 shows Aspen Plus Methane tank decanting flow network in dynamic environment. As explained above in static environment there are no flow controllers added which would define a definite flow path for the fluid flow. Once the general sketch for the flow network has been generated in static environment, the static file is exported to dynamic simulation interface in Aspen Plus. This exported file is a general flow network and still doesn't have any physical or thermal properties defined to any individual component. Before the flow simulation is initialized pressure controllers, flow controllers and temperature controllers are added between appropriate components to achieve a well-defined flow channel.

In **Figure 6-2** a pressure controller has been added between the valve ‘v1’ and the drum whose function is to cutoff the valve ‘v1’ once the drum reaches the required tank starting pressure condition. As you can see from **Figure 6-2** Methane enters into the drum through valve ‘v1’ from the feed system. As the pressure in the drum/tank increases and reaches the required starting point, the valve ‘v1’ is sent a control signal to stop the feed system from pumping Methane any further and thus no more Methane enters the drum from this point onwards.

A temperature controller is added between the inlet and outlet of the drum and the function of the temperature controller is to record the temperature within the tank and also before the decanting has started the fluid within the tank is lowered to required starting decanting temperature.

A flow controller is added between the outlet and inlet to valve ‘v2’ which is a vapor only valve. The valve ‘v2’ allows only vapors to flow through it and it blocks any liquid Methane trying to escape through the valve. The function of the flow controller is to adjust the outlet flow rate of valve ‘v2’ to selected flow rate. In GFSSP we have seen that the valve area is adjusted for number of time steps before the required fixed flow rate is achieved but in Aspen plus the outlet flowrate required is achieved instantaneously. The tank decanting is stopped once the pressure in the drum reaches preset pressure of 14bar.

Figure 6-3 shows the complete dynamic setup for Aspen plus dynamic simulation run. Here different windows can be custom opened as per user requirements. For the present simulation different windows to be monitored are process flowsheet, drum results table, S2 result table, feed results table, tank plot, flows plot, all global variables, pressure controller, flow controller and temperature controller, function of each will follow in next few paragraphs.

Process flowsheet shows the dynamic setup outlook for the flow network generated where all the controllers can be seen. **Drum results table** gives a dynamic view for decanting results generated by Aspen plus. Here instantaneous pressure, temperature values in the tank during decanting under specified conditions can be tracked. 'S2' is a flow node located at the outlet of the vapor valve 'v2' and the S2 results table allows users to track the fluid flow rate through the valve 'v2'. **Feed results table** though it doesn't play any role during decanting simulation, it is required for tracking the pressure and temperature in the tank during tank filling process. **Tank plot** as the name suggests it displays the results for temperature, pressure and vapor fraction for the fluid within the tank during decanting. The most important feature of Aspen plus is that it calculates vapor fraction at each time step and plot the value on the graph which allows the user to monitor if there is any liquid Methane formation within the tank. Aspen plus also allows the user to export these generated results in excel format which can be further used for post processing. **Flows plot** allows the user to track the flow rate, exit pressure from the selected valve. If any fluctuation in flow rates are observed, then the simulation can be stopped and proper steps can be taken to maintain the required flowrate. **'All global variables'** window allows the user to cross check all the fixed properties such as ambient temperature, surface area of tank, volume of the tank assigned to the flow network. The three different controllers in the flow network i.e. pressure, temperature and flow controllers allows the user to track the corresponding properties dynamically.

Figure 6-4 shows Aspen plus simulation window when tank decanting is in progress. As it can be seen the pressure, temperature in the tank is falling as the decanting is carried out.

6.1 Decanting Flow Rate Selected is 0.064kg/s

Figure 6-5, Figure 6-6 shows the pressure and temperature histories for Methane tank decanting with a flow rate of 0.064kg/s when the initial pressure and temperature were 218.2 bar and 0°C respectively. It is observed that the decanting takes 23688 seconds for the pressure in the tank to fall to 14bar with minimum observed temperature of fluid as -24.8°C. The minimum temperature in the tank was observed when the pressure in the tank was 58.9bar which is 17568seconds after the decanting has started. It can be observed that the temperature in the tank doesn't fall below the critical temperature of Methane and thus no liquid Methane formation is observed within the tank.

But as per the results obtained using GFSSP we found that from **Figure 4-3, Figure 4-4** the minimum observed temperature in the tank was -42.1°C which occurs 19909seconds after the decanting has started when the pressure in the tank was 47.3bar. This difference in values was expected as it was clearly stated earlier that Aspen plus is not capable of including the wall effects. In GFSSP during the start of the decanting process the tank ambient temperature, tank wall temperature and the tank fluid temperature are the same. Once the decanting starts the temperature of the fluid within the tank falls and thus the temperature of the inside of the tank wall starts to fall as well but the wall temperature is higher than the temperature of the adjacent fluid in contact. So due to this temperature difference between the tank wall and the fluid, the tank walls pumps heat into the system. Also as the ambient temperature is constant the outside surface of the wall gets increasing heat input with every time step as the temperature of the tank wall falls with the temperature of the fluid. Due to considerable thickness of the wall considerable heat energy gets stored in the tank wall and it doesn't allow the tank wall to get as cold as the fluid within the tank. Because of this complex heat exchange phenomenon happening within the tank and tank wall the temperature of the Methane observed is lower than that observed with Aspen plus as the amount of heat being pumped in the tank is decreasing with time in GFSSP.

In Aspen plus as the tank wall temperature is held constant with the ambient temperature the amount of heat pumped into the system increases with time during decanting as the temperature difference between the wall and tank fluid is increasing and thus more and more heat gets pumped into the system. Hence the temperature of the fluid observed is more than what is observed when Methane decanting is simulated in GFSSP.

Figure 6-7 shows the comparison of Pressure-Temperature (P-T) curve for Methane tank decanting with the saturation curve of Methane under the decanting conditions mentioned above. As it can be seen from **Figure 6-7** that the temperature of the Methane in the tank never fell below the critical temperature and hence there is no possibility of liquid Methane formation within the tank in the specified decanting conditions.

Figure 6-8 shows the comparison of pressure plots obtained from Aspen plus and GFSSP under similar conditions as specified above. As it is observed the pressure plots obtained from both the software closely trace each other and the observed differences in the two pressure plots is because of the absence of wall effects in Aspen Plus. The plot shows that the trends of pressure drop are similar in both the software's.

Figure 6-9 shows the comparison of tank fluid temperature plots obtained from Aspen plus and GFSSP under the conditioned specified above. The minimum fluid temperature observed during Methane decanting using Aspen plus and GFSSP are -24.8°C and -42.1°C respectively. There is a considerable difference in the tank fluid temperature plots which is justified as Aspen plus cannot include wall effects but it can be observed that even though the plots are not relatively close to each other their trends are similar.

Figure 6-10 shows a cumulative pressure plot obtained using Aspen plus for different system initial conditions with a decanting flow rate of 0.064kg/s. In all the decanting iterations the final pressure was set to be 14bar and the decanting was stopped as the pressure in the tank reached 14bar. The cumulative pressure plot **Figure 4-13** obtained using GFSSP under similar system initial conditions is comparable to the results obtained by Aspen plus. The trends for the pressure drop obtained by both the software match each other with close approximation suggesting that the results obtained are repeatable using any standard thermodynamic simulation software under the system boundary specified.

Figure 6-11 shows a cumulative temperature plot obtained using Aspen plus for different system initial conditions with a decanting flow rate of 0.064kg/s. The temperature values obtained from Aspen plus are not as comparable with GFSSP results as pressure values but the trend of the results are similar.

6.2 Decanting Flow Rate Selected is 0.11975kg/s

Figure 6-12, Figure 6-13 shows the pressure and temperature histories for Methane tank decanting with a flow rate of 0.11975kg/s when the initial pressure and temperature were 218.2 bar and 0°C respectively. It is observed that the decanting takes 11988 seconds for the pressure in the tank to fall to 14bar with minimum observed temperature of fluid as -36.9°C. The minimum temperature in the tank was observed when the pressure in the tank was 22.7bar which is 11988seconds after the decanting has started. It can be observed that the temperature in the tank doesn't fall below the critical temperature of Methane and thus no liquid Methane formation is observed within the tank.

Figure 6-14 shows the comparison of Pressure-Temperature (P-T) curve for Methane tank decanting with the saturation curve of Methane under the decanting conditions mentioned above. As it can be seen from **Figure 6-14** that the temperature of the Methane in the tank never fell below the critical temperature and hence there is no possibility of liquid Methane formation within the tank in the specified decanting conditions.

Figure 6-15 shows the comparison of pressure plots obtained from Aspen plus and GFSSP under similar conditions as specified above. As expected the pressure plots closely trace each other as the flow rate selected in both the simulation platforms are the same.

Figure 6-16 shows the comparison of tank fluid temperature plots obtained from Aspen plus and GFSSP under the conditioned specified above. As can be seen the minimum observed fluid temperature within the tank during decanting using GFSSP and ASPEN plus are -60.1°C and -36.9°C respectively. The difference in the temperature plots was expected as above due to absence of the wall effects.

Figure 6-17 shows a cumulative pressure plot obtained using Aspen plus for different system initial conditions with a decanting flow rate of 0.11975kg/s. In all the decanting iterations the final pressure was set to be 14bar and the decanting was stopped as the pressure in the tank reached 14bar.

Figure 6-18 shows a cumulative temperature plot obtained using Aspen plus for different system initial conditions with a decanting flow rate of 0.11975kg/s. The minimum temperature observed in all the decanting simulations with the flow rate of 0.11975kg/s was found to be -80.5°C which occurs when the system initial temperature was -50°C.

6.3 Decanting Flow Rate Selected is 0.3kg/s

Figure 6-19, Figure 6-20 shows the pressure and temperature histories for Methane tank decanting with a flow rate of 0.3kg/s when the initial pressure and temperature were 218.2 bar and 0°C respectively. It is observed that the decanting takes 5544 seconds for the pressure in the tank to fall to 14bar with minimum observed temperature of fluid as -53.8°C. The minimum temperature in the tank was observed when the pressure in the tank was 21.7bar which is 4788seconds after the decanting has started.

Figure 6-21 shows the comparison of Pressure-Temperature (P-T) curve for Methane tank decanting with the saturation curve of Methane under the decanting conditions mentioned above. The P-T curve suggests that the Methane in the tank always stays in the vapor region and also as it can be seen the minimum temperature of the fluid observed is well above the critical temperature of Methane.

Figure 6-22, Figure 6-23 shows the comparison of pressure and temperature plots obtained from Aspen plus and GFSSP under similar conditions as specified above. The pressure plots closely follow each other but the temperature plots as expected deviate from each other as the tank decanting approaches the preset final pressure of 14bar.

Figure 6-24, Figure 6-25 shows a cumulative pressure and temperature plot obtained using Aspen plus for different system initial conditions with a decanting flow rate of 0.3kg/s. The minimum temperature observed in all the decanting simulations was -93.6°C when the system initial temperature was -50°C.

Table 6-A provides a summary of results obtained by ASPEN Plus analysis for different tank decanting conditions. The system initial conditions for each simulation were kept consistent with the conditions used for Methane tank decanting as described above in **Chapter 4**. When the flow rate of 0.3kg/s was used the temperature of Methane went below the critical temperature when system initial temperatures were -40°C, -50°C and it is suggested to stop the tank decanting when the P-T curve crosses the saturation curve in these cases to prevent the cylinder liner material from any damage.

Table 6-A: Summary of results for Methane tank decanting at varying flow rates and different initial temperatures for the system.

Sl.No.	Flow rate (Kg/s)	System Initial Pressure (Bar)	System Initial Temperature (°C)	Pressure corresponding to Min Temp (kPa) **(Min Pressure)**	Min Fluid Temp (°C) **(M)**	Time at Min Temp occurs (sec) **(I)**	Time where phase transformation starts (Sec)	Pressure at which phase transformation occurs (kPa)	Time taken to empty the tank (Sec)
1.	0.064	250	20	1885.3	-10.8	22644	-	-	23364
2.		250	10	4461	-13.4	20988	-	-	24660
3.		218.2	0	5896	-25	17568	-	-	23724
4.		197	-10	5576	-34	17388	-	-	23508
5.		175.7	-20	5196.4	-43.2	17280	-	-	23292
6.		154.5	-30	4828	-52.4	17136	-	-	23076
7.		133.3	-40	4447	-61.5	16992	-	-	22788
8.		112.3	-50	3929	-70.4	17244	-	-	22428
9.	0.11975	250	20	1688.5	-18.5	12240	-	-	12600
10.		250	10	1755	-23.2	12888	-	-	13320
11.		218.2	0	2266	-37	11988	-	-	12780
12.		197	-10	2224	-46	11880	-	-	12672
13.		175.7	-20	2156	-54.4	11772	-	-	12564
14.		154.5	-30	2115	-63	11628	-	-	12420
15.		133.3	-40	2004	-72	11520	-	-	12276
16.		112.3	-50	1841	-80.5	11448	-	-	12096
17.	0.3	250	20	1943	-27	4968	-	-	5508
18.		250	10	2034	-35	5112	-	-	5724
19.		218.2	0	2170	-54	4788	-	-	5544
20.		197	-10	2117	-62	4752	-	-	5508
21.		175.7	-20	2116	-70	4680	-	-	5472
22.		154.5	-30	2097	-78	4508	-	-	5436
23.		133.3	-40	2055	-86	4536	3888	3252	5364
24.		112.3	-50	1996	-93.6	4464	2772	4295	5328

6.4 Chapter Conclusions

Studying Methane tank decanting was an important aspect of the present study and to extend it further ASPEN Plus was used to simulate the results under conditions mentioned above. It has been seen that the results obtained from GFSSP and ASPEN plus don't trace each other and reason for this has been discussed in detail in **Chapter 6**. Due to the absence of wall effects in ASPEN plus the heat pumped into the system by the wall increases as the decanting progresses. This increased heat input doesn't let the Methane within the tank to liquefy. Even though the simulation doesn't give a relativistic prediction for Methane liquefaction but indirectly these simulations give us a solution to avoid Methane liquefaction. If the wall temperature was maintained to the ambient temperature by external heating, Methane liquefaction could be avoided in most of the predicted cases and for the two cases where Methane liquefaction is still predominant there the decanting flow rate can be reduced to achieve the required results. From the results simulated it was found that the pressure plots from GFSSP and ASPEN plus trace each other closely i.e., their values lie within 5% error but the temperature plots though having the similar trend but their values differ greatly i.e., by almost 39% difference between them by the end of decanting, reason for which has been explained above.

Table 6-B: Final Phase of fluid after decanting to 14bar

System Initial Pressure (bar)	System Initial Temperature (°C)	Decanting Flow rate (Kg/s)		
		F1=0.064	F2=0.11975	F3=0.3
250	20	Gas	Gas	Gas
250	10	Gas	Gas	Gas
218.2	0	Gas	Gas	Gas
197	-10	Gas	Gas	Gas
175.7	-20	Gas	Gas	Gas
154.5	-30	Gas	Gas	Gas
133.3	-40	Gas	Gas	Liquid
112.3	-50	Gas	Gas	Liquid

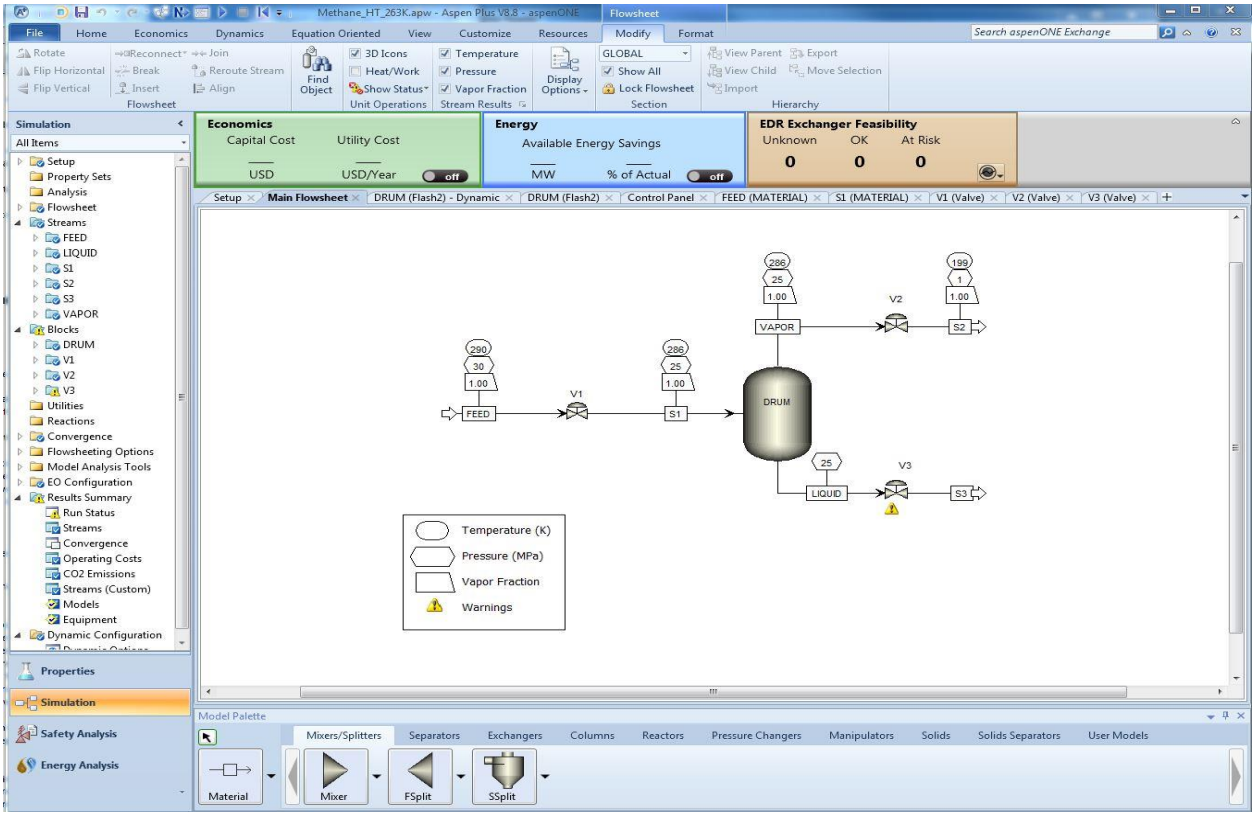

Figure 6-1: Aspen plus Flow Network (Static) for Pressurized Tank Decanting

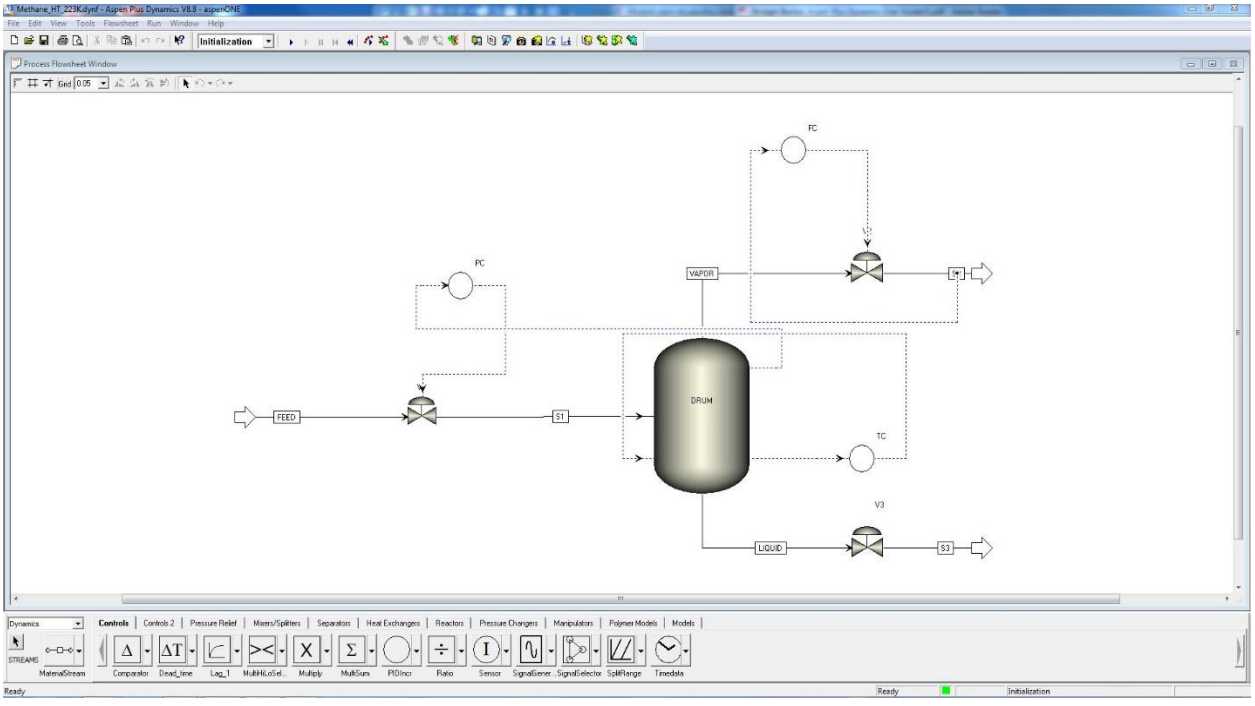

Figure 6-2: Aspen plus Flow Network (Dynamic) for Pressurized Tank Decanting

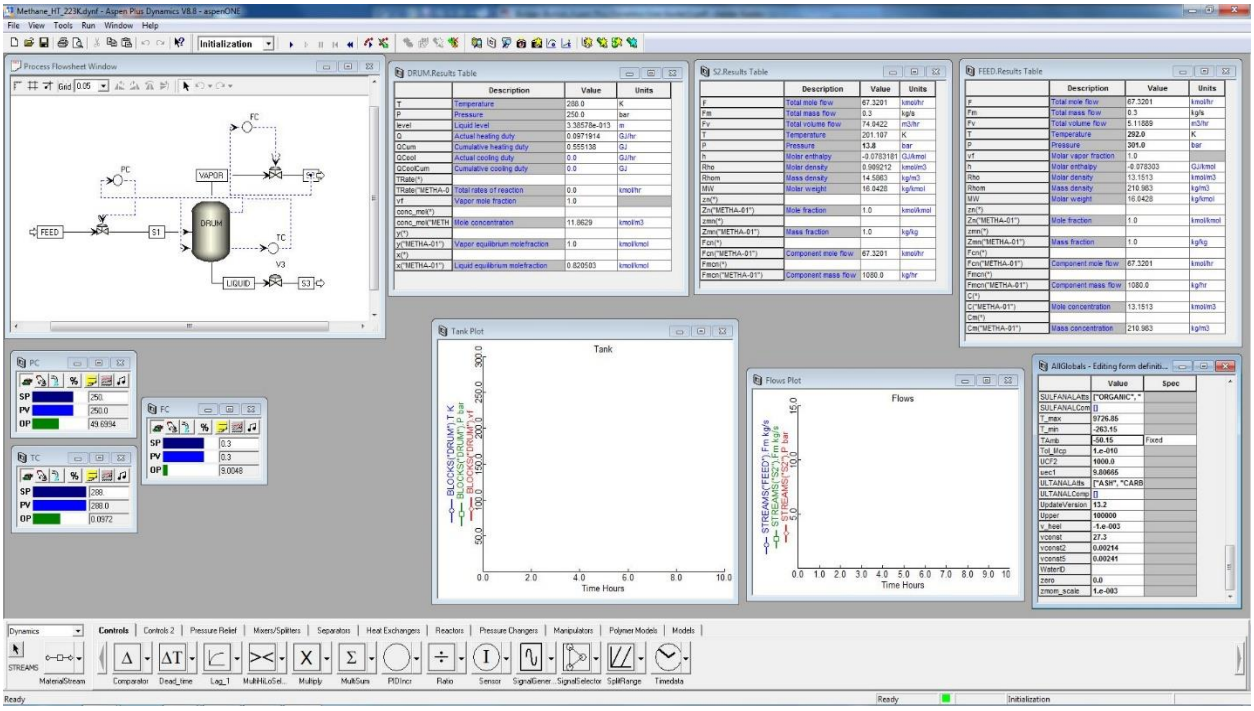

Figure 6-3: Aspen plus Dynamic simulation setup

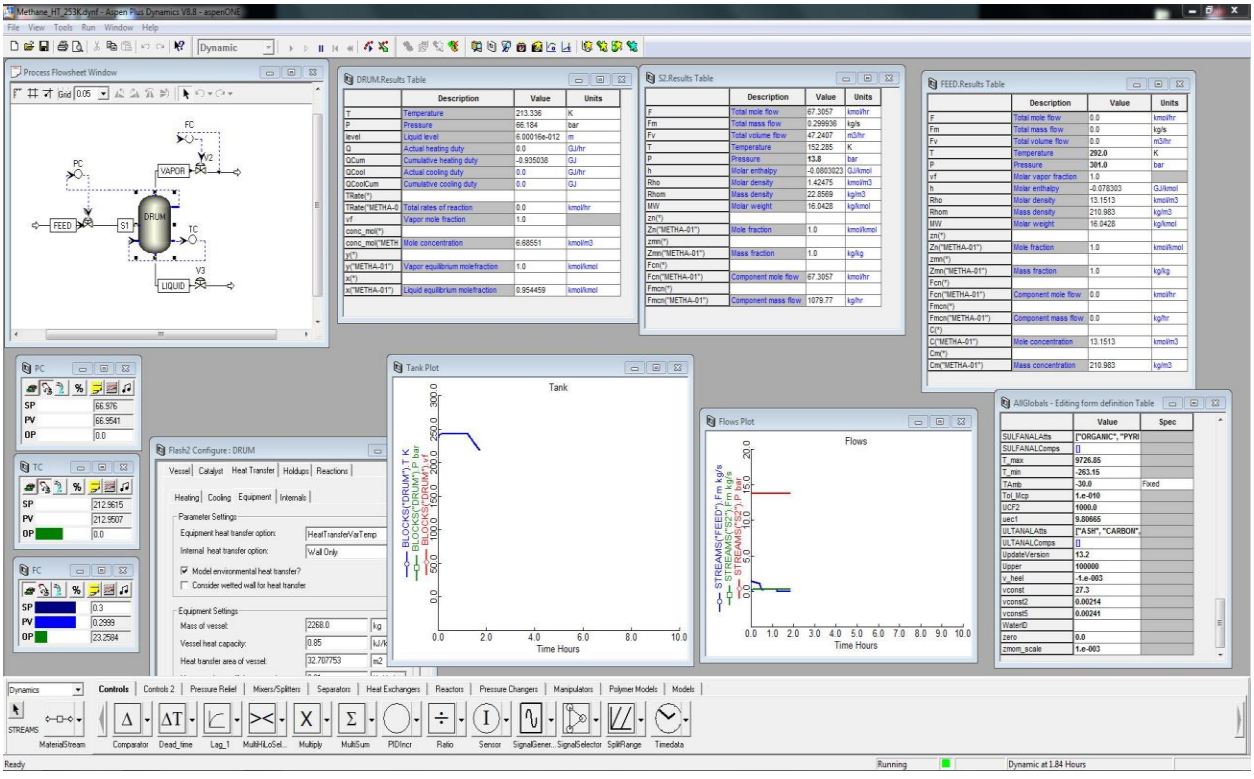

Figure 6-4: Aspen plus Dynamic simulation while running

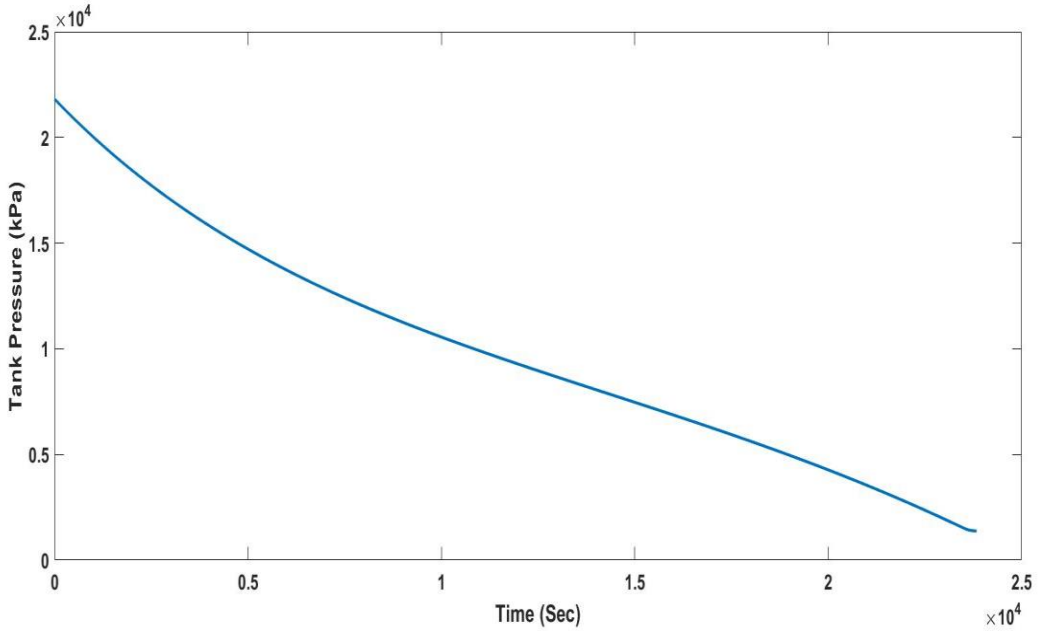

Figure 6-5: Tank Pressure Vs Time plot when the initial temperature of the system is 0°C and tank decanting rate is 0.064kg/s. Time taken to reach 14bar=23688s

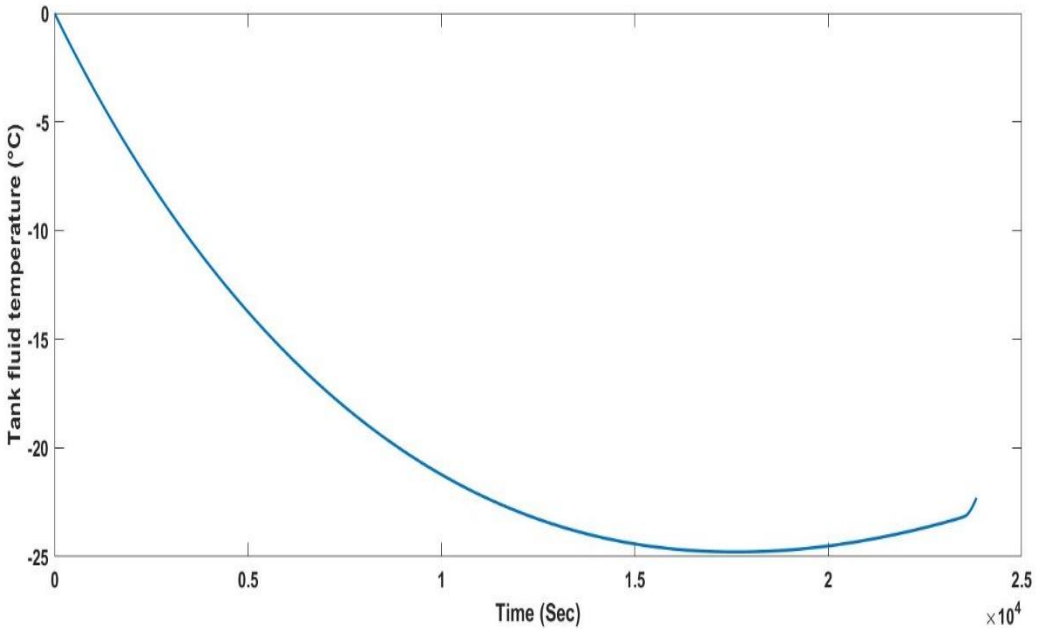

Figure 6-6: Tank Fluid (Methane) Temperature Vs time plot when initial temperature of the system is 0°C and tank decanting rate is 0.064kg/s. Minimum observed temperature of the fluid is -24.8°C.

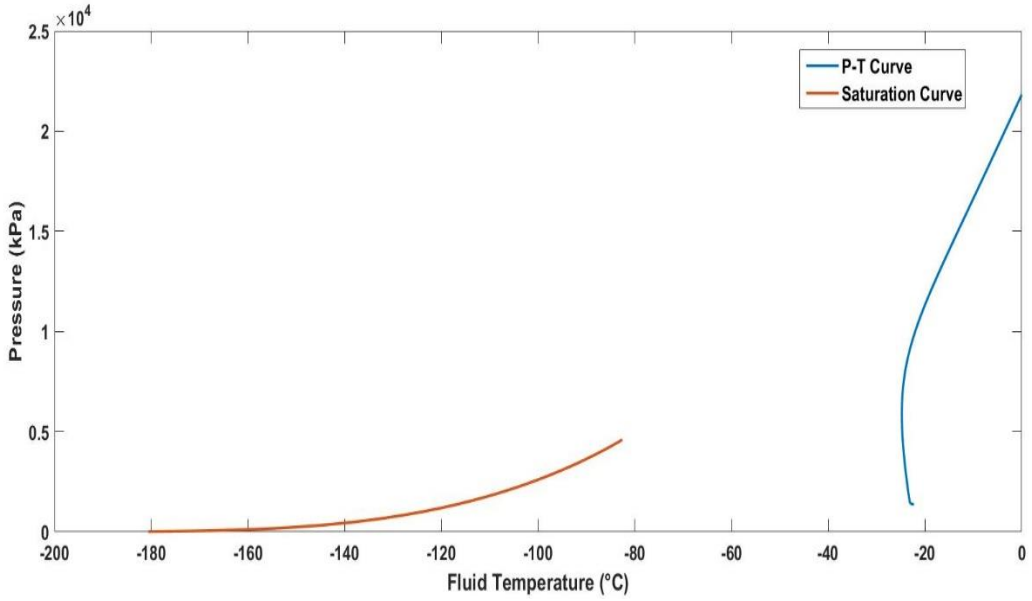

Figure 6-7: Pressure (kPa)-Temperature (°C) Vs Saturation Curve plot for Methane decanting at 0.064kg/s where the system initial conditions are at 218.2 bar and 0°C.

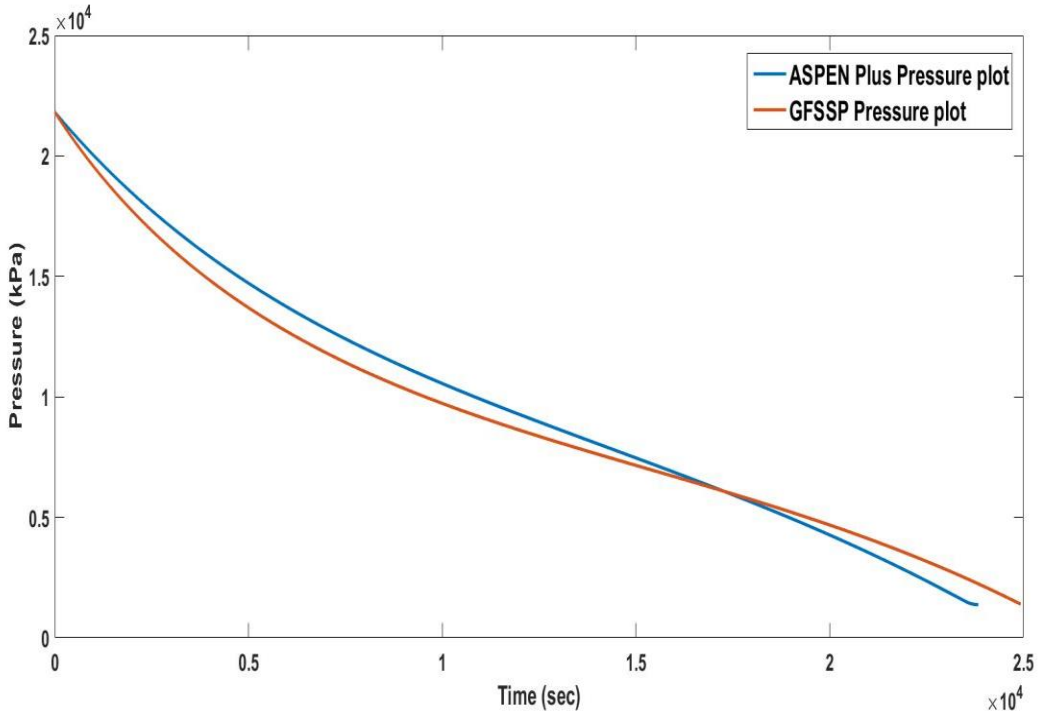

Figure 6-8: Pressure (kPa) Vs Time (sec) plot comparison for the results obtained from Aspen plus, GFSSP for Methane tank decanting at 0.064kg/s where the system initial conditions are at 218.2bar and 0°C.

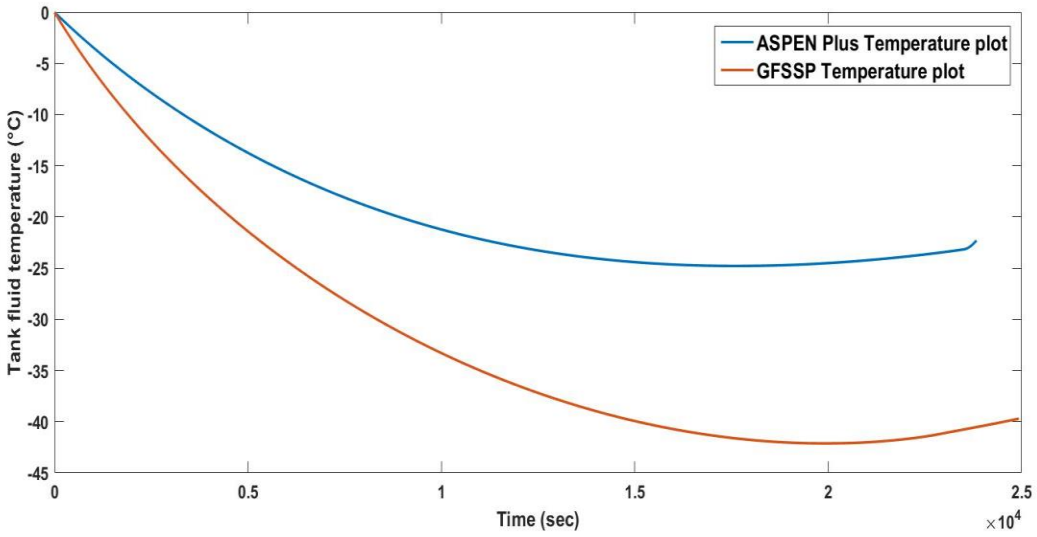

Figure 6-9: Tank Fluid (Methane) Temperature (°C) Vs Time (sec) plot comparison for the results obtained from Aspen plus, GFSSP for Methane tank decanting at 0.064kg/s where the system initial conditions are at 218.2bar and 0°C.

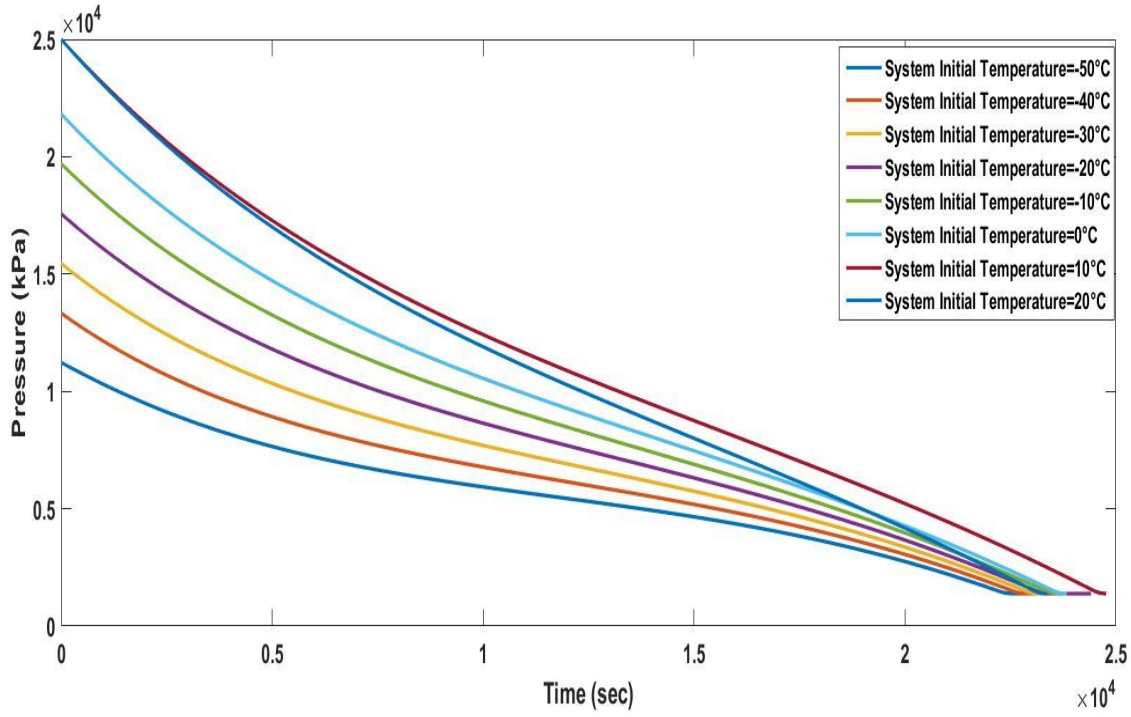

Figure 6-10: Cumulative Tank Pressure (kPa) vs Time (sec) plot obtained from Aspen plus for different system initial conditions with decanting rate of 0.064kg/s.

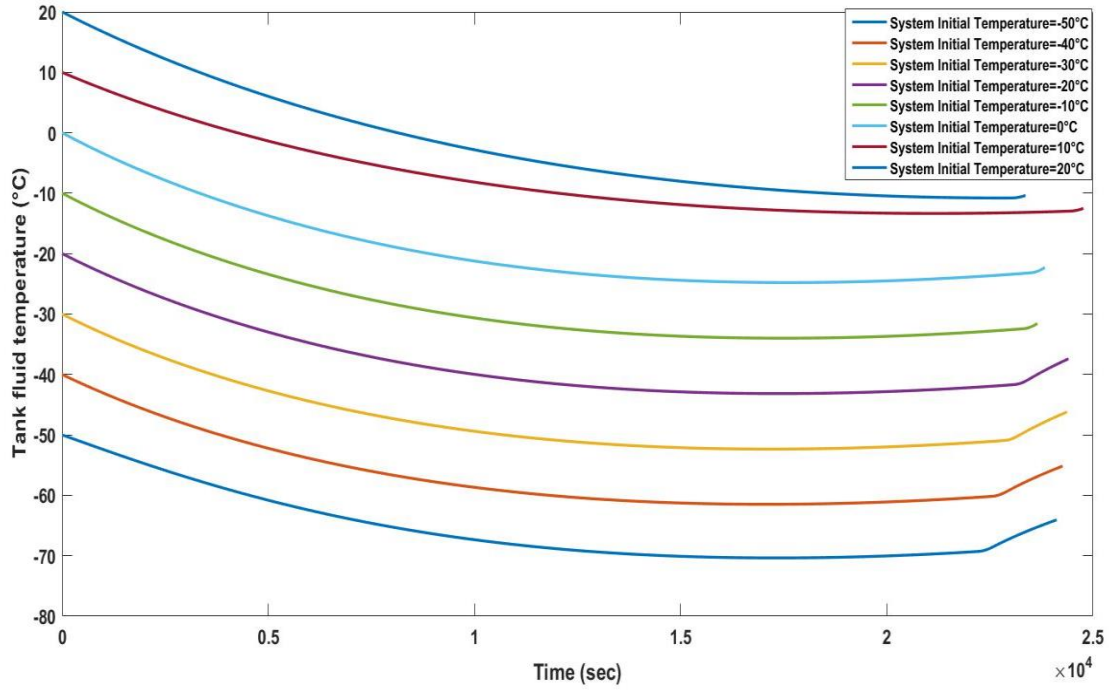

Figure 6-11: Cumulative Fluid temperature (°C) vs Time (sec) plot obtained from Aspen plus for different system initial temperatures with decanting rate of 0.064kg/s.

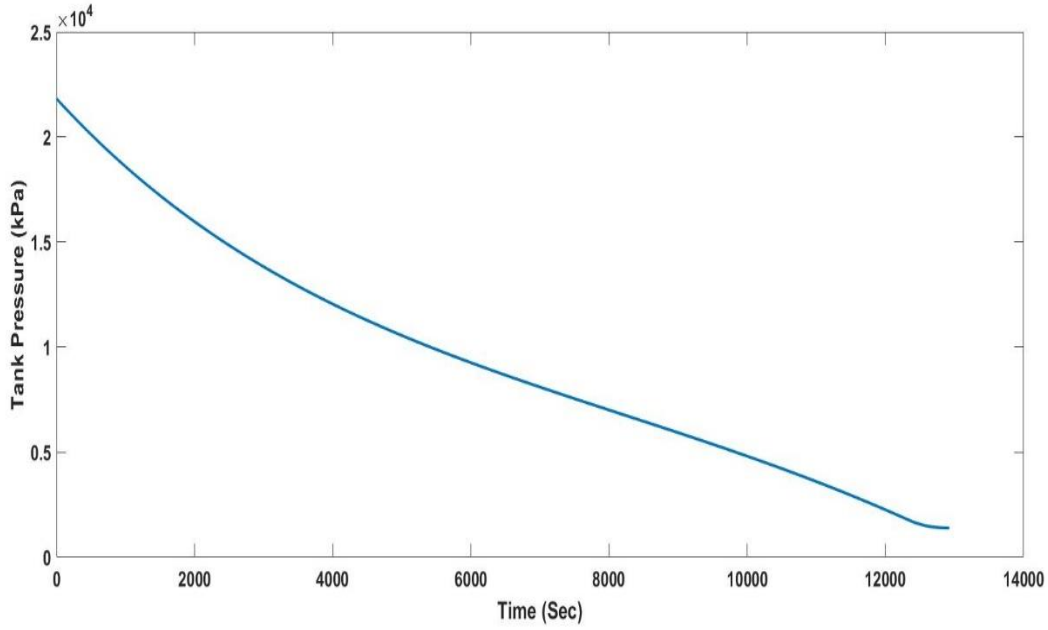

Figure 6-12: Tank Pressure Vs Time plot when the initial temperature of the system is 0°C and tank decanting rate is 0.11975kg/s. Time taken to reach 14bar=12780s

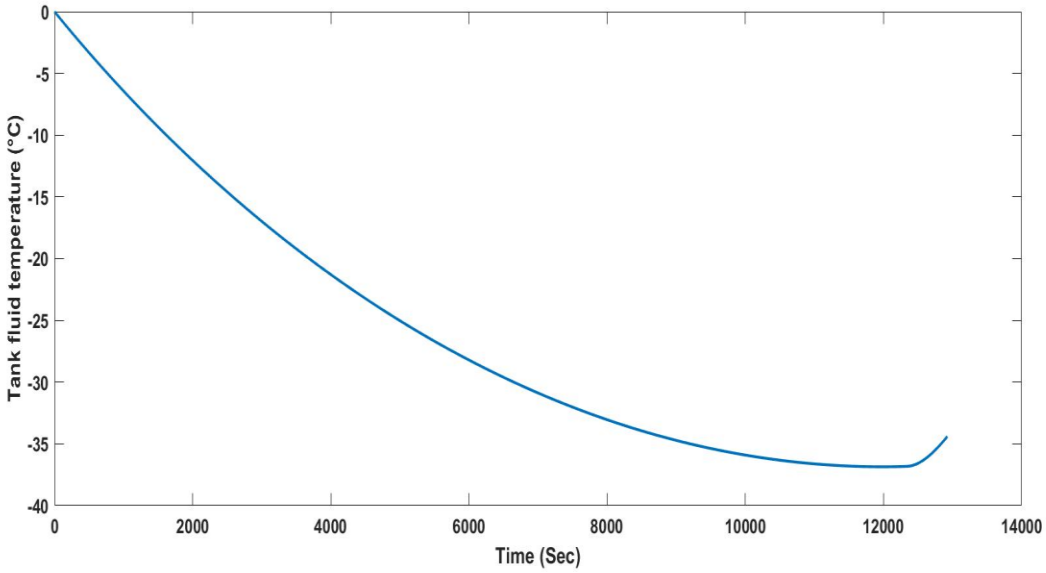

Figure 6-13: Tank Fluid (Methane) Temperature Vs time plot when initial temperature of the system is 0°C and tank decanting rate is 0.11975kg/s. Minimum observed temperature of the fluid is -36.9°C.

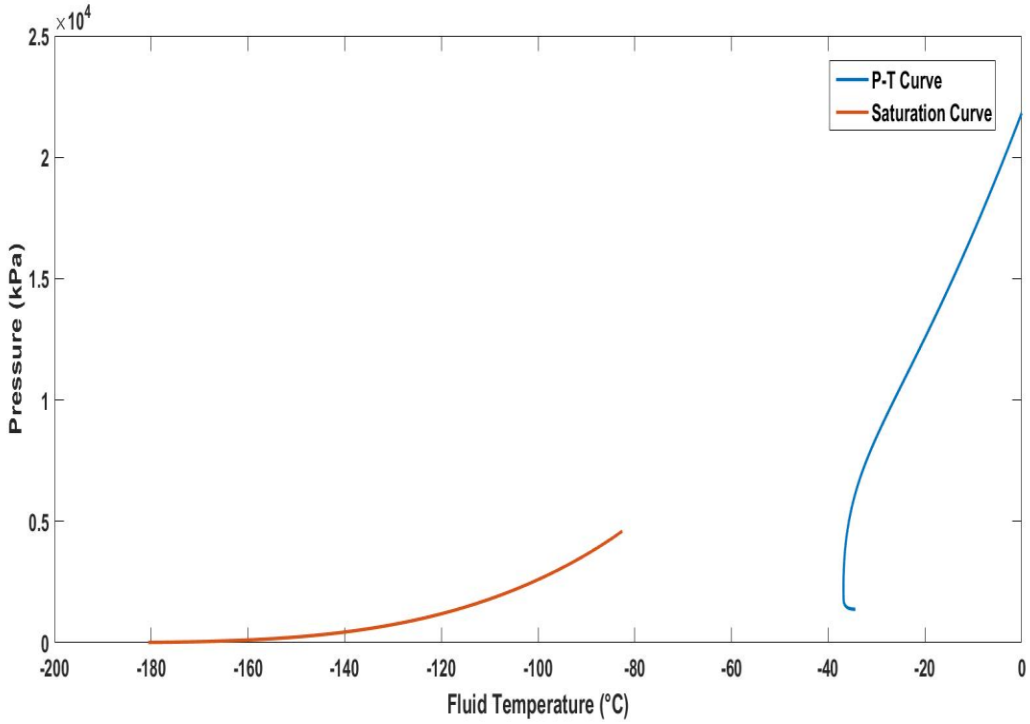

Figure 6-14: Pressure (kPa)-Temperature (°C) Vs Saturation Curve plot for Methane decanting at 0.11975kg/s where the system initial conditions are at 218.2 bar and 0°C.

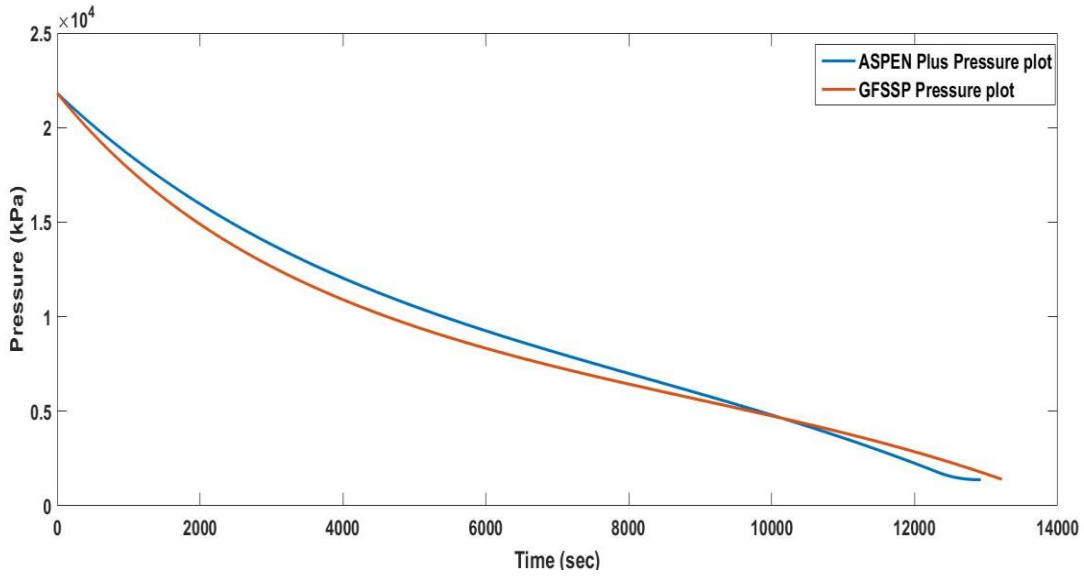

Figure 6-15: Pressure (kPa) Vs Time (sec) plot comparison for the results obtained from Aspen plus, GFSSP for Methane tank decanting at 0.11975kg/s where the system initial conditions are at 218.2bar and 0°C.

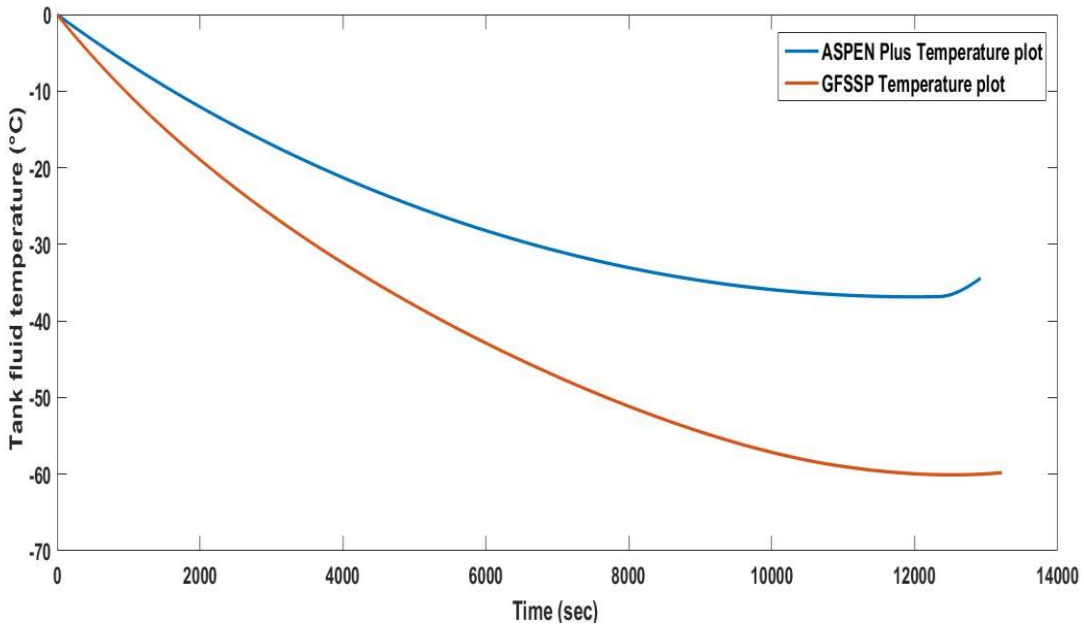

Figure 6-16: Tank Fluid (Methane) Temperature (°C) Vs Time (sec) plot comparison for the results obtained from Aspen plus, GFSSP for Methane tank decanting at 0.11975kg/s where the system initial conditions are at 218.2bar and 0°C

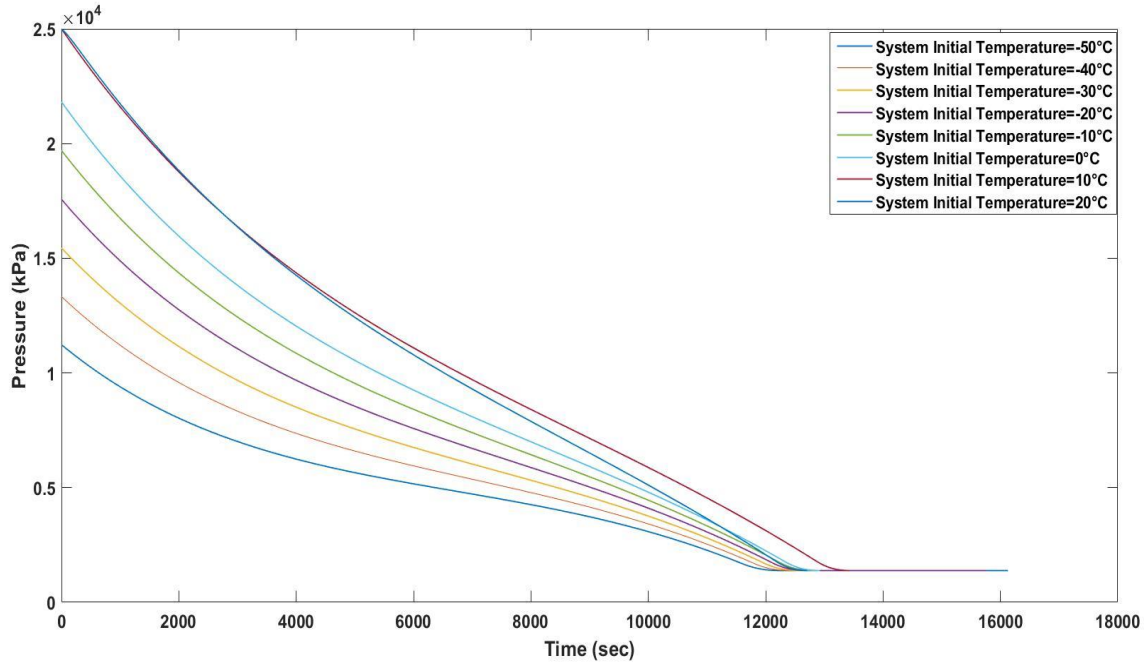

Figure 6-17: Cumulative Tank Pressure (kPa) vs Time (sec) plot obtained from Aspen plus for different system initial conditions with decanting rate of 0.11975kg/s

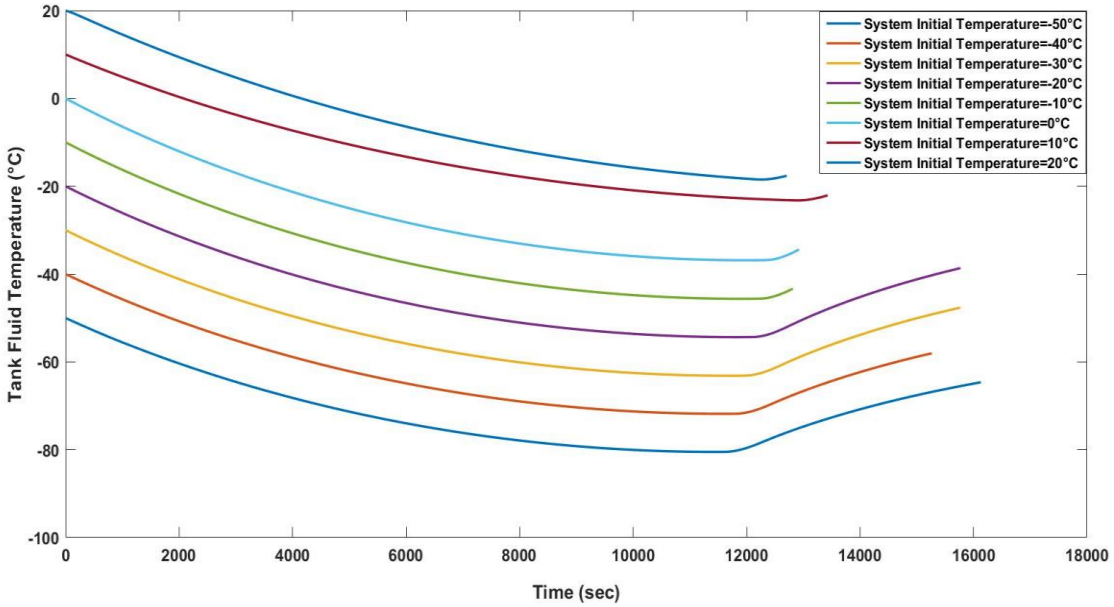

Figure 6-18: Cumulative Fluid temperature (°C) vs Time (sec) plot obtained from Aspen plus for different system initial temperatures with decanting rate of 0.11975kg/s

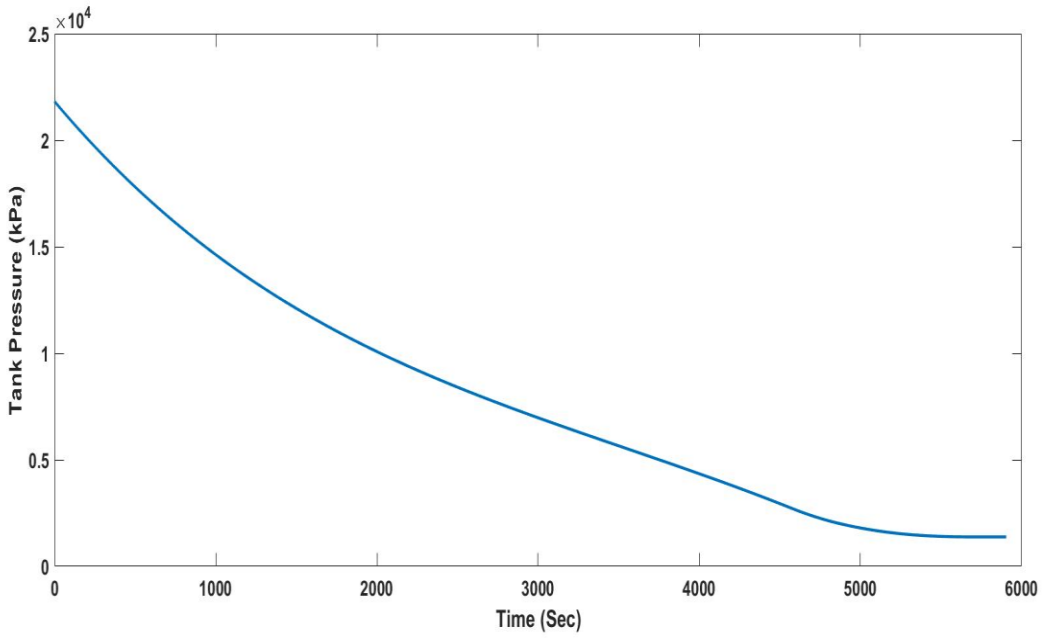

Figure 6-19: Tank Pressure Vs Time plot when the initial temperature of the system is 0°C and tank decanting rate is 0.3kg/s. Time taken to reach 14bar=5544s

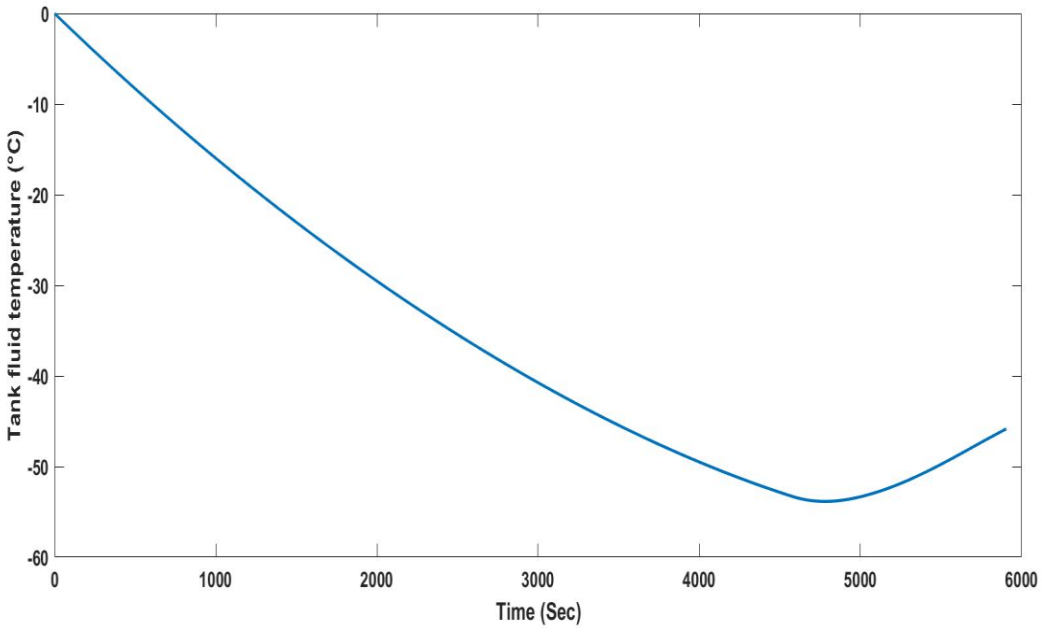

Figure 6-20: Tank Fluid (Methane) Temperature Vs time plot when initial temperature of the system is 0°C and tank decanting rate is 0.3kg/s. Minimum observed temperature of the fluid is -53.8°C

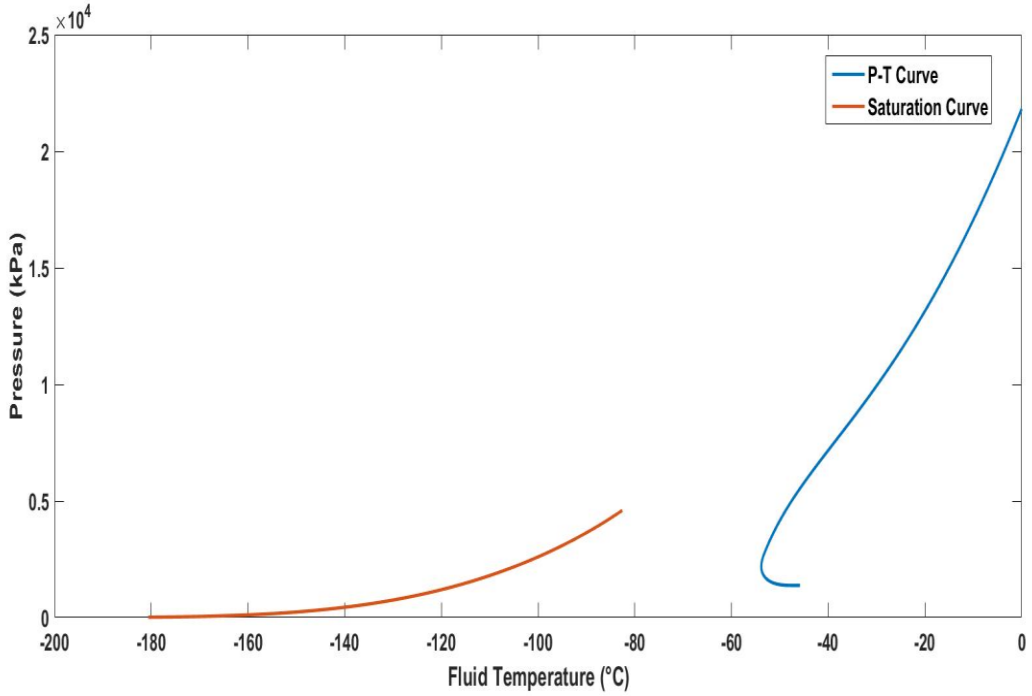

Figure 6-21: Pressure (kPa)-Temperature (°C) Vs Saturation Curve plot for Methane decanting at 0.3kg/s where the system initial conditions are at 218.2 bar and 0°C

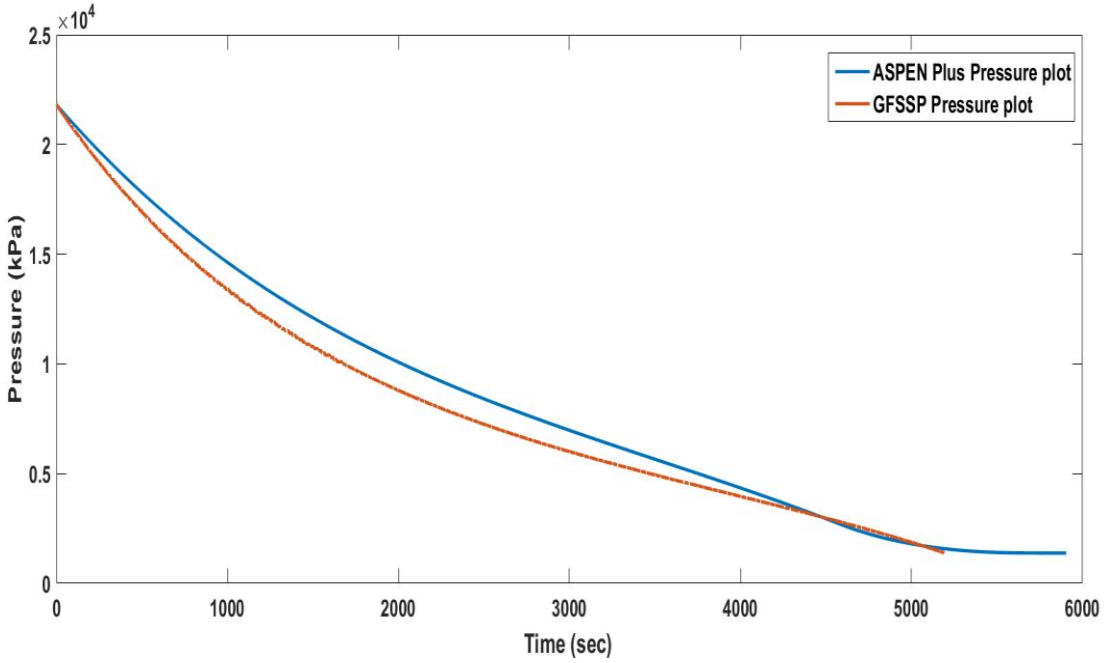

Figure 6-22: Pressure (kPa) Vs Time (sec) plot comparison for the results obtained from Aspen plus, GFSSP for Methane tank decanting at 0.3kg/s where the system initial conditions are at 218.2bar and 0°C.

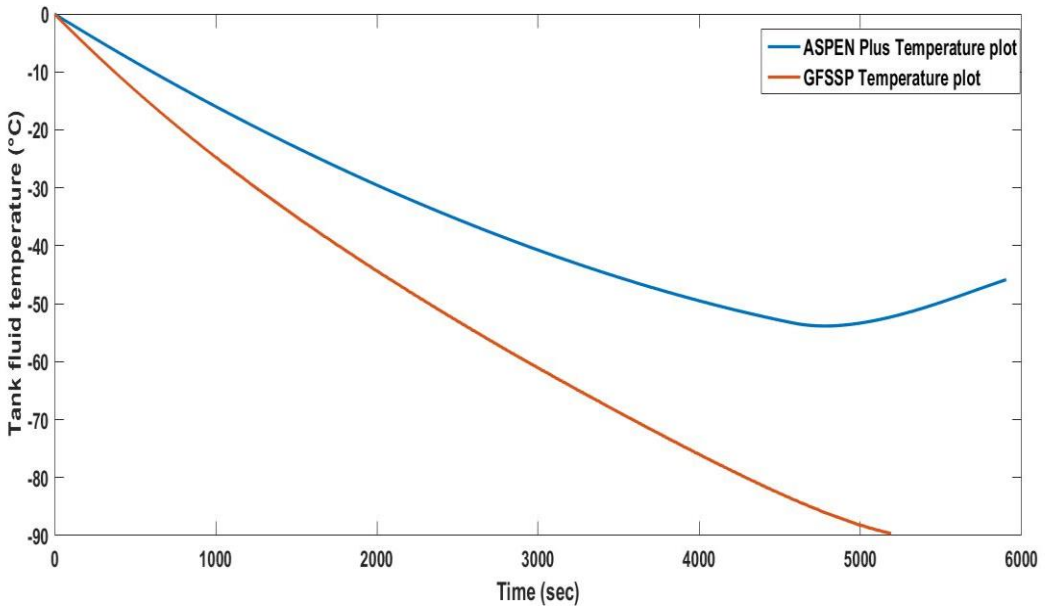

Figure 6-23: Tank Fluid (Methane) Temperature (°C) Vs Time (sec) plot comparison for the results obtained from Aspen plus, GFSSP for Methane tank decanting at 0.3kg/s where the system initial conditions are at 218.2bar and 0°C

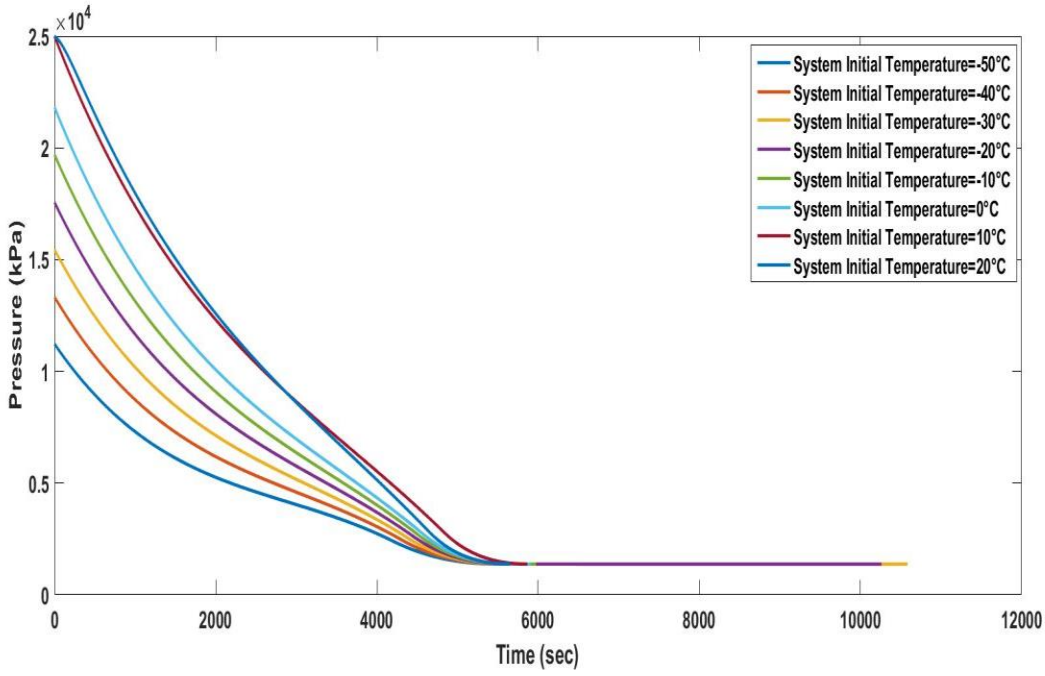

Figure 6-24: Cumulative Tank Pressure (kPa) vs Time (sec) plot obtained from Aspen plus for different system initial conditions with decanting rate of 0.3kg/s

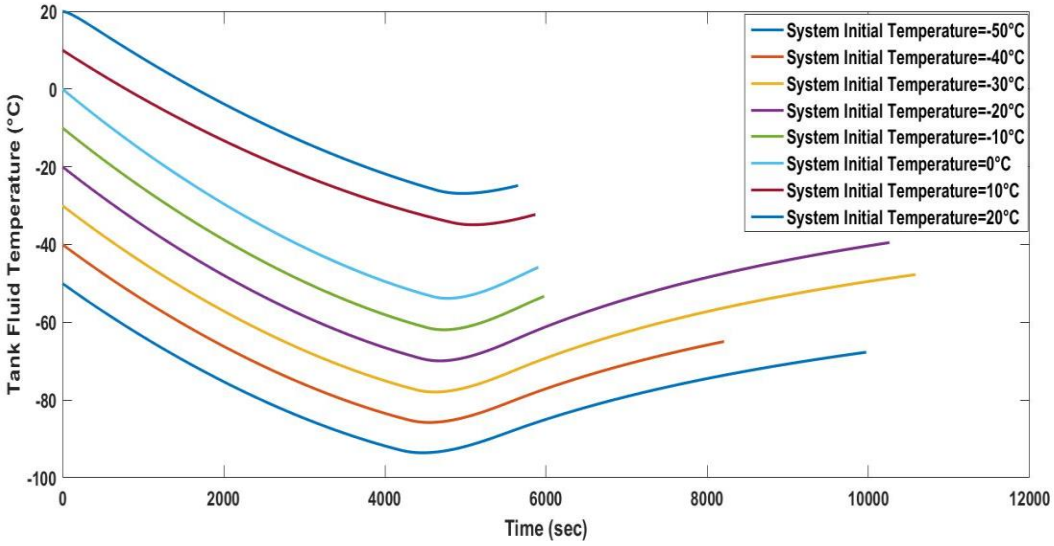

Figure 6-25: Cumulative Fluid temperature (°C) vs Time (sec) plot obtained from Aspen plus for different system initial temperatures with decanting rate of 0.3kg/s

Chapter 7 : Conclusions and Future work

7.1 Conclusions

Study of fast filling and decanting of fuels has long been a topic of interest for researchers around the world. Varied approaches have been utilized to study the fast filling of different fuels but little light was thrown towards the decanting of fuels particularly Methane. Throughout this report effort was made to study Methane tank decanting at different system initial conditions and at different decanting flow rates. Also focus was made on studying fuel mixture decanting and for this Biogas was chosen to be the fuel of interest. Many thermodynamic observations were made and the report was put together so that it may act as a guiding point for industries interested in fuel transportation. The major observations made and recommended suggestions for a safe fuel tank decanting are as follows:

1. Liquid Methane can prove to be fatal to the life of tank walls because of its ability to rapidly cool and damage tank walls. The purpose of this study is to determine when fuel condensation occurs during decanting.
2. The critical temperature of Methane is -82.59°C and during many of the decanting iterations the temperature within the tank went below this temperature. This shouldn't be considered to be only issue as critical pressure has a role to play. If the pressure in the tank at these points is greater than the critical pressure only, then the Methane liquefaction is observed otherwise Methane will remain as vapor in the tank.
3. Critical temperature and critical pressure are important points to be watched for, during decanting, but saturation curve is the guiding curve that should be taken as the base to predict any phase transformation happening within the tank walls.
4. It was observed that as the decanting flow rate increased, the chances of Methane liquefaction increased and also as the ambient temperature was decreased a similar effect was to be expected.

5. It was observed that system initial temperatures of -40°C and -50°C have always lead to the possibility of Methane liquefaction under all the studied decanting flow rates. The reason for this is that as the system initial temperature decreases the temperature drop required to reach liquefaction is relatively low which is met from all the decanting flow rates studied.
6. It was also observed that the decanting flow rates of 0.11975Kg/s and 0.3Kg/s mostly led to Methane liquefaction when the system initial temperatures were below -30°C.
7. The tank walls not only experience the thermal stresses due to fuel decanting but they are also under physical stress due to its own structure. The final pressure of 14bar is required by the manufacturer to make sure that the tank liner (HDPE polymer) doesn't pull away from tank structure (Carbon Epoxy fiber).
8. The behavior of Biogas during decanting is a bit different than pure Methane as the mixture is constituted of different gases and they behave differently in different thermodynamic conditions. The saturation curve derived from REFPROP was chosen as a base to predict liquefaction within the tank walls.
9. For the Biogas, the critical temperature and critical pressure derived from REFPROP were chosen to be the points to be watched for, during decanting. But as the decanting was continued beyond this point there were certain instances where individual gases started to condense as the partial pressure in the tank provided a perfect condition for individual gases to liquefy. Though it is still unclear on how all these gases behave individually throughout the decanting process, reasonable predictions were made from the results obtained from GFSSP simulations.
10. Though ASPEN plus was unable to include the wall effects but it provided an indirect solution to avoid liquefaction i.e. by maintaining the tank walls at ambient temperature by external heating.

11. Another suggested solution to avoid liquefaction is to decrease the decanting flow rate ahead of the liquefaction point so as the tank walls have enough time to pump heat into the system and also the rate of cooling of Methane is also decreased.

7.2 Future Work

The scope for future work are immense and below are few recommendations:

1. The system initial conditions can be varied over even wider range such as system initial temperature (ranging from -60°C to 100°C), pressure (ranging from 450bar to 100bar) depending on the structure of the tank and more flow rates (ranging from 1Kg/s to 0.03Kg/s) can be studied than the focused three in this report.
2. Similar studies can be made by choosing variety of tank materials ranging from metals to epoxy fibers. Only carbon epoxy tanks with HDPE polymer liner was studied in the present work.
3. Fuels other than Methane and Biogas are also needed to be studied and this would help the fuel transportation industry to improve their safe decanting standards.
4. It was assumed that the ambient conditions are constant throughout the process of decanting and there is a need to study the decanting in time varying ambient conditions.

References

A.K. Majumdar, A. L. a. R., 2013. *General Fluid System Simulation Program, Version 6.0,* HuntsVille: s.n.

Brittney Bridger Burton, K. C., 2016. *Modeling of Methane Tank Depressurization in Cold Weather.* [Online]
Available at: http://digitalcommons.unl.edu/ucareresearch/20/
[Accessed 11 June 2016].

Cole, K. D., June 12, 2015. *Safe Conditions for Decanting the Titan Tank: Simulations with a Caliberated Thermal Model,* Lincoln, Nebraska: Report Submitted to Hexagon Lincoln.

Consultants, J. S., 1991. *Comparision of CNG and LNG Technologies for Transportation Applications,* Colorado: National Renewable Energy Laboratory.

Eric W. Lemmon, M. L. H. M. O. M., 2007. *NIST Reference Fluid Thermodynamic and Transport Properties-REFPROP.* [Online]
Available at: http://www.nist.gov/srd/upload/REFPROP8.PDF

Javad Khadem, M. S.-T. M. F.-G., 2015. Mathematical modeling of fast filling process at CNG refueling stations considering connecting pipes. *Journal of Natural Gas Science and Engineering,* 11 June, Volume 26, pp. 176-184.

Khamforoush, M., Moosavi, R. & Hatami, T., 2015. Compressed natural gas behavior in a natural gas vehicle fuel tank during fast filling process: Mathematical modeling, thermodynamic analysis, and optimization. *Jornal of Natural Gas Science and Engineering,* 15 June, Volume 20, pp. 121-131.

Laurell, N., 2014. *Natural Gas Overview - Why is Methane a Clean Fuel?.* [Online]
Available at: http://www.nlaurell.com/natural-gas-overview-why-is-methane-a-clean-fuel/
[Accessed 26 July 2016].

Mazyan, W., Ahmadi, A. & Ahmed, H., 2016. Market and technology assessment of natural gas processing: A review. *Journal of Natural Gas Science and Engineering,* 13 February, Volume 30, pp. 487-514.

Melideo D., B. D. ,. B. A.-I. P. M. R. O. C., n.d. *CFD INVESTIGATION OF FILLING AND EMPTYING OF HYDROGEN TANKS,* Petten, The Netherlands: s.n.

Robert C. Hendricks, A. K. B. I. C. P., February, 1975. *GASP - A Computer Code for Calculating the Thermodynamic and Transport Properties for Ten Fluids: Parahydrogen, Helium, Neon, Methane, Nitrogen, Carbon Monoxide, Oxygen, Fluorine, Argon, and Carbon Dioxide,* Cleveland, Ohio: Lewis Research Center, National Aerodynamics and Space Administration.

Shipley, E., 2002. *Study of Natural Gas Vehicles (NGV) During the Fast Fill Process,* Morgantown: West Virginia University.

Appendix

The results obtained from GFSSP simulations have to be studied in order to understand the thermal behavior of Methane and Biogas during decanting under different system initial conditions of pressure and temperature. Different properties were selected from the results obtained and they were imported into MATLAB to get graphical data in order to understand the decanting simulations.

First different file naming pattern is explained below that will be used to import data from GFSSP to get graphical results and this pattern is kept constant throughout the study:

filenameFN.CSV: This is a .CSV type file where fluid node results are stored. The different fluid node property values that can be accessed from this file are pressure, temperature, compressibility, density, mole fraction, viscosity and thermal conductivity for the fluid in the tank.

filenameB.CSV: This file stores all the fluid branch results. The different results that are stored in this file are velocity of the fluid, pressure difference around the branch, mass flow rate of the fluid, entropy generation and area of the fluid branch.

filenameSN.CSV: This file is for storing solid node results. Specific heat and temperature of the solid node throughout the decanting at every time step can be accessed through this file.

filenameSF.CSV: Solid-Fluid conductor results are stored in this file. Convective enthalpy of the tank walls surface and fluid within the tank, enthalpy of solid-solid node, heat added to the fluid from the tank wall is the information stored in this file.

filenameSS.CSV: Solid-Solid conductor results are stored in this file. Thermal conductivity of the wall and head conducted from one solid node to other is the information that can be extracted from this file.

filenameSA.CSV: Solid-Ambient conductor results get stored in this file. Information such as convective enthalpy of solid-node and ambient surroundings, heat added by the ambient surroundings due to temperature difference between the wall surface and the surroundings is stored in this file.

Below is the MATLAB code used to import the results generated from GFSSP, Aspen Plus and plot the required graphs for the present analysis:

GFSSP results plot MATLAB Code

```
%% Plotting the Pressure and Temperature within the Tank with respect to time %%
a=csvread('finalmodelFN.CSV',2,0);      % Imports the fluid node results file from GFSSP into MATLAB
u=a(:,2);                               % Reads the pressure values in the tank at each time step
v=a(:,4);                               % Reads the temperature values in the tank at each time step
c=size(v);                              % Gives the number of time steps taken to empty the tank
for i=1:c
   if v(i,1)<=-82.59        % Condition to check if the temperature in the tank falls below critical temperature
      i;
      pressure_phasechange=u(i,1)
      fprintf('critical point has reached \n');
      break;
   end
end
[M,I]=min(v(:));
min_pressure=a(I,2); % Gives the pressure in the tank when the temperature in the tank is at critical temperature %
plot(v);                                % Plots the temperature of fluid vs time
xlabel('Time (Sec)');
ylabel('Tank fluid temperature (°C)');
figure;
plot(u);                                % Plots the pressure in the tank vs time
xlabel('Time (Sec)');
ylabel('Tank Pressure (kPa)');
%% End of code for plotting Pressure and Temperature in the Tank with respect to time %%
```

```
%% Code for plotting Pressure-Temperature Vs Saturation Curve in the Tank %%
a=csvread('finalmodelFN.CSV',2,0);          % Imports fluid node results from GFSSP in MATLAB
b=xlsread('Methane saturation data.xlsx'); % Imports Methane saturation data obtained from REFPROP
plot(a(:,4),a(:,2));                    %Plots P-T curve based on results obtained from GFSSP tank decanting
hold on;
plot(b(:,1),b(:,2));                     %Plots P-T Curve from the Saturation data obtained from REFPROP
xlabel('Fluid Temperature (°C)');
ylabel('Pressure (kPa)');
legend('P-T Curve','Saturation Curve');
%% End of code for plotting Pressure-Temperature Vs Saturation Curve %%

%% Code for plotting Solid Node Temperature %%
a=csvread('finalmodelSN.CSV',2,0);  % Imports Solid node results from GFSP into MATLAB
u=a(:,12);                  % Reads the solid node temperature closest to the ambient surroundings
v=a(:,21);                  % Reads the solid node temperature closest to inner surface of the tank
 [M,I]=min(v(:));           % Gives the Minimum observed temperature of the tank wall during decanting
plot(u);                    % Plots 'TS2'
hold on;
plot(v);                     % Plots 'TS11'
xlabel('Time (Sec)');
ylabel('Tank wall temperature (°C)');
legend('TS2','TS11');
%% End of code for plotting Solid Node Temperature %%

%% Code plotting Tank Fluid Temperature Vs Solid Node Temperature %%
a=csvread('finalmodelFN.CSV',2,0); % Imports fluid node results from GFSSP into MATLAB
b=csvread('finalmodelSN.CSV',2,0); % Imports solid node results from GFSSP into MATLAB
plot(a(:,4));                           % Plots fluid temperature in the tank during decanting
hold on;
plot(b(:,21));                  % Plots the solid node temperature closest to inner surface of the tank wall
xlabel('Time (sec)');
ylabel('Temperature (°C)');
legend('Fluid Temperature','Wall Temperature')
%% End of code for Tank Fluid Temperature Vs Solid Node Temperature %%


%% Code for plotting Pressure/Temperature cluster %%
a=csvread('20C,f3,MethaneFN.CSV',2,0); % Imports fluid node results when initial system temperature is 20°C
b=csvread('10C,f3,MethaneFN.CSV',2,0);
c=csvread('0C,f3,MethaneFN.CSV',2,0);
d=csvread('-10C,f3,MethaneFN.CSV',2,0);
e=csvread('-20C,f3,MethaneFN.CSV',2,0);
f=csvread('-30C,f3,MethaneFN.CSV',2,0);
g=csvread('-40C,f3,MethaneFN.CSV',2,0);
h=csvread('-50C,f3,MethaneFN.CSV',2,0);
%% Continued in next page %%
```

```
s=a(:,4); % Plots temperature/ pressure values during tank decanting
t=b(:,4);
u=c(:,4);
v=d(:,4);
w=e(:,4);
x=f(:,4);
y=g(:,4);
z=h(:,4);
plot(s);
hold on;
plot(t);
hold on;
plot(u);
hold on
plot(v);
hold on
plot(w);
hold on
plot(x);
hold on
plot(y);
hold on
plot(z);
xlabel('Time (sec)');
ylabel('Tank Fluid Temperature (°C)');
legend('System Initial Temperature=20°C','System Initial Temperature=10°C','System Initial Temperature=0°C','System Initial Temperature=-10°C','System Initial Temperature=-20°C','System Initial Temperature=-30°C','System Initial Temperature=-40°C','System Initial Temperature=-50°C');
%% End of code for plotting Pressure/Temperature cluster %%

%% Code for plotting Saturation data %%
a=xlsread('saturation data.xlsx'); % Imports Methane saturation data into MATLAB obtained from REFPROP
plot(a(:,1),a(:,2));
xlabel('Temperature (°C)');
ylabel('Pressure (kPa)');
%% End of code for plotting Saturation data %%
```

ASPEN Plus results plot MATLAB code:

Before the code used is explained below is the little detailed explanation for the file naming pattern used to store and plot the results obtained from ASPEN Plus:

File naming: 273.xlsx is the main Excel file in which many excel sheets were added for the results obtained. 293,f3 means that the system initial temperature was 293 Kelvin with a flow rate f3=0.3kg/s.

```
%% Pressure Plot %%
a=xlsread('273.xlsx','293,f3'); % Imports the tank decanting results from Aspen Plus into MATLAB
plot(a(:,4),a(:,6));
xlabel('Time (Sec)');
ylabel('Tank Pressure (kPa)');
%% End of code for plotting Pressure %%
```

```
%% Temperature Plot %%
a=xlsread('273.xlsx','293,f3');
plot(a(:,4),a(:,5));
xlabel('Time (Sec)');
ylabel('Tank fluid temperature (°C)');
%% End of code for plotting Temperature %%

%% P-T vs Saturation Curve Plot %%
a=xlsread('273.xlsx','293,f3');
b=xlsread('Methane saturation data.xlsx');
plot(a(:,5),a(:,6));
hold on;
plot(b(:,1),b(:,2));
xlabel('Fluid Temperature (°C)');
ylabel('Pressure (kPa)');
legend('P-T Curve','Saturation Curve');
%% End of code for plotting P-T Vs Saturation Curve Plot %%

%% Plotting Pressure from ASPEN Vs Pressure from GFSSP %%
a=xlsread('273.xlsx','sheet6');
plot(a(:,1),a(:,3));
hold on
plot(a(:,4),a(:,5));
xlabel('Time (sec)');
ylabel('Pressure (kPa)');
legend('ASPEN Plus Pressure plot','GFSSP Pressure plot');
%% End of code for plotting Pressure from ASPEN Vs Pressure from GFSSP %%
```

```
%% Plotting Temperature from ASPEN Vs Temperature from GFSSP %%
a=xlsread('273.xlsx','sheet6');
plot(a(:,1),a(:,2));
hold on
plot(a(:,4),a(:,6));
xlabel('Time (sec)');
ylabel('Tank fluid temperature (°C)');
legend('ASPEN Plus Temperature plot','GFSSP Temperature plot');
%% End of code for plotting Temperature from ASPEN vs Temperature from GFSSP %%

%% Cumulative Pressure and Temperature plot ASPEN results %%
a=xlsread('273.xlsx','cumulative,f3');
plot(a(:,1),a(:,2));
hold on;
plot(a(:,4),a(:,5));
hold on;
plot(a(:,7),a(:,8));
hold on;
plot(a(:,10),a(:,11));
hold on;
plot(a(:,13),a(:,14));
hold on;
plot(a(:,16),a(:,17));
hold on;
plot(a(:,19),a(:,20));
hold on;
plot(a(:,22),a(:,23));
xlabel('Time (sec)');
ylabel('Tank Fluid Temperature (°C)');
legend('System Initial Temperature=-50°C','System Initial Temperature=-40°C','System Initial
Temperature=-30°C','System Initial Temperature=-20°C','System Initial Temperature=-10°C','System
Initial Temperature=0°C','System Initial Temperature=10°C','System Initial Temperature=20°C');
%% End of code for plotting Cumulative Pressure and Temperature plot ASPEN results %%
```